

**EXPLORING MICROWAVE ASSISTED ROCK BREAKAGE  
FOR POSSIBLE SPACE MINING APPLICATIONS**

By

**Hemanth Satish**

June, 2005

Department of Mechanical Engineering  
McGill University  
Montreal, Quebec, Canada

A thesis submitted to  
McGill University  
in partial fulfillment of the requirements for the degree of  
Master of Engineering

© Hemanth Satish, 2005



Library and  
Archives Canada

Bibliothèque et  
Archives Canada

Published Heritage  
Branch

Direction du  
Patrimoine de l'édition

395 Wellington Street  
Ottawa ON K1A 0N4  
Canada

395, rue Wellington  
Ottawa ON K1A 0N4  
Canada

*Your file* *Votre référence*  
*ISBN: 978-0-494-22671-1*  
*Our file* *Notre référence*  
*ISBN: 978-0-494-22671-1*

**NOTICE:**

The author has granted a non-exclusive license allowing Library and Archives Canada to reproduce, publish, archive, preserve, conserve, communicate to the public by telecommunication or on the Internet, loan, distribute and sell theses worldwide, for commercial or non-commercial purposes, in microform, paper, electronic and/or any other formats.

The author retains copyright ownership and moral rights in this thesis. Neither the thesis nor substantial extracts from it may be printed or otherwise reproduced without the author's permission.

**AVIS:**

L'auteur a accordé une licence non exclusive permettant à la Bibliothèque et Archives Canada de reproduire, publier, archiver, sauvegarder, conserver, transmettre au public par télécommunication ou par l'Internet, prêter, distribuer et vendre des thèses partout dans le monde, à des fins commerciales ou autres, sur support microforme, papier, électronique et/ou autres formats.

L'auteur conserve la propriété du droit d'auteur et des droits moraux qui protègent cette thèse. Ni la thèse ni des extraits substantiels de celle-ci ne doivent être imprimés ou autrement reproduits sans son autorisation.

---

In compliance with the Canadian Privacy Act some supporting forms may have been removed from this thesis.

Conformément à la loi canadienne sur la protection de la vie privée, quelques formulaires secondaires ont été enlevés de cette thèse.

While these forms may be included in the document page count, their removal does not represent any loss of content from the thesis.

Bien que ces formulaires aient inclus dans la pagination, il n'y aura aucun contenu manquant.

  
**Canada**

# Abstract

---

As humanity prepares to migrate to the frontiers of the Moon and other planets, the area of mining in space must go along for the purpose of exploration and in-situ resource utilization. In the present work the literature that has been developed over the years in the area of mining in space as applicable to Lunar and Martian environments is reviewed. Subsequently, the key mining technologies that are most suitable for Lunar and Martian environments are identified. From the literature review, it is concluded that an optimal combination of both mechanical methods and novel energy (lasers, microwaves, nuclear energy) methods for rock destruction drawing a trade off between the energy and mass would be the most ideal option for space applications.

One such technique of applying low power microwaves to the rocks to thermally weaken them without actually melting them before employing mechanical methods of rock destruction is investigated. Finite element simulations were carried out to simulate microwave heating of a calcareous rock to determine the temperature profiles and thermal stresses at different microwave heating times and powers. Preliminary experiments were carried out in order to determine the microwave susceptibility of terrestrial basalt (which has similar composition as Lunar and Martian rocks). Temperature and strength of the rock sample before and after microwaving was measured.

The results of the finite element simulation indicated that a calcareous rock with microwave responsive phase and a microwave non-responsive phase developed thermal stresses of large magnitudes exceeding the actual strength of the rock. The simulation methodology can be applied to other rock types as well, provided the thermal, electrical and structural properties of constituent mineral phases are available.

The preliminary experimental results showed that the basalt rock specimens used were quite susceptible to the low power microwaves. There was a decreasing trend in terms of the point load index of the rock samples as the microwaving exposure times were increased, with some rock samples showing visible cracks at higher microwaving times.

## Résumé

---

Comme l'humanité se prépare à migrer vers la Lune et les autres planètes, le domaine minier devra suivre dans l'espace pour les fins d'exploration et d'exploitation des ressources. Dans le présent travail la littérature relative au domaine minier dans l'espace, plus spécifiquement en ce qui a trait aux environnements lunaire et martien a été revue. Par la suite les éléments technologiques clefs les plus prometteurs pour les environnements lunaire et martien ont été identifiés. De cette revue de la littérature il est conclu que la combinaison optimale des méthodes mécaniques et d'énergies nouvelles (laser, micro-ondes, nucléaires ou autres) pour le cassage de la roche permettant un compromis entre l'énergie et la masse serait l'option idéale pour les applications spatiales.

Plus spécifiquement, une telle technique combinant les micro-ondes de faible puissance au roc dans le but de l'affaiblir sans produire la fusion au préalable a l'application d'une méthode mécanique de destruction du roc est étudiée. Des simulations par éléments finies pour une roche calcaire ont été réalisées pour simuler l'application de micro-ondes et prédire les profils de température et de contraintes induits pour divers niveaux de puissance et de temps d'exposition. Ensuite, des essais préliminaires ont été conduits pour déterminer la susceptibilité d'un basalte (choisi parce que sa composition s'apparente aux roches lunaires et martiennes. La température et la résistance mécanique des échantillons de roche ont été mesurés.

Les simulations numériques ont montré qu'une roche contenant des phases susceptibles et non susceptibles aux micro-ondes développaient des contraintes de tension aux interfaces grains/matrice excédant la résistance en tension du roc. La méthode d'analyse peut être appliquée à divers types de roche dans la mesure où les propriétés thermiques, diélectriques des diverses phases constituantes sont connues.

Les résultats des essais préliminaires montrent que les échantillons de Basalte utilisés sont très susceptibles aux micro-ondes de faible puissance. La résistance, mesurée avec l'essai de double poinçonnement, tend à diminuer lorsque la durée d'application des micro-ondes augmente. Pour certains échantillons l'apparition de fissures visibles à l'œil nu a été notée lorsque la durée d'application des micro-ondes augmentait.

# Acknowledgements

---

## “SRI GURUBYO NAMAH”

I would like to express my sincere gratitude and thanks to my thesis supervisors Prof. Peter Radziszewski and Prof. Jacques Ouellet for their constant guidance, encouragement and patience through out the course of this project. Their concern for my problems, professional or otherwise, invaluable advice at appropriate times went a long in motivating me to successfully complete this project.

The present work is a part of the Design for Extreme Environments under the McGill University CDEN node and I would like to thank Prof. Peter Radziszewski for supporting me financially through out the course of my thesis.

My sincere thanks to Prof. G.S.V. Raghavan, Dept of Bioresource Engineering, McGill University for his inputs and allowing me to use his microwave test facilities, without which this project work would not have been complete. I would also like to thank Mr. Yvan Gariépy for teaching me how to use the microwaving facility. I would like to thank Mr. John from the department of Civil Engineering, McGill University for helping me to core and cut my samples.

Last but not the least I would like to thank my parents for their love, understanding and support during the course of the study.

# Table of Contents

---

Abstract.....	ii
Résumé .....	iii
Acknowledgements .....	iv
Table of Contents .....	v
List of Tables.....	viii
List of Figures.....	x
Nomenclature .....	xiii
CHAPTER 1 INTRODUCTION.....	1
1.1 Introduction .....	2
1.2 Motivation and organization of the thesis .....	3
1.3 Thesis objectives .....	4
1.4 Outline of the thesis.....	4
CHAPTER 2 REVIEW OF MINING IN SPACE.....	6
2.1 Typical Terrestrial mining operations .....	7
2.2 Design for Lunar/Martian mining .....	9
2.3 Space Mining.....	12
2.3.1 Drilling .....	14
2.3.2 Blasting .....	21
2.3.3 Excavation .....	24
2.3.4 Comminution, classification and beneficiation .....	28
2.4 Issues of mining on Moon/Mars.....	31
2.5 Conclusions .....	33

CHAPTER 3	MICROWAVE ASSISTED ROCK BREAKAGE .....	35
3.1	Introduction .....	36
3.2	Basic Concepts of Microwave Heating .....	36
3.3	Microwave Heating Equipment.....	38
3.4	Research in the use of microwave treatment of mineral ores.....	40
3.5	Use of microwave energy for drilling and excavation of rocks .....	42
3.6	Issues .....	45
3.7	Conclusions .....	46
CHAPTER 4	SIMULATION OF MICROWAVE HEATING .....	48
4.1	Introduction to Maxwell's equations.....	49
4.1.1	Boundary conditions.....	50
4.2	Dielectric properties .....	51
4.3	Dielectric heating equation.....	53
4.4	Simulation methodology .....	55
4.4.1	High Frequency Electromagnetic analysis .....	56
4.4.2	Transient thermal analysis.....	59
4.4.3	Estimation of thermal stresses.....	62
4.5	Results and Discussions .....	64
4.6	Conclusion.....	77
CHAPTER 5	EXPERIMENTAL STUDIES.....	78
5.1	Introduction .....	79

5.2	Theory of point load strength test.....	80
5.2.1	Calculation.....	81
5.3	Experimental Setup .....	83
5.3.1	Microwaving setup .....	83
5.3.2	Point load tester .....	84
5.3.3	Test Specimens.....	85
5.4	Experimental Procedure .....	86
5.4.1	Microwaving experiments.....	86
5.4.2	Point load strength testing.....	88
5.5	Results and Discussion.....	89
5.6	Conclusions .....	98
CHAPTER 6 CONCLUSIONS AND RECOMMENDATIONS .....		99
6.1	Conclusions .....	100
6.2	Recommendations .....	102
REFERENCES .....		104

## List of Tables

---

Table 2.1 Important design parameters .....	9
Table 2.2 Candidate planetary drilling technologies .....	20
Table 2.3 Applicability of various drilling methods in Lunar environment.....	21
Table 2.4 Applicability of blasting methods in Lunar/Martian environment.....	24
Table 2.5 Alternate excavation and haulage (for surface mining) methods for space .....	27
Table 2.6 Applicability of under ground mining methods to Lunar and Martian .....	28
Table 2.7 Candidate screening, comminution and beneficiation methods as applied to Moon/Mars .....	29
Table 3.1 Qualitative analysis of microwave heating of minerals .....	40
Table 3.2 Microwave heating of minerals .....	41
Table 4.1 Dielectric Constant ( $\epsilon'$ ) and loss factor ( $\epsilon''$ ) for various materials at 3000MHz .....	53
Table 4.2 Dimensions for high frequency electromagnetic analysis.....	57
Table 4.3 Material properties for electromagnetic analysis .....	58
Table 4.4 Thermal conductivity as a function of temperature .....	61
Table 4.5 Specific Heat capacity as a function of temperature of calcite and pyrite .....	61
Table 4.6 Density of the mineral Phases .....	61
Table 4.7 Strength Properties of pyrite and calcite .....	63
Table 4.8 Thermal Coefficient of expansion as a function of temperature .....	64
Table 4.9 Maximum Electric Field Intensity at different input Microwave Powers.....	64
Table 5.1 Comparison of chemical composition of terrestrial basalt with Lunar and Martian composition .....	80

Table 5.2 Generalized value of C .....	82
Table 5.3 Megascopic and microscopic description of the rock .....	86
Table 5.4 Microwave exposure times used .....	88
Table 5.5 Average point load index and compressive strengths at different times of microwave exposure.....	94

# List of Figures

---

Figure 2.1 Stages in the operation of mine.....	8
Figure 2.2 Broad picture of mining on Moon/Mars .....	13
Figure 2.3 (a) Multirod Drill (b) Drill tool schematics .....	15
Figure 2.4 Sample collection and discharge sequence .....	16
Figure 2.5 Bottom Hole assembly .....	16
Figure 2.6 Rock Melting bits .....	17
Figure 2.7 Self contained down hole drilling system.....	18
Figure 2.8 Ultrasonic Driller/Corer .....	19
Figure 2.9 Plasma Blasting system.....	23
Figure 2.10 Lunar Comminution and beneficiation circuit.....	30
Figure 3.1 Microwave interactions with materials.....	37
Figure 3.2 Typical Components of a microwave Heating system.....	39
Figure 3.3 Schematic Representation of the Microwave Drill.....	43
Figure 4.1 Geometric model for the high frequency electromagnetic analysis.....	56
Figure 4.2 Schematic Representation of the boundary condition.....	58
Figure 4.3 Variation of Dielectric loss factor with temperature for pyrite .....	59
Figure 4.4 Geometric model for the transient thermal analysis .....	60
Figure 4.5 typical contour plots for the electric field distribution within the dielectric load for an input power of 150Watts at a microwave frequency of 2450MHz.....	65
Figure 4.6 Typical contour plot showing the electric field distribution for the whole electromagnetic structure for an input power of 150Watts at a microwave frequency of 2450MHz.....	66

Figure 4.7 Microwave Power absorption density of pyrite at 2450MhZ, 150W cavity at various temperatures.....	66
Figure 4.8 Microwave Power absorption density of pyrite at 2450MhZ, 750W cavity at various temperatures.....	67
Figure 4.9 Microwave Power absorption density of pyrite at 2450MhZ, 1000W cavity at various temperatures.....	67
Figure 4.10 Temperature profiles at different microwave heating times and at input microwave power of 150 W, 2450 MHz.....	68
Figure 4.11 Temperature profiles at different microwave heating times and at a input microwave power of 750 W, 2450 MHz.....	69
Figure 4.12 Temperature profiles at different microwave heating times and at input microwave power of 1000 W, 2450 MHz.....	69
Figure 4.13 Temperature profile at a microwave heating time of 10s and at input microwave power of 750 W, 2450 MHz.....	71
Figure 4.14 Temperature profile at a microwave heating time of 60s and at input microwave power of 750 W, 2450 MHz.....	71
Figure 4.15 Stress profile for a microwave input power of 150W at various exposure times .....	72
Figure 4.16 Stress profile for a microwave input power of 750W at various exposure times .....	72
Figure 4.17 Stress profile for a microwave input power of 1000W at various exposure times .....	73
Figure 4.18 Stress profile for a microwave input power of 1000W for microwave exposure time of 10seconds.....	74
Figure 4.19 Stress profile for a microwave input power of 750W for microwave exposure time of 10 seconds .....	74
Figure 4.20 Solution dependency of the high frequency analysis on the mesh size .....	76
Figure 4.21 Solution dependency of the transient thermal analysis on the mesh size .....	77
Figure 5.1 Size Correction Factor Chart.....	82

Figure 5.2 Relationship between point load strength index and uniaxial compressive strength .....	83
Figure 5.3 Photograph of the microwaving setup .....	84
Figure 5.4 Photograph of the point load tester .....	85
Figure 5.5 Dimensions of the rock specimen .....	85
Figure 5.6 Schematic representation of the loading points in point load testing .....	88
Figure 5.7 Temperatures of the rock specimens at different microwave exposure times ..	89
Figure 5.8 Specimens after 60 seconds (a) and 120 seconds (b) microwave exposure times .....	90
Figure 5.9 Some specimens that showed cracking after 180seconds microwave exposure times .....	91
Figure 5.10 Some specimens that showed cracking after 360seconds of microwave exposure times .....	91
Figure 5.11 Experimental results of the point load tests .....	92
Figure 5.12 Correlated compressive strengths from point load index.....	93
Figure 5.13 Mean Compressive strengths at different Microwave exposure times .....	93
Figure 5.14 Typical failure patterns of the specimens during the diametral point load testing .....	94
Figure 5.15 Specimen showing local failures at the point of loading during point load tests after microwaving.....	95
Figure 5.16 Penetration rate vs. uniaxial compressive strength for percussive drilling ...	96
Figure 5.17 Penetration rate vs. Microwave exposure times for percussive drilling .....	97

# Nomenclature

---

$\bar{E}$  = Electric Field intensity (V/m)

$H$  = Magnetic field intensity (A/m)

$E_t$  = Tangential electric field intensity (V/m)

$E_n$  = Normal electric field intensity (V/m)

$E_i$  = Internal electric field intensity within the dielectric load (V/m)

$H_n$  = Normal magnetic field intensity (A/m)

$D$  = Electric Flux density ( $C/m^2$ )

$B$  = Magnetic flux density ( $W/m^2$ )

$J$  = Conduction electric current density ( $A/m^2$ )

$\epsilon$  = Permittivity (F/m)

$\mu$  = Permeability (H/m)

$\sigma$  = Conductivity (S/m)

$\rho_e$  = Electric charge density ( $C/m^3$ )

$\epsilon_r$  = Relative permittivity

$\epsilon_0$  = Permittivity of free space (F/m)

$\epsilon'$  = Relative dielectric constant

$\epsilon''$  = Relative dielectric loss factor

$\mu_0$  = Permeability of free space

$\mu''$  = Relative magnetic loss factor

$\tan \delta$  = Loss tangent

$P_d$  = Microwave power dissipation density ( $W/m^3$ )

$f$  = Microwave frequency (Hz)

$t$  = Microwave exposure time(seconds)

$T$  = Temperature (Kelvin)

$r$  = radial spatial coordinate (mm)

$z$  = Axial spatial coordinate (mm)

$\theta$  = Angular spatial co-ordinate (rad)

$\rho$  = Density (Kg/m<sup>3</sup>)

$C_p$  = Specific heat capacity (J/Kg-K)

$K$  = Thermal conductivity (W/m-K)

$\epsilon_{ij}$  = various components of strains

$\sigma_{ij}$  = Various components of normal Stresses (MPa)

$\tau_{ij}$  = Various components of shear stresses (MPa)

$E$  = young's modulus (GPa)

$\nu$  = Poisson's ratio

$\alpha$  = Co-efficient of thermal expansion (1/K)

# CHAPTER 1

## INTRODUCTION

---

## 1.1 Introduction

When humanity expands its horizons to the Moon and other planets in the solar system the utilization of the in situ space resources will become imperative due to the high cost of re-supplying from the Earth. It will be impossible to establish self-sufficient settlements on other planets without making extensive use of the indigenous resources. The Earth sits in a deep gravity well; it requires considerable energy and money to escape the Earth's gravity - a rocket velocity of 9.2 Km/s just to reach the low Earth orbit at a cost of about \$10000/Kg. It takes an additional 5.6 Km /s to land on the Lunar surface and about 8.5 Km/s to land on the surface of Mars (Jeffery, G.T. *et al.* 2003). Clearly it will be essential to use the local materials when building large economically and physically self-sufficient space settlements. A NASA study for the need of space resources concluded that near Earth resources can not only foster the growth of activities in space, but are essential to any long-term space activities.

Moon and Mars are the likely places where humans will try to migrate and try to establish a permanent base. It is certain that if mankind is prospecting Moon and Mars, many different branches of engineering like geosciences, geotechnical, mining, mechanical, electrical electronics among others must go along. In the various Lunar or Martian exploration missions, interplanetary transportation becomes highly unproductive in the absence of some insitu mining or production systems. Mars Design Reference Mission (DRM) (Noever, D.A., 1998) calls for insitu production of methane/oxygen propellant for crew's ascent vehicle and surface mobility, as well as the necessary water and life support gases for the crew's entire surface stay

It is certain that if mankind is to migrate to the frontiers of Moon and Mars, mining must go along. We have the responsibility to understand the harsh conditions and operating parameters of this new environment so as to design space-mining equipment that is cost effective, simple and dependable, developed from the existing terrestrial counterparts.

Developing space mining and processing technology is very similar to advancing terrestrial mining and processing technology. However, there are two modifying factors

1. Space logistics and associated economics
2. The environment

The logistics and economic constraints impose limits on the size, weight and power available for the mining equipment in addition to requiring increased simplicity and reliability. The environment on Moon and Mars will greatly influence all aspects of mining on Moon and Mars (Podnieks, E.R., *et al.* 1992).

## **1.2 Motivation and organization of the thesis**

The motivation for the current thesis is a lack of knowledge in the area of mining and mineral processing in space and Canada's commitment to space exploration.

The thesis is organized into two parts; the first part generally focuses on a very broad literature review pertaining to mining in space. Research work done in the area of common mine unit operations like drilling, blasting, excavation, comminution and beneficiation as applied to Moon/Mars has been reviewed. In the second part of the thesis the scope of the project is narrowed down to the exploration of microwave assisted rock breakage for its potential application in space with possible terrestrial applications as well.

From the extensive literature review, it is concluded that an optimal combination of both mechanical methods and novel energy (lasers, microwaves and nuclear energy) methods for rock destruction drawing a trade off between the energy and mass would be the most ideal option for space applications. Novel energy methods have the advantage of being less bulky and are less affected by the environment when compared to conventional mechanical methods of rock destruction. Novel methods are well suited for space because there is no attenuation or dispersion during propagation and remote generators can beam the energy in to work location with minimal loss (Lindroth *et al.*, 1988).

In the present work one such technique of applying microwaves to rocks in order to thermally weaken them without actually melting them before employing mechanical methods is investigated. Use of such methods is precluded on the terrestrial environments because the process becomes uneconomical owing to its energy intensive nature (Kingman *et al.*, 1998, Lauriello, P.J. *et al.*, 1974), however such methods can be beneficial to space applications where there can be a tradeoff between mass and energy. There has not been much work done in studying the effect of low power microwaves on rocks in terms of their temperature response and strength properties.

### **1.3 Thesis objectives**

1. Identify the key technologies that are best suited for Lunar and Martian environments
2. Identify the design issues for developing space-mining equipment as applicable to Moon and Mars.
3. To apply commercially available FEA software ANSYS 7.1 to simulate the thermal effect of microwave radiation on an artificial rock.
4. To experimentally study the susceptibility of the selected rock (basalt) to microwave radiation

### **1.4 Outline of the thesis**

This thesis is divided in to six chapters. Chapter 1 covers a general introduction, aim and motivation for this thesis, as well as the objectives and a short thesis outline for the study.

Chapter 2 covers the broad overview of mining in space with particular focus on Lunar and Martian environment. The chapter reviews the literature that has been developed regarding the issues and technologies feasible for Moon and Mars. The chapter concludes with a summary of work done up till now in the area of Lunar and Martian mining.

Chapter 3 covers the fundamentals of microwave heating and the application of microwaves for rock breakage and identifies the issues associated with microwave application for rock breakage.

Chapter 4 covers the finite element simulation of microwave heating to compute the temperature distribution and thermal stresses in a dielectric rock sample due to microwave exposure. The chapter also covers a finite element simulation for the calculation of electric fields in a dielectric material when exposed to microwave radiation.

Chapter 5 is devoted to the experimental part of the thesis. A description of various experimental apparatus used is given along with the experimental methodology. Sample material used for experimental work and measurement techniques are presented.

Chapter 6 covers the conclusions from the present work and recommendations for the future work.

# CHAPTER 2

## REVIEW OF MINING IN SPACE

---

*This chapter focuses on the literature that been developed over the years in the area of mining in space with particular focus on Lunar and Martian environments. Typical terrestrial mining operations are presented before developing a scenario for Lunar/Martian mining. Various technologies for drilling, blasting, excavation, comminution and beneficiation as applicable to Moon/Mars are reviewed. Key technologies and design issues suitable for Moon/Mars are identified. The chapter is concluded with a summary of the work that has been done till now in the area of mining in space.*

## 2.1 Typical Terrestrial mining operations

The process of terrestrial mining is largely an abstract and ill-defined operation; it has 5 main stages: prospecting, exploration, development, exploitation and reclamation. In the prospecting stage the mineral deposits which are either located at the surface or below the surface are assessed, with the aid of geologic studies, aerial photography, geophysics geochemistry among others. The exploration stage estimates as accurately as possible the size and value of the mineral deposit and helps in making the decision of developing or abandoning the mine. The development stage involves opening up the ore deposit for production, acquire mining rights, construct the infrastructure facilities and excavate the deposit. Exploitation involves large-scale production of the ore employing either surface or underground mining methods or a combination of both. Reclamation, which is the final stage, ensures restoration of the site, monitoring the discharges and removal of plant and buildings (Hartman, H.L., *et al.*, 2002).

Further, irrespective of the mining method employed (surface or underground methods), the mining unit operations remain common, differing only in the scale of operations. The operations that aid exploitation of ore on a large scale are termed as production operations. Usually they are grouped under rock breakage, overburden clearance and material handling. Primary breakage involves drilling and blasting and secondary breakage involves comminution (crushing and grinding). Overburden clearance and material handling involves excavation, loading and haulage.

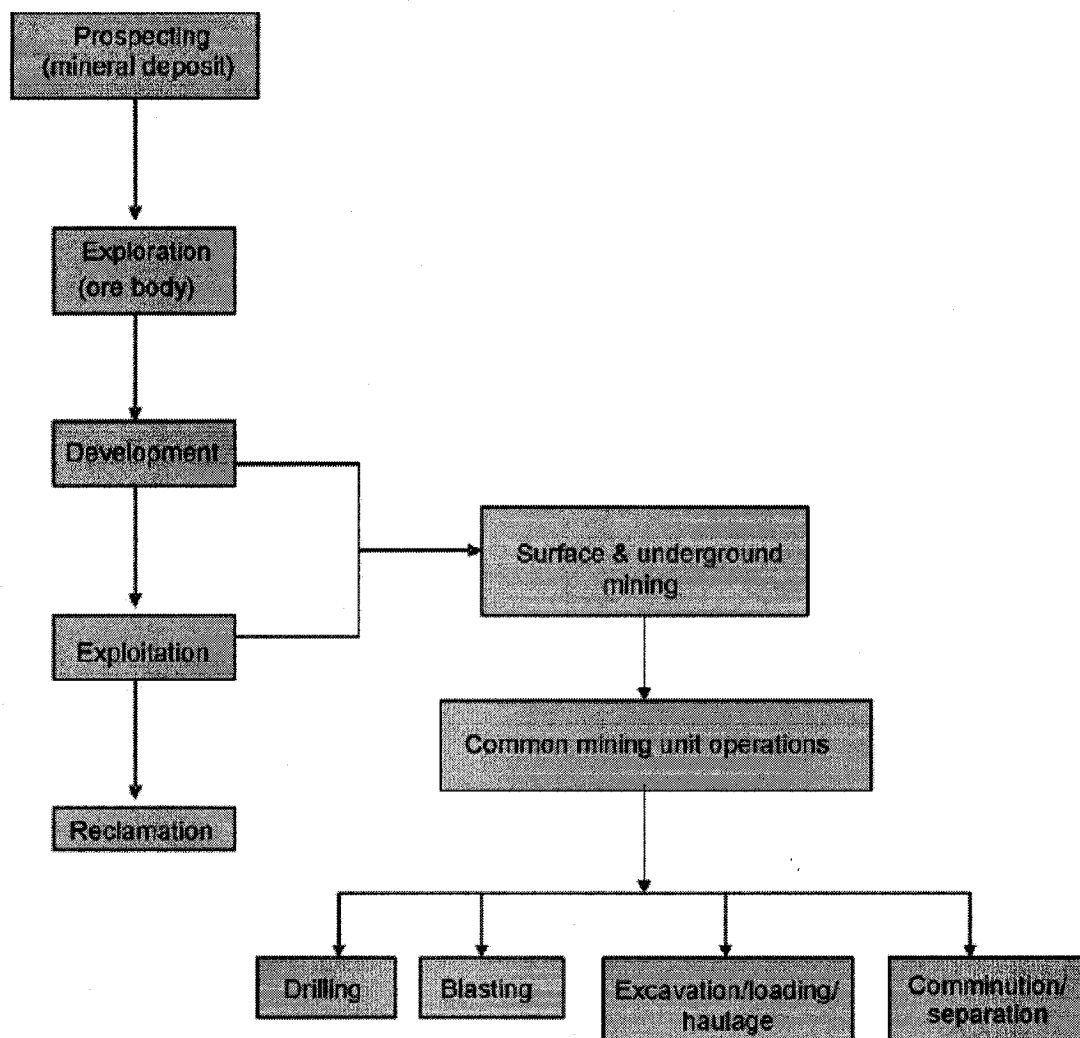


Figure 2.1 Stages in the operation of a mine

## 2.2 Design for Lunar/Martian mining

Before reviewing the scenario for Lunar/Martian mining, it is necessary to define the environment and specify the parameters within which the system must operate.

**Table 2.1 Important design parameters (Horneck *et al.* 2001)**

Parameter	Earth	Moon	Mars
Gravity	1xg	0.166g	0.377g
Diurnal temperature range	10 °C to 20°C (Standard temperature)	-171 °C to 111 °C (Apollo data)	-90 °C to -30 °C (Viking data)
Pressure	1000 mbar	$3 \times 10^{-12}$ mbar	~6mbar
Atmosphere	78.1 % N <sub>2</sub> , 20.9 % O <sub>2</sub> , 0.03% CO <sub>2</sub>	No Significant atmosphere	95.3% CO <sub>2</sub> , 2.7% N <sub>2</sub> , 1.6%Ar, 0.1%O <sub>2</sub>
Length of the day	23h 56' 4. 1"	29.53 Earth days	24h 37' 22. 7"
Escape velocity	40,248 km/h	8,568 km/h	18,072 km/h
Shielding against radiation	1000g/cm <sup>2</sup>	None	16g/cm <sup>2</sup>
Cosmic ionizing radiation	1-2 mSv/a	~0.3Sv/a	0.1-0.2 Sv/a
Solar particle events	Not applicable	Up to ~0.1 Sv/h	Up to 0.4-0.6Sv/h
Others	NA	Lunar surface dust Impact by meteorites and micrometeorites	Martian surface and dust storms

Over the years, a considerable amount of work has been done by the researchers in conceptualizing the idea of mining on Moon and more recently on Mars. In the process, they have come up with some design criteria (listed below) for the equipment during the initial stages of mining machine design for extraterrestrial bodies. (Podnieks, E.R. *et al.*, 1993, Gertsch, R.E. 1990, Lewis, J *et al.*, 1993, Benaroya, H *et al.*, 2002).

1. Low machine mass: Any mining machine that is designed for Moon/Mars cannot be mass intensive because of the high cost of transporting from the deep gravity well of Earth. A trade off should be drawn between the mass and energy requirements of the machine. Novel methods using electromagnetic energies/lasers have to be combined with the conventional mechanical methods so as to reduce the mass of the machine.
2. Operational and design simplicity: The very first machines that are going to be designed for operation on Moon /Mars should be very simple before specialized equipment is used. By keeping the design simple and versatile, the probability of failure decreases and it becomes much easier for any kind of modification/remediation in case of problems in the future.
3. Flexibility: During the early stages of mining on Moon/Mars multipurpose mining machines that can accomplish excavation, loading, hauling, navigation and such other operations should be used. More specialized machines can be employed once the operations become more productive
4. Low energy requirement: The energy requirement should be kept at an optimum level, according to a NASA study, the energy requirement for excavation and transport should not exceed 70KW. Alternative forms of energy sources should be advocated such as fuel cells, solar energy and nuclear energy and insitu H<sub>2</sub>/O<sub>2</sub> generation, for catering to the fuel requirements.
5. Automation and teleoperation potential: Automation of the machines during the early stages of operation is not desirable because it makes the machine more complex and requires high maintenance and loses flexibility. Rather, teleoperation is desirable, wherein the operator can operate the machine remaining in a safe environment. This is more economical than automation and renders the machine more flexible because of the human presence in the control loop.
6. Minimize the need for working fluids: Because of the extremes in pressure and temperature on Moon/Mars, most oils, cooling fluids, greases would outgas, disintegrate or evaporate. Care should be taken while designing the machines for Moon/Mars so as to

develop newer working fluids or alternate methods employing a minimum use of the working fluids.

7. Special attention to the tribology part of the design: All the mining machines depend on some kind of bearings for their motion, power transmission and any other kind of motion. All the bearings that go in to these machines should be specially designed to withstand the abrasive environment, dust and extremes in pressures and temperatures. The design should include redundancy to some extent so that the bearings can perform satisfactorily in case of unexpected emergencies. The seals which would be used serve two purposes, to protect the bearings and to confine the working fluids in their spaces.

8. Special shielding requirement: Special shielding will be necessary for mining machines employed on the surface of Moon/Mars to protect them from the extreme radiation (typically three orders greater than that on Earth) and micro meteoritic bombardment.

9. Availability of advanced fabrication materials: Advanced materials that have high strength to weight ratios, good durability, the ability to withstand the temperature and pressure extremes and the ability to combat radiation influx have to be used for machines operating in Lunar/Martian environments (for e.g. Al-Cu, Al-Ag, Ti, hybrid composites etc). New failure modes such as those due to high velocity micro meteoritic impact, severe thermal loading and pressure variations have to be considered.

10. Long term operation with minimal maintenance: As far as possible, Lunar/Martian mining equipment should be designed to minimize breakdowns. The components should be replaceable, interchangeable and easily accessible. Overall the equipment must be rugged and robust enough to sustain the Lunar/Martian environment with optimal performance.

## 2.3 Space Mining

Resource recovery on Moon/Mars can be done on surface, underground or a combination of both. Initially, the mining operations will be essentially surface based, this means excavating the Lunar/Martian regolith and subjecting it to further processing operations to extract oxygen, hydrogen, iron and other useful building blocks. Underground methods will eventually follow because of the need to provide shelter to humans working and also to combat the hostile environmental conditions on Moon/Mars. Podnieks, E.R. *et al.* (1990), Lewis, J *et al.* (1993) considers the Apollo mission data and ensuing research on the Lunar regolith relevant to mining operations and compares surface mining scenarios and underground operations for Lunar resource utilization. They conclude that shelters are required to provide human habitats and facilities for mine equipment maintenance and repair. The construction process in the near vacuum will be complex, expensive and equipment intensive operation. The structures will have to counter severe tensile stresses caused by the internal pressure of nearly 10000 Kg/m<sup>2</sup>. Considering these factors, it becomes apparent that underground habitats and service facilities provide an excellent alternative to surface structures because the creation of habitable space is combined with mining the resources and diversified equipment required for surface mining, transportation and construction will be reduced.

Further as shown in the figure 2.2, following the stages of a terrestrial mine, irrespective of the mining method used there are some basic operations such as drilling, excavation, blasting, comminution and separation that has been given some thought by many researchers. It is obvious that Earth-based methods cannot be directly applied on Moon/Mars because of the differences in the design parameters as enunciated in table 2.1. Below we concentrate on each of these operations, separately identifying the issues and technologies that would be feasible on Lunar and Martian environments.

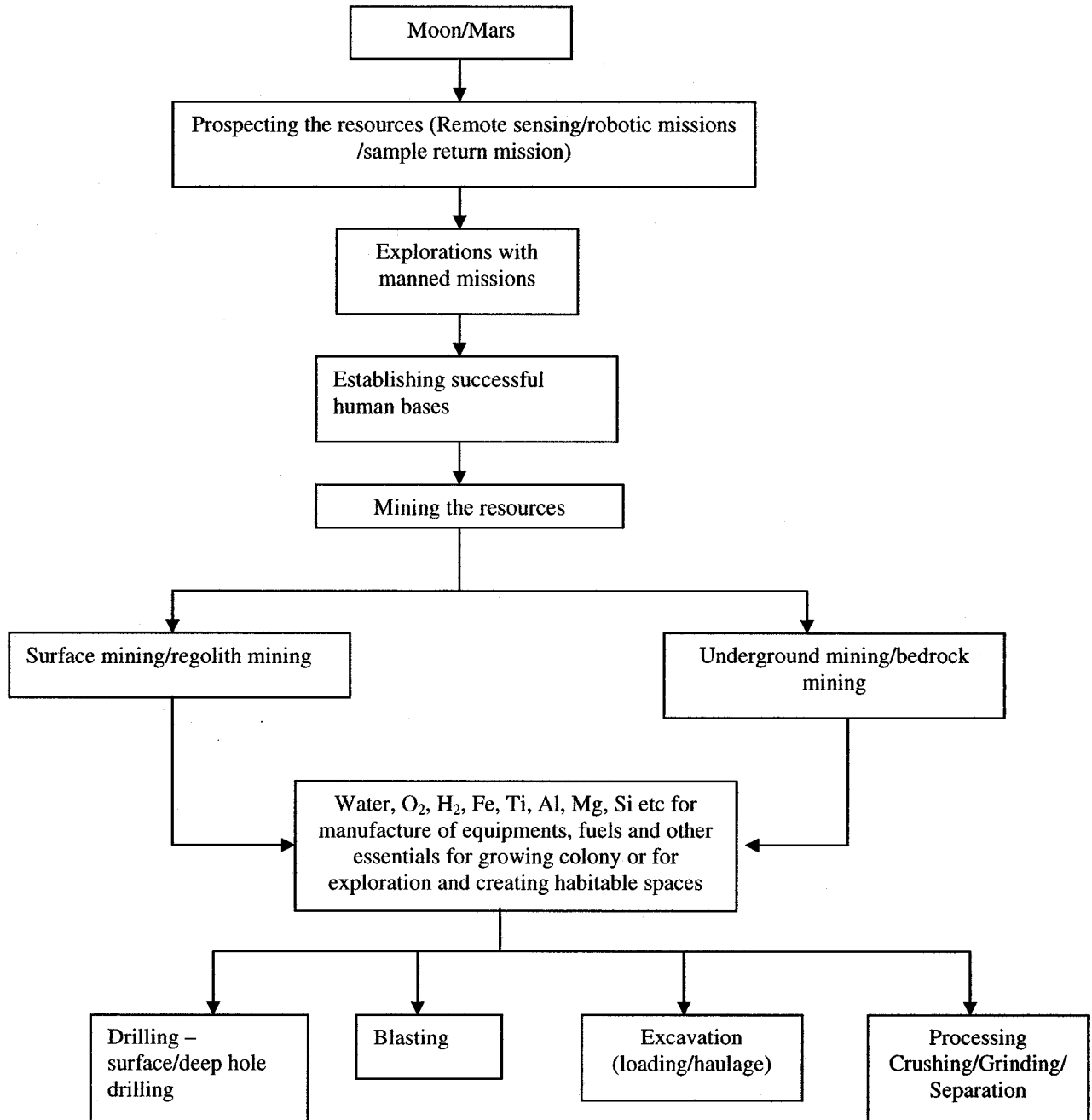


Figure 2.2 Broad picture of mining on Moon/Mars

### 2.3.1 Drilling

Different types of drilling methods are likely to be required on Moon/Mars for the purposes of sample collection, anchoring structures, explosive placement and exploration purposes. Drilling happens to be the first and most important step towards any planetary exploration or mining operation. In the preceding paragraphs we provide a review of the research work that has been done in the area of extraterrestrial drilling.

The idea of drilling on Moon dates back to Apollo mission times. Hughes tool co, USA in 1960 had developed a drilling system to collect samples of the Moon's surface for analysis. The drill system developed was a miniature drill that stood 5ft tall and weighed 60lb and capable of penetrating dust or granite like rock (Anon, 1960). Other technical details pertaining to materials, capacity, cooling and flushing systems are not cited in the publication.

A NASA sponsored research team (Phillips M, 1971) developed a dry drill system for collecting Lunar rock core samples from depths in excess of 100ft with internal chip cooling and dry chip flushing. Diamond crystals ( $\pm 0.004$  in tolerance) were used for the drill bits. Burns *et al.* (1966) suggest that rotary percussive system is the most favored for Moon drilling, because of the simplicity and following reasons (Rostami, J, 1998):

- Lower energy requirement
- Durability of tools
- High level of reliability
- Ease of transportation and deployment.
- Wealth of knowledge acquired over centuries of using mechanical tools

Blair (1996) reviews the use of fluid based cuttings removal and cooling for Lunar production drilling and technical factors affecting the same. Use of non-reactive fluid (gas or liquid) source, insulated fluid transfer lines and drilling technology based on terrestrial experience is advocated. From Nathan *et al.* (1992) and Klosky (1996) it can be inferred that vibrating penetrator is more efficient than a rotating drill or a penetrator for

Lunar regolith. Significant reduction in forces was observed for very shallow depths operations, however force required to penetrate the regolith increased when digging at greater depths using vibration.

Blacic *et al.* (1986) suggest drilling methods for sampling, emplacing explosives constructions and rapid excavation remote emergency shelters (rocket exhaust drill) on Mars; they are rather straightforward adaptation of terrestrial equipment and procedures. They also advocate the use of compressed CO<sub>2</sub> in Martian atmosphere as the circulating fluid (for cooling and chip removal).

Magnani *et al.* (2004) summarized the major developments being performed by Galileo Avionica with particular reference to the on going deep drill program under Italian space agency, including hardware prototyping and testing, suitable to operate in planetary and cometary environment. The preliminary design of integrated drill systems, both employing a single drill tool or multiple rod assembled during operation, shows their ability to achieve performances in line with resources allowed by a Mars vehicle and feasibility of drill tools to operate in very different types of soils and capable of reliably collecting the samples. Single rod design suitable is for 1m depth and weighs 7.32Kg and multirod design is suitable for 3m depth and weighs 8.3Kg.

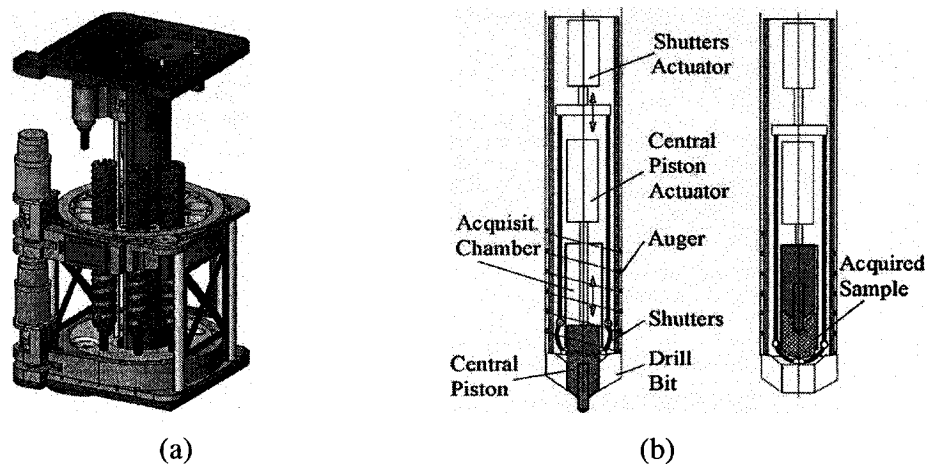


Figure 2.3 (a) Multirod Drill (b) Drill tool schematics (Magnani *et al.*, 2004)

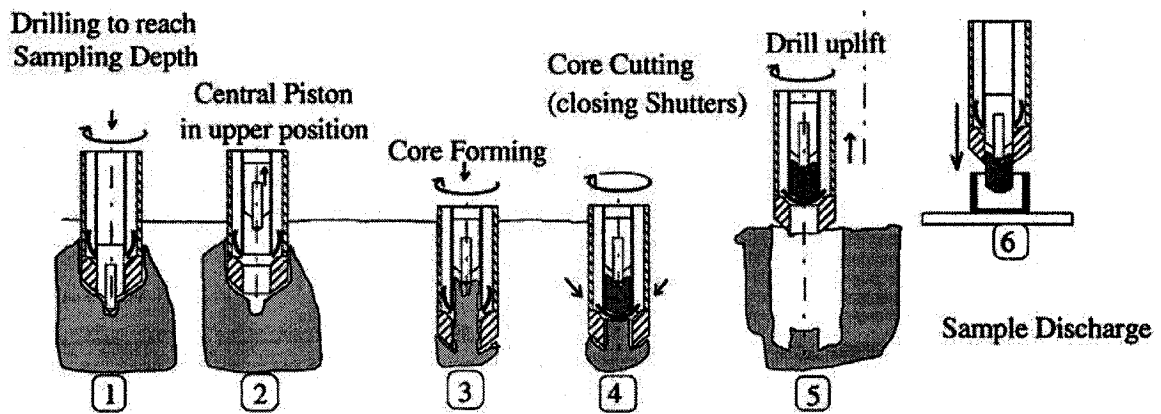


Figure 2.4 Sample collection and discharge sequence (Magnani *et al.*, 2004)

Briggs *et al.* (2003) (a part of NASA's Astrobiology Technology and Instrument Development Program ASTID) are developing a low mass (~20Kg) drill that will be operated without drilling fluids and at very low power levels (~60W electrical) to access and retrieve samples from permafrost regions of Earth and Mars. The drill designed and built as a joint effort by NASA Johnson Space Center and Baker Hughes incorporated takes the form of a down hole unit attached to a cable so that it can be scaled readily to reach significant depths (figure 2.5).

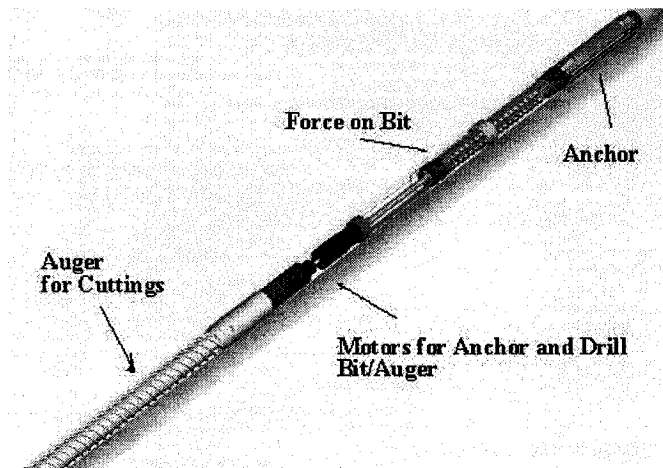


Figure 2.5 Bottom Hole assembly (Briggs *et al.*, 2003)

Briggs.G.A. *et al.* (2002) discuss the technical challenges of deep drilling on Mars. They also emphasize geological and biological motivations of drilling on Mars as well as the technologies required to successfully reach greater depths (see Table 2.2).

An alternative to the standard drilling procedure is to gain access to the Martian deep subsurface by melting the surrounding rock. This technology eliminates the need for casing material, drilling fluids and drill bit replacement. This technique employs an electrically heated probe that melts the rock moving downward from a small-applied force and gravity. The borehole is lined with glass created by resolidified rock melt obviating the need for casing. Three bits have been used in preliminary testing—consolidating, extruding and coring (Mancinelli, R.L., 2000), however, this technology is still in the developmental stage and it has to be properly authenticated on terrestrial environment to further facilitate its use on Mars.

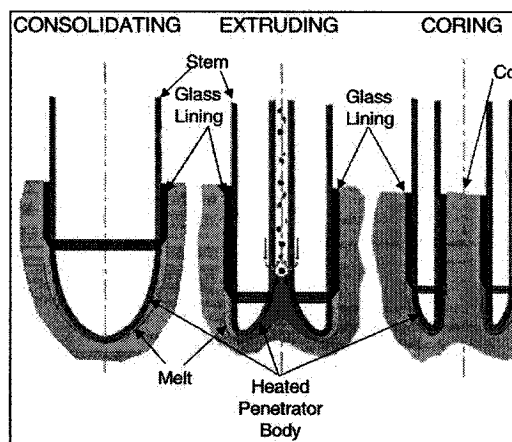


Figure 2.6 Rock Melting bits (Mancinelli, RL, 2000)

In addition to penetration by melting, novel drilling techniques like thermal spalling, vaporization drills and chemical drills (Maurer, 1968, Poirier *et al.* 2003) can also be used for Moon/Mars penetration projects. The use of these novel techniques is precluded on the terrestrial environment because of their energy intensive nature, however on Moon/Mars they can be used because they are lighter, can be easily automated and obviates the use of drilling fluids

Hill *et al.* (2003) present the basic concept of tethered down hole motor drilling, as it might be developed to work with a broad range of available basic down hole drilling equipment. This system includes a revolutionary new bit system that drilled an 80mm diameter hole in medium strength sandstone to a depth of 2m at a total power consumption that is five times less than the conventional drilling methods.

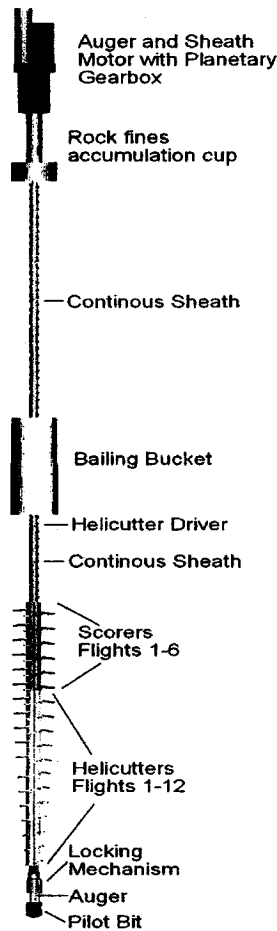
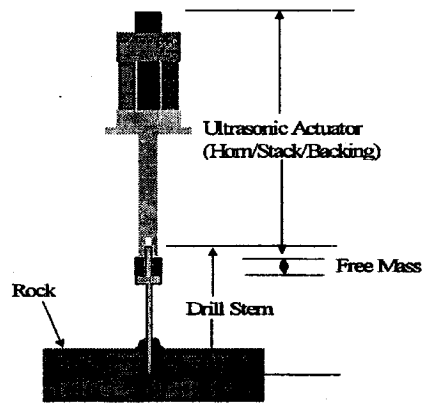


Figure 2.7 Self contained down hole drilling system (Hill *et al.*, 2003)

Cohen *et al.* (2001) have developed an Ultrasonic Driller/Corer (USDC) to address the problem of drilling on extraterrestrial bodies. The USDC is based on an ultrasonic horn that is driven by a piezoelectric stack; the device weighs 450g, requires low preload (<5N) and can be driven at low power (5W). It has been shown to drill various rocks including granite, diorite, basalt and limestone. The USDC can be used to accomplish sampling, insitu probing and analysis.



**Figure 2.8 Ultrasonic Driller/Corer (Cohen *et al.*, 2001)**

Peeters, M., *et al.* (2000) reviewed oil industry drilling and geophysical bore hole techniques that could be adopted for space applications. Coiled tubing drilling has many advantages because the surface facilities are compact, and an electrical cable in tubing can transmit power and data. If kevlar is used for the coiled tubing, laser beam could be transmitted via optic fibers in the coiled tubing wall. Using this beam to cut the rock would virtually eliminate the mud and down hole motor requirements, and save a lot of weight.

Finzi *et al.* (2004) present a method of modeling a drilling process to be carried on in the space by a dedicated payload. The interaction between the soil and the tool has been modeled using the 2D Nishimatsu's theory for rock cutting for rotation perforation tools. The numerical model was validated with the experimental results by considering the Deep Dri system (described earlier) as the reference tool.

A lot of research has been done in testing the prototype drills developed by many agencies on the harsh Moon/Mars like environment on Earth or simulated harsh environments, prime among them are the testing of a low mass drill (ASTID) in the permafrost regions of Northern Canada (Briggs, G.A *et al.*, 2003), simulated drilling project by ESA and NASA for future Mars missions at the Tinto river in Spain (Fernandez *et al.* 2004). MARTE, an experimental system for drilling simulated Lunar rock in ultra high vacuum by the US Bureau of Mines (Roepke, 1975).

**Table 2.2 Candidate planetary drilling technologies**  
 (Briggs .GA, 2002,Blacic. J, 2000)

Drilling method	Rock and soil comminution	Drill conveyance
Percussion drills	Mechanical rotary/percussion	T &C Drill Steel
Cable deployed drills	Mechanical percussion	Umbilical sand line
Rotary drills	Mechanical Rotary	T &C drill Steel
Down hole motor and rotary hammer drills	Mechanical rotary/percussion	Continuous tubing
Piercing soil drills	Local formation compaction	T&C push rods
Overburden drilling systems	Coring, local compaction erosion	Special piercing casing
Subterranean moles	Local formation compaction	Self propelled mole/umbilical
Jet and cavitations drills	Hydraulic impact /Erosion	Continuous tubing with utilities
Thermal spallation drills	Thermal stress spallation	Continuous tubing with utilities
Rock melting drills	Thermal fusion	Continuous tubing with utilities

**Table 2.3 Applicability of various drilling methods in Lunar environment**

Method	Basis	Advantages	Disadvantages	Applicability
Mechanical	Mechanical breakage of rock	Demonstrated application on Earth, versatile, simple and ease of operation	Power intensive, bulky, wear of drill tools	Medium
High pressure fluid drilling	Fluidized breakage of Rock (fluid medium-water)	Demonstrated applicability for soft rock mining (coal mining)	Involves use of a fluid, cannot be used for very hard rocks	Low
Thermal/Microwave drilling	Spalling of the rocks	Less bulky, demonstrated applicability, no fluids, no moving components, no wear	Power intensive, new technology, expensive	High
Nuclear drilling	Nuclear fission Nuclear fusion	Conceptual stage	Conceptual stage	Medium

### 2.3.2 Blasting

Rock blasting is the breakage function carried out on a large scale to fragment masses of rock when large-scale production or construction operations have to be undertaken. Based on the way energy is applied to fragment the rock, the process can be either chemical or electrical. Electrical fracturing of rock has been used sparingly for secondary breakage of boulders in surface mines on Earth. However, blasting using chemical explosives has wide spread application for all consolidated material in both surface and underground mining on Earth.

Extensive research has been done in the area of use of explosives on Lunar environment. The projects such as research for Lunar seismic experiments conducted by the Naval Ordnance Laboratory (NOL), the Stanford research institute's study of the expansion of detonation products in vacuum, the bureau of mines study on the use of explosives in

vacuum, the air force institute of technology's research in various vacuums and gravities, Martin Marietta's study to determine explosive and pyrotechnic stability in space and of sterilization are of prime importance. The following important conclusions can be drawn from these works: 1) HNS/Teflon explosive developed by NOL was successfully used for Lunar seismic experiments during the Apollo 16 flights to Moon (HNS/Teflon has the detonation velocity of TNT and is capable of sustaining the harsh Lunar conditions). 2) Crater dimensions produced by the explosives in the simulated Lunar gravity and vacuum were greater than that achieved in terrestrial environment. 3) Accidental detonation due to micrometeorite impact will not be a problem and only limited particles due to detonation would achieve the Lunar orbit (Watson, 1988). Some of the other candidate explosives other than HNS/Teflon that can be used in space are DATB, ALD, LX04, ALX, ALH, MFH and ALOX (Joachim, 1988).

An excavation research program has shown that small-scale explosives blasting in a Lunar soil simulant will greatly reduce the digging forces required for scoop and dragline excavators. Some crater blasting parameters were determined for the Lunar soil simulant at one Earth gravity and at 10 Earth gravities using a centrifuge. The size of the craters produced at 10-Earth g's matched those formed at 1g by scaling according to the weight of the explosive. These data can be applied to explosive excavation problems such as habitat construction, burial of nuclear power sources and rapid construction of shelters remote from the main base to shield against solar flare activity (Goodings, D.J., 1992, Dick, D.R., 1992). Joachim (1988) compares the space drill developed by NASA and directed energy charge devices (explosively formed penetrators) for emplacement hole formation and comes to the conclusion that the later appears to be better of the two.

Cox (2000) has used the prediction equations used to design blasting patterns on Earth and modified it to account for the reduced gravity on Moon and used the same to plan blasting operations for Lunar rock excavation. These resulting equations predicted specific explosive charge of  $0.04 \text{ kg/m}^3$  for soft rocks and  $0.12 \text{ kg/m}^3$  for hard rocks. Also explosive quantity ranging from 0.002 to 0.005 Kg/Kg of water is estimated to produce water on Moon from hydrous Lunar rock (1% water).

Apart from chemical explosives the technique of electrical blasting was also extensively investigated for terrestrial conditions in mining industry for a number of years, however its use on Earth is precluded because of the high-energy consumption. But this blasting technique using electricity has tremendous advantage for space industry in reducing drastically the payload and eliminating the transport and handling of potentially hazardous substances such as chemical explosives with detonating devices. Noranda's plasma blasting technology has these characteristics. It is based on the fast discharge of stored electrical energy into a small amount of electrolyte, suitably located in the rock. This transfer of energy to the electrolyte is accomplished through a coaxial blasting electrode, which in turn is suitably coupled to a capacitor bank. Under these conditions the electrolyte quickly turns in to a high temperature high-pressure plasma, which induces shockwaves producing stress fields inside the rock accomplishing the breaking process. But electrodes are destroyed, which makes the costs excessive when new electrodes must be used each time (Nantel, J., 1996, Hamelin *et al.*, 1993).

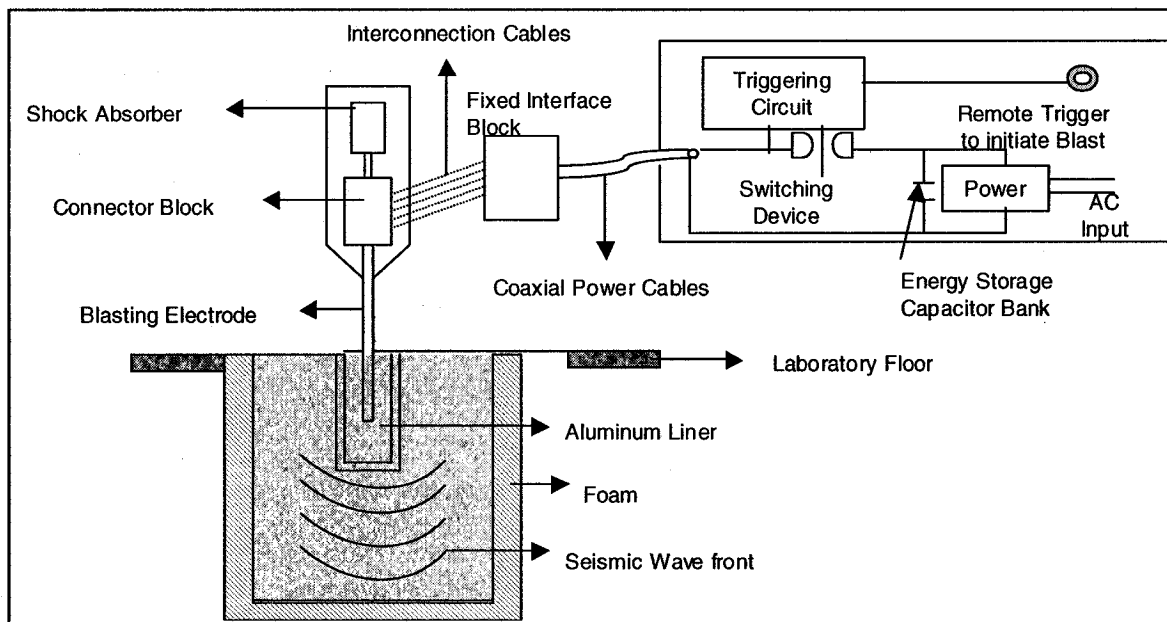


Figure 2.9 Plasma blasting system (Hamelin, M. *et al.*, 1996)

**Table 2.4 Applicability of blasting methods in Lunar/Martian environment**

Method	Basis	Advantages	Disadvantages	Applicability
Chemical blasting	Chemical explosive (high velocity exothermic reaction-liberation of gases at tremendous pressure)	Very versatile, economic Large amounts of energy release accomplished	Large amount of gaseous discharge-poses problem in extreme Lunar vacuum Sensitivity, storage, transportation of the explosives	Low/medium
Electrical Blasting	Use of electricity (electro hydraulic effect to fracture rock)	Discharge generates small quantities of gas, low energy process requires less energy to remove the fragmented rock after impact,	High cost due to electrode consumption Electrolyte stability might be a problem in the harsh environment	High

### 2.3.3 Excavation

Early space mining activities will involve excavating the Lunar/Martian regolith for resource extraction and various other construction and anchoring purposes. Numerous researchers have proposed excavation/mining methods for their use on Moon. This is because of its proximity to Earth, nevertheless similar methods could be applied on the Martian surface as well because of the fact that Lunar environment is much more hostile than the Martian environment. As mentioned previously the mining activities can be surface, underground or a combination of both, one can't arrive at a method conclusively. Lot of issues like mass constraint, power constraint, exact mission objectives, thorough understanding of the composition and nature of Lunar/Martian surface have to be resolved. The brief review provided below could be a stepping-stone for developing mining machines that can operate in the hostile outer space environment and still achieve their objective.

Podnieks, E.R. *et al.* (1992) present the results of a NASA sponsored assessment of the various proposed Lunar mining surface mining equipment. Based on this assessment, two pieces of mining equipment were conceptualized by the bureau for surface mining operations: ripper excavator loader (REL), also capable of operating as a load-haul dump vehicle and haulage vehicle (HV), capable of transporting feedstock from pit, liquid oxygen containers from the processing plant and materials during construction. The general findings indicate that reliable and durable Lunar mining equipment is best developed by the evolution of proven terrestrial technology adapted to the Lunar environment. Podnieks, E.R. *et al.* (1993) examine some of the equipment, like the REL and HV which were previously proposed in addition to the teleoperated mine firefighting vehicle (which represents a present day application of advanced electronics technology to protect the miner), radial axial rock splitter-used on Earth for secondary breakage, generates tensile breaking force by pulsing against its own anchoring system requiring no external thrust, well suited for low gravity since it does not require large external reaction forces and teleoperated compact load-haul dump or minimucker

Gertsch, L.E. *et al.* (1990) analyzed three terrestrial surface mining systems: truck and loader, dragline and continuous miner - to determine how well they meet the design criteria derived from the unusual conditions on the Lunar surface. Hall, R.A. *et al.* (1992) address the issue of functional flow of Lunar surface mining right from the preparation phase to operation phase (not from a technical perspective but rather a conceptual perspective). The paper also addresses the conceptual design of a relocatable mining system; it is based on the equipment that is currently in use on Earth. Gertsch, R.E. (1983) present a conceptual design of a Lunar strip mining system known as three drum cableway scraper-bucket or slusher, selected for its simplification, it lessens the project startup problems, eliminates low 'g' traction dependency, lowers lift weight and lowers capital and operating costs without sacrificing production flexibility.

Bernold (1991) describes the result of experiments that were developed to evaluate empirically, if and how soil could be excavated on the Moon and Mars. The goal of the present study was rather to establish a sound knowledge base to use for more detailed

studies needed to design an operational system that will be successful on the Moon and Mars. It is demonstrated that this problem needs special attention and the study shows that traditional excavation below 20cm is extremely difficult due to the high density of Lunar soil; the existence of large boulders could further complicate the problem.

Boles, W.W. *et al.* (1997) present results of experiments that provide bounds for excavation technology for Lunar regolith, the following important notions are drawn, first a fractional reduction in gravity does not mean that a corresponding and a similar fractional reduction in digging force will occur. In fact, a somewhat lesser effect on digging force is observed as compared to the fractional reduction in the gravity. The optimal conditions for maximum soil matrix fragmentation are a densely compacted soil matrix, a downward trajectory and a steep blade angle. Finally the authors conclude that material, blade configurations nonlinearities need further research.

Lewis *et al.* (1993) as a first step give a review of some technologies that can be used for underground and surface mining activities in outer space (see Tables 2.5 and 2.6).

Apart from the mechanical methods for rock fragmentation and excavation US bureau of mines has conducted preliminary research on fragmenting terrestrial basalts using laser, microwave and solar energy under atmospheric and vacuum conditions. The results of the experiments are very promising indicating that rock fragmented due to thermal stresses and that the vacuum had a positive effect on rock disintegration by these unconventional forms of energy (Lindroth D.P., *et al.*, 1988).

**Table 2.5 Alternate excavation and haulage (for surface mining) methods for space**  
 (Lewis *et al.* 1993, Schrunck, D *et al.* 1999)

Excavation method	Haulage Method
Front end loader	Conveyor system
Clamshell	Cable tram
Dozer	Rail tram
Continuous drum type mining machine	Pipeline
Scraper	Magnetically levitated containers
Slusher	Ballistic throwing
Backhoe	Electrostatic transport
Bucket wheel excavator	
Dragline	
Explosive casting	
Auger	
Rotating brush	

**Table 2.6 Applicability of under ground mining methods to Lunar and Martian Environment (Lewis *et al.* 1993)**

Mining system	Operation	Advantages and disadvantages	Applicability
TBM's (Tunnel Boring Machines)	Developed for terrestrial applications requiring long straight tunnels such as railway tunnels. Machines are rather inflexible and massive	High mass and inflexible	Low
Drum type continuous miners	Developed for mining coal, can mine soft to medium hard material (200-700mt/hr).	High power requirement and dependence on machine weight to counteract cutting forces.	Low
Road header	Originally intended to enlarge access headings in coalmines. The main attraction is the boom mounted cutter head.	Dependence on machine weight to counteract cutting forces	Medium
Hydraulic Rock Splitter	Used on Earth for secondary breakage, generates tensile breaking force by pulsing against its own anchoring system requiring no external thrust	Requires no external thrust, low power requirement	High
Novel methods	Such methods are mainly energy intensive, include thermal fragmentation with electromagnetic energy in the form microwaves /Lasers	High-energy requirement, low mass and less massive.	High

### 2.3.4 Comminution, classification and beneficiation

The Lunar and Martian surface is composed primarily of a loose, fine grained material known as regolith. The formation of regolith has resulted from the breakup of surface rocks by mostly small meteoritic impacts. The largely unconsolidated nature of the Lunar regolith makes it the material of choice for most processes, but certain schemes for oxygen production (ilmenite reduction by hydrogen) requires sizing, possible grinding and beneficiation.

Mason (1992) addresses the applicability of terrestrial based comminution (particle grinding and sizing) and beneficiation equipment for their use in the Lunar environment. Classification techniques (screening, settling, cyclonic and pneumatic), grinding operations (tumbling, fluid energy, impact and ultrasonic mills) and beneficiation techniques (magnetic and electrostatic) are assessed for their use on Lunar surface. The question of optimal source material (rock or regolith) is also addressed. Of the equipments surveyed, screens, ultrasonic grinding mills and magnetic and electrostatic separators are the most applicable for their use on Lunar surface. Mason (1992) also suggests a conceptual design of a complete Lunar beneficiation and comminution circuit for a liquid oxygen plant.

**Table 2.7 Candidate screening, comminution and beneficiation methods as applied to Moon/Mars (Mason, 1992)**

Method	Basis	Advantages	Disadvantages	Applicability
Screening (classification)	Physical separation	Dry, no fluids	Reduced gravity	High
Ultrasonic mill (comminution)	Ultrasonic compression	High through put High efficiency, no fluids, narrow size dist produced	Immature technology	High
Magnetic (beneficiation)	Paramagnetic particle properties	Demonstrated application independent of particle size	Power intensive	High
Electrostatic (beneficiation)	Dielectric particle properties	Demonstrated applicability, low power	Non specific, works best with narrow size distribution	High

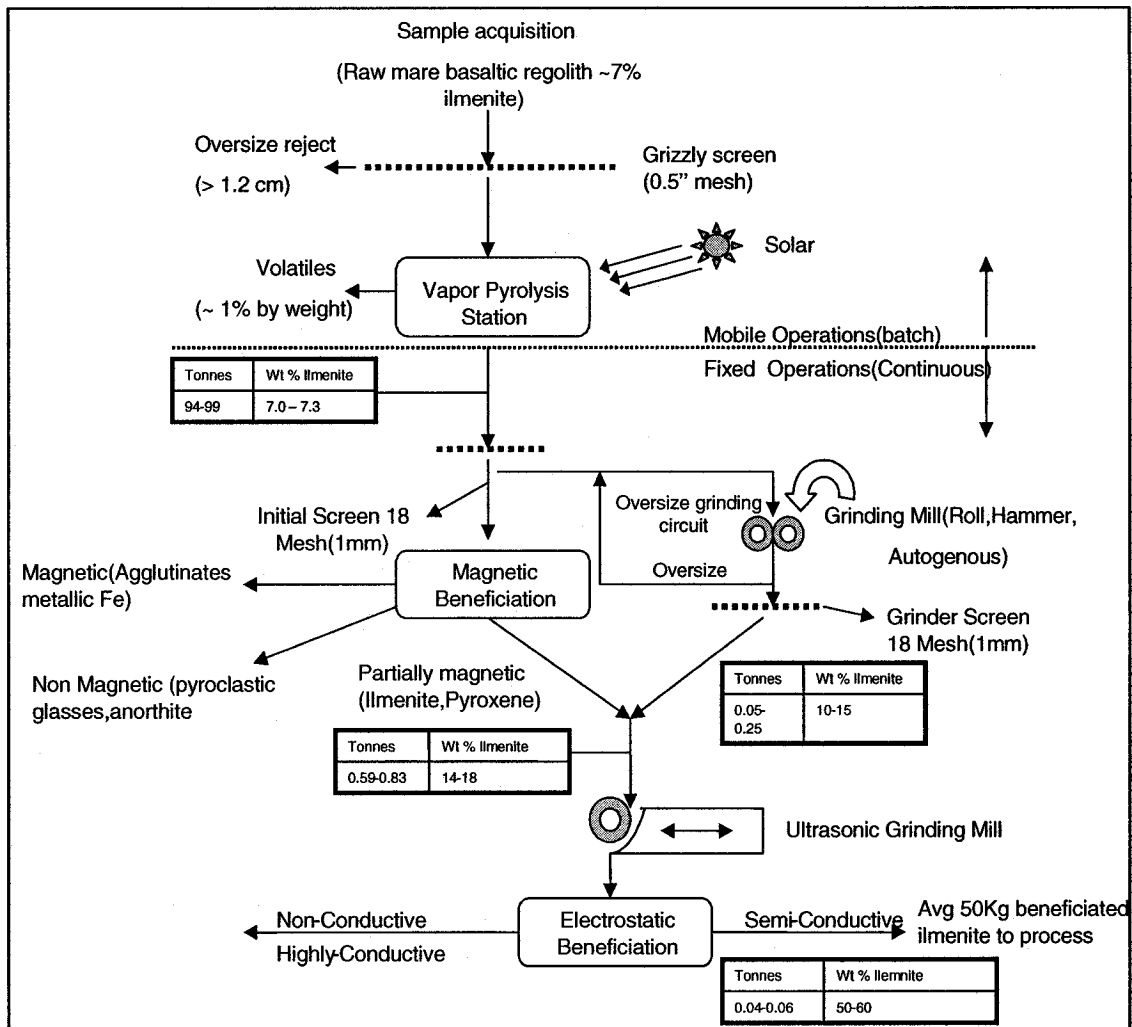


Figure 2.10 Lunar Comminution and beneficiation circuit (Mason, 1992)

However, it can be inferred from the review, that not much work has been done on looking in to beneficiation, comminution and classification for Martian surface as the chemistry and composition of its surface is largely undetermined, nevertheless except for its distance from the Earth, Mars is considered much more hospitable than the Moon. Even when it comes to Lunar surface over 20 methods (Taylor, G.F., 2003) have been suggested for oxygen extraction but very little work has been done on the beneficiation, comminution and classification aspect of processing the regolith.

## 2.4 Issues of mining on Moon/Mars

The problem of designing mining equipment for the hostile Lunar/Martian environment is a tough challenge. Understanding the Lunar/Martian environment thoroughly is of paramount importance. The Lunar environment is quite well understood from the wealth of information from the Apollo mission data, however we do not have a good understanding of the Martian environment. Some cursory issues are discussed in the present work, but a more rigorous analysis is necessary for a detailed study.

1. Lunar/Martian dust will hamper the visibility, coat lenses and mirrors, clog moving parts. The Lunar dust consists of pulverized regolith (powder) that is very abrasive and clings to the space suits, robots and all other machinery. The lack of atmosphere on Moon sets up the dust particles at high speeds and long distances, because of the mining operations and exhaust from the launch vehicles that land and take off from the surface (Schrunk, D *et al.*, 1999). The Martian dust on the other hand is not so well understood, but from the numerous satellite pictures it is learnt that there are periodic dust storms that rise high in the atmosphere up to several kilometers obstructing the sunlight. Both Lunar and Martian dusts will be a constant threat to both humans and machines, and its negative impacts should be very well understood before planning any future missions.
2. The low atmospheric pressure and absence of magnetic field on the Moon (near vacuum) and Mars (atmospheric pressure of 600 Pa) means that there won't be any protection from the harmful influx of ionizing radiation of galactic and solar origin. However on Mars it is found that there is an atmospheric shielding of  $16\text{g/cm}^2$  against the harmful radiation, amounting up to a 100 times more radiation doses than that encountered on Earth (Horneck *et al.*, 2001). Low atmospheric pressure will create severe lubrication problems (most lubricants are volatile and will outgas in vacuum), which will prevent component movement and prevent some mechanisms from working. Radiation hazards and micrometeorite

bombardment (velocities up to 20000 Km/hr) calls for the need of automation, teleoperation computer assistance and efficient shielding for all the equipments. High radiation may interfere with the electrical and electronic devices.

3. Tremendous temperature fluctuations on Moon (from  $-150\text{ }^{\circ}\text{C}$  to  $110\text{ }^{\circ}\text{C}$ ) and Mars (from  $-85\text{ }^{\circ}\text{C}$  to  $-5\text{ }^{\circ}\text{C}$ ) will greatly restrict equipment design, especially the material selection part of the design. The equipment will be subjected to significant thermal stresses.
4. Low gravitational force on Moon ( $1.62\text{ m/sec}^2$ ) and Mars ( $3.27\text{ m/sec}^2$ ) presents stability and traction problems that must be overcome.
5. Our knowledge of the material on the Moon/Mars is very limited, consisting information mainly on the surface materials (which is also highly localized) and almost no information on the type and formation about the bedrocks. Therefore a thorough characterization of the soils and rocks on Moon/Mars has to be accomplished before planning any mission.
6. Communication lag between Earth and Moon/Mars has to be accounted for during the design of any mining equipment.
7. The strength of frozen sand can reach up to 10MPa making it extremely difficult to penetrate with conventional tools. It has been previously estimated that ice exists at Lunar poles and just below the Martian surface, excavating frozen regolith on Moon/Mars is obviously a serious concern given the fact that freezing greatly increases the ground strength (Boles *et al.*, 2002).
8. During drilling on Moon or Mars chip removal and cooling the drill bit are source of great problem.

9. There are serious differences between the Earth and Moon/Mars blasting that need to be studied and determined. A few examples are soil density, rock characteristics, gravity differences, lack of oxygen atmosphere and soil and rock temperatures and their possible quenching effects on explosive energy.
  
10. Loaders digging tough or compacted regolith materials will require sufficient weight to anchor them while they perform (Delinois, S.L., 1966). The work of Klosky *et al.* (1998) show that the experiments using helical anchors to provide down force were quite successful and anchors may be necessary for excavating the frozen soil, however such systems become bulky and less agile.
  
11. The problem of vacuum welding will be pronounced on Moon because of the near vacuum conditions, which has to be accounted for during the selection of any mining machine (Delinois, S.L., 1966).

## 2.5 Conclusions

From the brief review carried out here it can be concluded that much of the work done up until now has been mainly focused on Moon because of its proximity to Earth and better understanding of the Lunar surface by a series of Apollo and Luna machines. Of all the operations reviewed in a typical mining scenario extraterrestrial drilling has drawn lot of attention because of its importance in exploration of subsurface, anchorage of structures and production. Most of the research work that has been done till now on the extraterrestrial drilling focuses mainly on exploration, which is only a preliminary part of the mining operations

Chemical explosives have already been used for seismic experiments during the Apollo experiments on Moon, other methods of blasting like the plasma blasting technique seems very promising for their use in space because of the relative advantages it offers over chemical blasting.

Brief thought has been given by researchers in designing comminution beneficiation circuits for Lunar oxygen production plant. Screens, ultrasonic grinding mills and magnetic and electrostatic separators seem to be the most applicable technologies for their use in these kinds of circuits.

Mechanical methods of rock breakage are being suggested by many authors as being the most appropriate given the design constraints of simplicity, flexibility and ruggedness to name only a few. Nevertheless novel methods of rock destruction using electromagnetic energy and lasers are also being investigated for their use in space. Optimal combination of both mechanical methods and novel energy methods for rock destruction drawing a trade off between the energy and mass (payload) would be the most ideal option for space applications

# CHAPTER 3

## MICROWAVE ASSISTED ROCK BREAKAGE

---

*As enunciated in chapter 2, optimal combination of mechanical methods and novel energy methods of rock destruction could prove to be beneficial for space applications in terms of large-scale production drilling or rock removal processes. For the present study one such method of application of microwaves to induce thermal cracks in the rocks prior to use of mechanical methods is investigated with possible space bound and terrestrial applications.*

*This chapter focuses on the basics of microwave heating and also reviews the work that has been done till now in the application of microwaves for rock breakage. The chapter concludes with important issues pertaining to application of microwaves to rock breakage.*

### 3.1 Introduction

Microwave energy is a non-ionizing electromagnetic radiation with frequencies in the range of 300Mhz to 300Ghz. Microwave frequencies include 3 bands: the ultrahigh frequency (UHF: 300MHz to 3GHz), the super high frequency (SHF 3GHz to 30GHz) and extremely high frequency (EHF: 30GHz to 300GHz). It is well known that microwaves have extensive applications in communication. However, the industrial application of microwave heating was suggested in the forties when the magnetron was developed. It was finally implemented in the fifties after the extensive work on material properties. Four microwave frequencies have been designated for industrial, scientific and medical applications (ISMI): 915MHz, 2450MHz, 5800MHz and 22,125MHz (Metaxas *et al.* 1983). When microwaves are studied as a source of energy they are immediately linked to the heating of dielectric materials.

### 3.2 Basic Concepts of Microwave Heating

Microwaves cause molecular motion by migration of ionic species and /or rotation of dipolar species. Microwave heating of a material depends to a great extent on its dissipation 'factor' which is the ratio of the dielectric loss or loss factor to dielectric constant of the material. The dielectric constant is a measure of the ability of the material to retard microwave energy as it passes through: loss factor is a measure of the ability of the material to dissipate energy. In other words, loss factor represents the amount of input microwave energy that is lost in the material by being dissipated as heat. Therefore the material with high loss factor is easily heated by microwave energy (Metaxas *et al.* 1983)

All the materials can be classified into one of the three groups, conductors, insulators and absorbers (Church *et al.*, 1983). Metals in general have high conductivity and are classed as conductors. The microwaves are reflected from the surface of the metals and hence do not heat them. Conductors are often used as conduits (waveguide) for microwaves. Materials, which are transparent to the microwaves, are classed as insulators. Insulators are often used to support the material to be heated. Materials, which are excellent

absorbers of microwave energy, are easily heated and are classed as dielectrics. Figure 3.1 shows these properties (Haque, K.E., 1999).

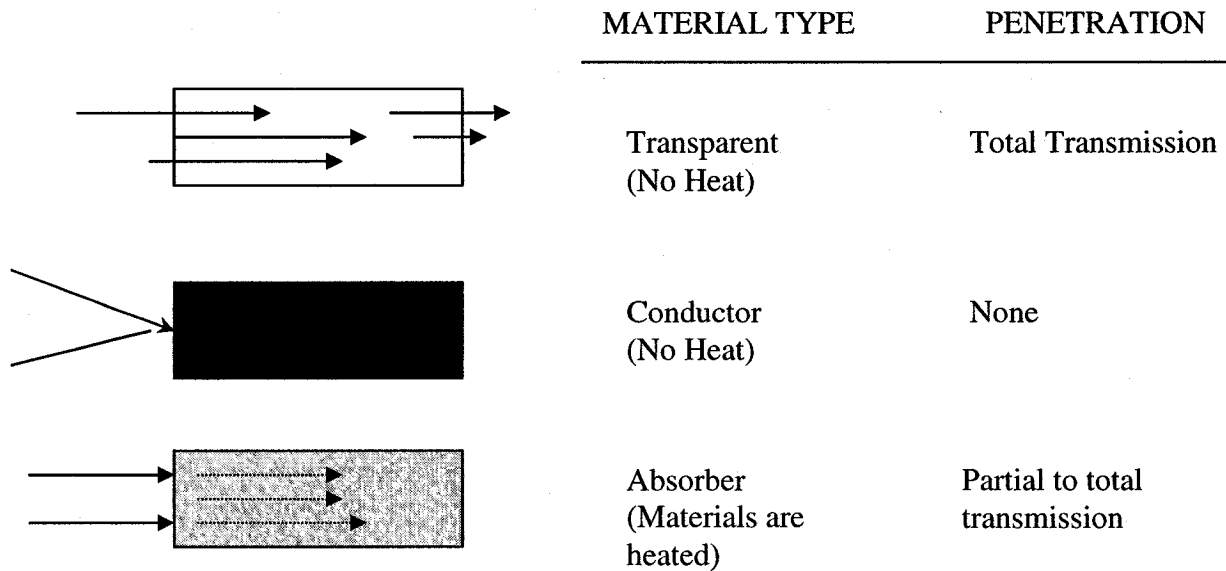


Figure 3.1 Microwave interactions with materials (Haque, K.E., 1999)

Advantages of microwave heating over conventional heating

- Non-contact heating
- Energy transfer and not heat transfer
- Rapid heating
- Material selective heating
- Volumetric heating
- Quick startup and stopping
- Heating starts from the interior of the material body
- High level of safety and automation.

### **3.3 Microwave Heating Equipment**

Microwave equipment for industrial applications consist of three major components: the microwave generator, a waveguide and an applicator. Other Auxiliary devices like the transformer, rectifier and devices such as the circulators and tuners are required for smooth operation of the equipment. The power output of microwave generators ranges from 500W to 10KW at 2450MHz and for a frequency of 915MHz the generator output can be as high as 75KW. At microwave frequencies where the wavelength is comparable with the dimensions of the equipment, waveguides are used to transport the produced microwave power from the generator to the applicator or to the load directly (Sanga, E., 2002).

Microwave generators come in two classes namely the solid-state devices and vacuum tubes. Solid-state devices are expensive and short of power output requirements when compared to vacuum tubes and hence are not used for industrial applications. Vacuum tube generators are of three types namely magnetron, klystron and traveling wave tubes. Magnetrons are the most commonly used microwave generators because of the fact that they are low cost, are compact, are useful for low power devices and have excellent frequency stability (Meredith, 1998).

The most commonly used microwave applicator is the multimode type, for many domestic and industrial applications. This type of applicator has the advantage of being mechanically simple, versatile in being able to accept a wide range of heating loads, although non-uniform heating is a frequently encountered problem. The multimode applicator is essentially a closed metal box with means of coupling microwave power from a generator. The dimensions of such a box are several wavelengths long and at least two dimensions. Such a box will support a large number of resonant modes in a given frequency range. Another type of applicator known as the single mode applicator is used in many branches of engineering whenever very high power densities are required. Essentially a single mode cavity consists of a metallic enclosure into which microwave signal of correct electromagnetic field polarization will undergo multiple reflections. The

superposition of reflected and incident waves gives rise to a standing wave pattern that is very well defined in space. The precise knowledge of electromagnetic field enables the dielectric material to be placed in the position of maximum electric field strength, which in turn helps to achieve the maximum heating. However, such cavities lack the versatility of multimode cavities (Metaxas *et al.*, 1983).

Wave-guides are metallic conduits, which can have either a rectangular or a circular cross section depending on the mode of transmission. For a detailed description of different waveguide types and the different modes supported by them the reader is referred to Meredith *et al.* (1998) and Gandhi, O.P. (1981). Microwave energy conversion efficiency from electricity is between 45 to 50 %. This efficiency includes the losses in converting the AC to DC and DC to microwaves, it also includes the losses associated with waveguide and applicators (Sanga, E, 2002).

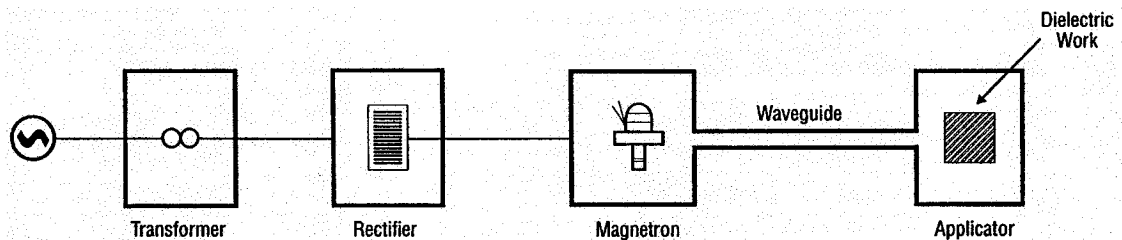


**Figure 3.2 Typical Components of a microwave Heating system (Haque K.E. 1999)**

Also most of the standard microwave heating equipments are instrumented with temperature measurement devices. Nevertheless, continuous measurement of temperature is a major problem in microwave heating. Luxtron fluoroptic or accufibre is used to measure temperatures up to 400°C. Optical pyrometers and thermocouples are used to measure higher temperatures. Optical pyrometers can measure the surface temperature only and metallic thermocouples have the problem of arcing. A recent development is the ultrasonic temperature probe, which covers temperatures of up to 1500 °C (Haque, K.E., 1999)

### 3.4 Research in the use of microwave treatment of mineral ores

In 1978 Zavitsanos obtained a US patent for the desulphurization of coal using microwaves, his was the first recorded attempt to expose minerals to microwave radiation (Kingman *et al.*, 1998). It was not until 1984 that interest was renewed with the publication of the pioneering paper by Chen *et al.* (1984) concerning the relative transparency of minerals to microwave energy (table 3.1).

Walkiewicz *et al.* (1988) completed more detailed, quantitative study of the microwave heating characteristics of various minerals and compounds. The materials selected were irradiated in a 1KW, 2.45 GHz heater and the resulting temperatures and rates of heating determined.

**Table 3.1 Qualitative analysis of microwave heating of minerals (after Chen *et al.*, 1984)**

Mineral	Power (W)	Heating response
Arsenopyrite	80	Heats, some sparking
Bornite	20	Heats readily
Chalcopyrite	15	Heats readily, sulphur fumes
Covellite	100	Difficult to heat
Galena	30	Heats readily with arcing
Pyrite	30	Heats readily; emission of sulphur fumes
Pyrrhotite	50	Heats readily
Cassiterite	40	Heats readily
Hematite	50	Heats readily
Magnetite	30	Heats readily
Monazite	150	Does not heat

Chapter 3  
 Microwave Assisted Rock Breakage

---

From the work of Walkiewicz *et al.* (1988) and Chen *et al.* (1984) the following important conclusions can be drawn:

- Highest temperatures were obtained with carbon and most metal oxides.
- Most metal sulphides heated well but with consistent pattern. Metal powders and some heavy metal halides also heated well.
- Gangue minerals such as quartz, calcite and feldspar did not heat.
- Most silicates, carbonates, sulphates, some oxides and sulphides do not heat so well and their mineral properties remain essentially the same.
- Low lossy materials ( $\text{SiO}_2$ ,  $\text{CaCO}_3$ ) do not heat well at any power levels, high lossy materials ( $\text{PbS}$ ,  $\text{Fe}_3\text{O}_4$ ) heated rapidly at all power levels.

**Table 3.2 Microwave heating of minerals (after Walkiewicz *et al.*, 1988)**

Mineral	Maximum temp (°C)	Time (min)
Albite	69	7
Chalcocite	746	7
Chalcopyrite	920	1
Chromite	155	7
Cinnabar	144	8.5
Galena	956	7
Hematite	182	7
Magnetite	1258	2.75
Marble	74	4.25
Molybdenite	192	7
Orthoclase	67	7
Pyrite	1019	6.75
Pyrrhotite	586	1.75
Quartz	79	7
Sphalerite	88	7
Tetrahedrite	151	7
Zircon	52	7

Kingman *et al.* (2000) exposed massive Norwegian ilmenite ore, massive sulphide ore (from Portugal), highly refractory gold ore from Papua, New Guinea and an open pit carbonatite from South Africa to microwave radiation for varying times and showed reductions in the work index of a particular ore. Ores that have consistent mineralogy and contains a good absorber of microwave radiation in a transparent gangue matrix have demonstrated to be more responsive to microwave treatment. Ores that contain small particles that are finely disseminated in discrete elements are shown to respond poorly to microwave treatment in terms of reductions in required grinding energy.

Kingman *et al.* (2004) elucidated the influence of high electric field strength on copper carbonatite. It has been shown that very short exposure times can lead to significant reductions in ore strength as determined by point load tests. It was shown that reductions in required comminution energy of over 30% could be achieved for microwave energy inputs of less than 1KW h per tonne. Whittles *et al.* (2003) show by their numerical simulation (Finite Difference Time Domain method) that microwave power density is very important in thermally fracturing rocks, and also usage of high microwave power densities for short duration of time reduces the grinding energy requirements.

### **3.5 Use of microwave energy for drilling and excavation of rocks**

*Drilling:* Jerby, E *et al.* (2002) present a drilling method that is based on the phenomenon of local hot spot generation by near field microwave radiation. The microwave drill is implemented by a coaxial near field radiator fed by conventional microwave source. The near field radiator induces the microwave energy into a small volume in the drilled material under its surface and a hot spot evolves in a rapid thermal runaway process. The center electrode of the coaxial radiator itself is then inserted into softened material to form the hole. During this study microwave drills were successfully inserted into a variety of materials including concrete, ceramics, basalt, glass and silicon. The experimental laboratory setup for the drill consisted of standard Richardson's components, including switched power supply for magnetron (0-2KW adjustable), a

2.45GHz magnetron, isolator, reflectometer with incident and reflected power indicators and an EH tuner, the setup also includes a specific transition from WR340 waveguide to the coaxial microwave drill and a chamber in which microwave drill is installed. Typically a 600W microwave drill can penetrate easily into a concrete slab to form a hole of 2mm diameter and 2cm depth within less than a minute.

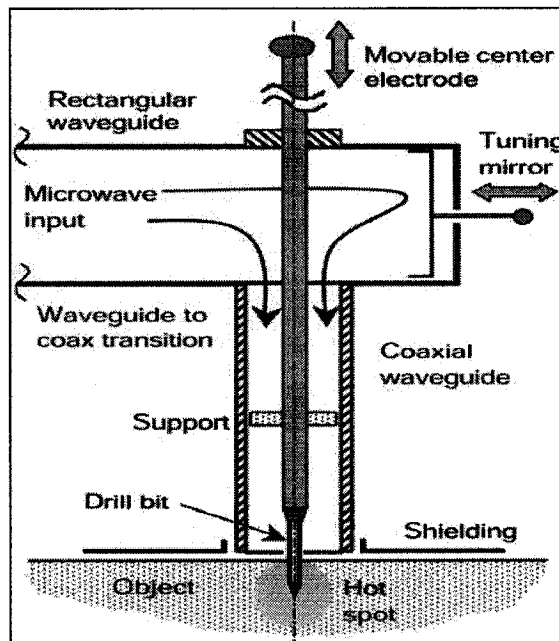


Figure 3.3 Schematic Representation of the Microwave Drill (Jerby, E *et al.*, 2002)

Rock Excavation: Breaking rocks with microwaves is primarily based on inducing stresses by differential thermal expansion. The principle is similar to fire setting technique, which was used from the Bronze Age until the nineteenth century (Santamarina, 1989)

Analytical modeling has been used to a very limited extent to study the breakage of rocks with microwaves. The reason being the large number of variables and phenomena involved (Nekrasov, 1974). Indeed, most studies have been experimental and have primarily taken place in Japan and Russia.

Considerable amount of work has been done in applying microwave radiation alone to rocks like granite, schist, pumice slate and sandstone. The type of applicator used in all

these works was resonant cavities, surface applicators or internal applicators. The power used by various researchers was as high as 100KW with frequency being kept constant at either 2.45GHz or 915MHz. In most of the cases it was observed that hotspots developed varied from a depth of 30mm to 150mm, within 5 to 15 minutes cracks formed and melted material flowed (Santamarina, 1989, Okamoto, R. *et al.* 1982)

The following important observations were made

- As the compressive strength of the rock increases, the rate of advance and the specific energy consumption decreases when electromagnetic waves are used. Opposite is true for the case of mechanical excavation.
- Energy consumption in the electro-thermal method decreases as the cross section increases.
- The rate of advance with the electro-thermal method increases with irradiated power density.

The combination of two or more energy processes has the potential to overcome the fragmentation limitations of separate processes. Researchers in USSR studied the combined use of mechanical and electro-thermal excavation methods for frozen ground, in order to reduce the cutting resistance and combined energy. A prototype was developed using rotary heading machine for hard rock excavation, more than 30m of tunnel were cut, they found that the combined mode resulted in a 250% reduction of cutting tool wear per meter of tunnel (Santamarina, 1989).

Lindroth *et al.* (1993) selected two igneous rocks for their study, namely dresser basalt and St Cloud grey granodiorite for drilling combining both microwave and mechanical methods. The experimental apparatus consisted of a Richmond model AR-16 horizontal boring machine with a 5.4 KW air motor, added to the machine were a double acting hydraulic cylinder to provide a thrust force of 454 Kg and sample holder for testing blocks up to 380mm x 360mm x 200mm thick, a kennametal tungsten carbide, 50mm diameter spade bit (rake 25°, 0.4 radius: clearance +10°, 0.2 radius) was used. During the entire test the drilling parameters were held constant, with variables being microwave power and time of irradiation. Also held constant were the 401 kg drill thrust, rotation of

36rpm and the 1min drilling time. Used for the rock sample heating was a high power microwave generator built by Gulf Radiation technology, providing power up to 25KW at a frequency of 2.45 GHz. All the experiments were performed inside a closed copper screen room used for containing microwave energy.

Microwave assisted rotary drag bit cutting has demonstrated the ability in selected hard rock, to increase dramatically the penetration rate compared to the untreated rock. Penetration rate in granodiorite at 1093°C (2000F) were in excess of three times the rates at 25°C. In addition negligible bit wear was observed. Since bit temperatures remained low, no destruction of the carbide to steel brazing occurred and all the bits remained in good condition.

The cost estimate for a terrestrial road header in hard rock was (bulk heating costs excluded), the cost to mine 0.9 tonne of hard rock was \$5.3 for microwave assisted method and \$8 for the unassisted method.

### **3.6 Issues**

As discussed in the brief literature review, there has been a lot of sporadic work focusing on the combined use of mechanical methods and microwave energy, but there is a need to select the proper frequency and power when the microwave energy is combined with a mechanical system, which requires an optimization analysis that relates numerous variables. Also there is a need to assess the economics of energy when microwaves are combined with mechanical methods of rock removal.

There is a need for evaluating the strength of the rock experimentally after exposure to low power microwaves and characterize its behavior. Much of the work that has been done on the microwave-assisted breakage of rocks used very high power levels (~10-100KW) and such high power levels would render the microwave-assisted breakage uneconomical both in terrestrial and space environments.

Also very little work has been done in the area of numerical modeling of microwave assisted rock breakage. Numerical models able to predict the temperature evolution during microwave treatment of rocks would be very useful tool because of the difficulty in measurement of interior temperature during the process.

Efficient numerical models incorporating the effect of microwave radiation on the rock (modeled with appropriate strength models and compositional features) have to be developed. The models should be able to predict the thermal cracks developed in the rock due to microwave radiation and reduction in the strength of the rock at different power levels.

There is a need for evaluating the most common rock drilling methods, like percussive drilling, rotary drilling and diamond drilling when combined with microwave radiation. Much of the work that has been done either focuses on the large scale excavating machines or comminution circuits (grinding), almost no work has been done to systematically evaluate the effect of microwaves on the penetration rate, tool bit wear, thrust force and other drilling parameters of various common drilling methods as mentioned above. There is a need to relate the drilling parameters that are affected by change in dominant rock properties due to microwave irradiation.

### **3.7 Conclusions**

Chen *et al.* (1984), Walkiewicz *et al.* (1988) have studied the microwave heating characteristics of most common minerals and reagent grade materials. Kingman *et al.* (2000) have demonstrated the increased grinding efficiency after the exposure of ores to microwaves. Also there has been lot of sporadic work in Russia and Japan in using very high power microwaves to destruct the rock by actually melting and blasting it (Santamarina, 1989). Jerby *et al.* (2002) demonstrate the method of penetrating various materials including rocks using focused microwave beams. Lindroth *et al.* (1993) observed considerable improvements in drilling rate after exposing the rocks to high power microwaves.

### Chapter 3

#### Microwave Assisted Rock Breakage

---

Microwaves when used solitarily for the purposes of rock excavation or removal, the process becomes highly energy intensive and hence is rendered uneconomical. However they can be optimally combined with mechanical methods of rock removal. But there hasn't been a systematic approach in optimally combining microwave energy with mechanical methods so that the process is rendered economical.

# CHAPTER 4

## SIMULATION OF MICROWAVE HEATING

---

*Development of efficient numerical models to predict the thermo mechanical behavior of geotechnical materials like rocks and minerals is very useful in terms of understanding the physics of microwave assisted rock breakage.*

*This chapter addresses the basic simulation methodology for estimating the electric field strength in a dielectric load; determine the temperature distribution and thermal stresses in the rock specimen due to continuous low power microwave radiation. These simulations are planned as a precursor for the ensuing experimental studies that is described in chapter 5. The simulation results give a first order indication of how a microwave responsive dielectric material might behave when exposed to microwave power levels within 1000 W within a cavity. However the simulation is not a direct validation of the experiments because of the nonavailability of the properties. The objective was rather to develop a methodology to better understand the physics of the process with a further scope of improvement.*

## 4.1 Introduction to Maxwell's equations

In the nineteenth century, J.C. Maxwell proposed a set of postulates, which related time varying electric and magnetic field quantities. His postulates were based upon the experimental work of Faraday, Ampere and others and were combined into a set of vector equations known as the Maxwell's equation. They are a system of partial differential equations, which are the mathematical basis for modeling electromagnetic phenomena.

Maxwell's equations are

$$\nabla \times \bar{E} = -\partial B / \partial t \quad (4.1)$$

$$\nabla \times H = J + \partial D / \partial t \quad (4.2)$$

$$\nabla \cdot D = \rho_e \quad (4.3)$$

$$\nabla \cdot B = 0 \quad (4.4)$$

Where,

$\bar{E}$  = Electric field intensity (V/m)

H = Magnetic field intensity (A/m)

D = Electric flux density (C/m<sup>2</sup>)

B = Magnetic flux density (We/m<sup>2</sup>)

J = Conduction electric current density (A/m<sup>2</sup>)

$\rho_e$  = Electric charge density (C/m<sup>3</sup>)

These field variables are real vector quantities and vary in space and time. Constitutive relations exist which relate the field variables to the physical properties of the medium.

These equations are

$$D = \epsilon \bar{E} \quad (4.5)$$

$$B = \mu H \quad (4.6)$$

$$J = \sigma \bar{E} \quad (4.7)$$

Where,

$\epsilon$ = Permittivity (F/m)

$\mu$ =Permeability (H/m)

$\sigma$ =Conductivity (S/m)

Maxwell's equations essentially state that if  $\vec{E}$  is changing with time at some point, then H has curl at that point and thus can be considered as forming a small closed loop linking the changing  $\vec{E}$  field. Also, if  $\vec{E}$  is changing with time, then H will in general change with time, although not necessarily the same way. Further, a changing H produces an electric field which forms small closed loops about the H lines, but this changing field is present a small distance away from the point of original disturbance (Hayt, H.W., 1974)

In microwave heating applications, Maxwell's equations are used to find the intensity of the electric fields in the dielectric load, which in turn is used to find the power deposition density into the dielectric load (Smith, J.W., 1999).

#### 4.1.1 Boundary conditions

Maxwell's equations are solved by finding solutions to the fields to match the requirements of the field intensities, which must exist at the boundaries of the structure. The principal boundary conditions are presented below:

The electric field intensity at the surface of the conductor, in a direction parallel to the surface, i.e. grazing the surface is zero. For a perfect conductor there can be no potential difference between two points however great the current flowing.

i.e.  $E_t=0$

However the component of the electric field normal to a conducting surface has in general a nonzero value.

The component of magnetic field normal to a conducting surface is zero because it is not otherwise possible to create a magnetic loop i.e.

$$H_n=0$$

But there can exist a magnetic field grazing the surface of the conductor and can have with it associated surface current.

Third most important boundary condition is that there must be a continuity of displacement current across the boundary between two dielectric regions. This is a particularly important condition in the electro heat because in part it determines the relative values of electric field inside and outside the workload (Meredith, 1998)

## 4.2 Dielectric properties

The complex permittivity of a material defines the interaction of the material with electromagnetic waves. When the complex permittivity is normalized with respect to the constant permittivity of the vacuum  $\epsilon_0$  ( $8.854 \times 10^{-12}$  F/m) it is termed as the complex relative permittivity  $\epsilon_r$ .

$$\epsilon_r = \epsilon' - j\epsilon'' \quad (4.8)$$

$$\tan(\delta) = \epsilon''/\epsilon' \quad (4.9)$$

Where,

$\epsilon_r$  = Complex relative permittivity

$\epsilon'$  = Relative dielectric constant \*

$\epsilon''$  = Relative dielectric loss factor \*

$\tan\delta$  = loss tangent

The relative loss factor combines all forms of losses including polarization and conduction losses. The ratio of the real part to the imaginary part is called the loss tangent

---

\* In the preceding sections  $\epsilon'$  and  $\epsilon''$  will be referred to as dielectric constant and loss factor respectively, omitting the term relative.

and can be used to characterize materials: in a low loss material  $\epsilon''/\epsilon' \ll 1$ , in a high loss material  $\epsilon''/\epsilon' \gg 1$ . The dielectric constant  $\epsilon'$  for rock forming minerals ranges between 3 and about 200, however most values are between 4 and 15, the loss factor  $\epsilon''$  ranges between  $10^{-3}$  and 50 and it is sensitive to frequency and temperature (Santamarina, 1989).

Much of work has been devoted in the past for determining the thermal properties of rock forming minerals, but the data available on the loss tangents and permittivity of important rock types are either inadequate or non existent. Only a few references are available on the dielectric properties of minerals, much of the published data omits the frequency range of 30MHz to 3GHz. It is this frequency range that is of interest, as it includes the 915MHz and 2.45GHz frequency bands allocated for the use in industrial, scientific and medical (ISM) applications. Even when the published data is available it cannot be applied to a particular sample under study unless all parameters (the moisture content, frequency, temperature, composition) have been clearly identified (Church *et al.*, 1988). Dielectric properties of various geotechnical related materials are given in table 4.1

**Table 4.1 Dielectric Constant ( $\epsilon'$ ) and loss factor ( $\epsilon''$ ) for various materials at 3000MHz (Santamrina *et al.*, 1989)**

Material*	$\epsilon'$	$\epsilon''$
Andesite, Hornblende	5.1	0.03
Basalt (9 types)	5.4-9.4	0.08-0.88
Gabbro	7	0.13
Granite	5-5.8	0.3-0.2
Muscovite	5.4	0.0016
Marble	8.7	0.14
Obsedian	5.5-6.6	0.1-0.2
Tuff	2.6-5.8	0.04-0.36
Pumice	2.5	0.03
Sandy Soil Dry	2.55	0.016
Water	76.7	12.04
Ice pure	3.2	0.003

\*The temperature is at 25°C

### 4.3 Dielectric heating equation

Microwave heating involves the conversion of electromagnetic energy into heat. The amount of thermal energy deposited (power density) into a material due to microwave heating is given by the equation

$$P_d = 2\pi f \epsilon_0 \epsilon'' E_i^2 \quad (4.10)$$

Where,

$P_d$  = Power dissipation density ( $W/m^3$ )

$f$  = frequency of Microwave radiation (Hz)

$\epsilon_0$  = Permittivity of free space ( $8.854 \times 10^{-12}$  F/m)

$\epsilon''$  = Relative dielectric loss factor

$E_i$  = Electric field intensity within the dielectric load due to the microwave power (V/m)

Some of the very important features of the dielectric heating equation are (Meredith *et al.*, 1998)

- a. The power density dissipated in the workload is proportional to the frequency, where the other parameters are constant. This means that volume of the workload in the applicator can be reduced as the frequency rises, resulting in a more compact applicator.
- b. The power density is proportional to the loss factor
- c. For a constant power dissipation density the electric field stress  $E_i$  reduces with  $\sqrt{f}$ , this means that, if  $\epsilon''$  remains constant with the frequency, the risk of voltage breakdown reduces as the chosen operating frequency rises. Which makes it desirable to use higher microwave frequencies.
- d.  $\epsilon''$  usually varies with the frequency especially in the materials where dipolar loss dominates. Generally  $\epsilon''$  rises with frequency adding to the effects (a) and (d).
- e. The electric field  $E_i$  is usually not a constant but varies in space depending on the microwave applicators, the dielectric constant of the workload ( $\epsilon'$ ) and the geometry of the workload.
- f. In practice the value of  $\epsilon''$  not only varies with frequency, but also with temperature, moisture content, physical state (solid or liquid) and composition.
- g. It is important to consider both  $\epsilon''$  and  $E_i$  as variables during the microwave heating process.

However, if the material exhibits magnetic losses as well, the permeability of the material attains the complex form similar to the permittivity and term  $2\pi f \mu_0 \mu'' H^2$  will be added to the eqn (4.10) resulting in eqn (4.11), which includes magnetic losses, but for the present study the dielectric losses are considered and magnetic losses are not considered.

$$P_d = 2\pi f \epsilon_0 \epsilon'' E_i^2 + 2\pi f \mu_0 \mu'' H^2 \quad (4.11)$$

## 4.4 Simulation methodology

The microwave heating process was simulated in 3 steps using finite element numerical model: first an electromagnetic analysis is performed to calculate the electric field within the dielectric load, second a transient thermal analysis is conducted to predict the temperature response of the dielectric load and third a stress equilibrium calculation is done to estimate the resulting thermal stresses due to the microwave heating. The finite element analysis software ANSYS 7.1 was used in all the three steps of the simulation.

ANSYS is a general-purpose finite element-analysis package for numerically solving a wide variety of physical problems. These problems include: static/dynamic structural analysis (both linear and non-linear), heat transfer and fluid problems, as well as acoustic and electro-magnetic problems. ANSYS physics environments can be used to solve the coupled field problems like thermal stress problems, coupled solid fluid interaction, coupled electromagnetics and thermal problems just to mention a few.

The simulation methodology followed was similar to that proposed by Salsman *et al.* (1996). However the loading conditions and dimensions for the present study was selected in anticipation of the experiments that is described in chapter 5. Present simulation study has following differences when compared to the previous work of Salsman *et al.* (1996)

- An electromagnetic analysis is performed in order to estimate the electric field intensity within the dielectric load; this methodology can further be extended to the condition when there is only surface exposure of the dielectric load instead of a cavity. However, for the present study the case of dielectric sample in a cavity is considered.
- The microwave power absorption density, which is input as a body load during the thermal analysis, is a function of temperature and the microwave power absorption densities are quantified in terms of the input microwave power.

- Also the input power levels are aimed at much lower levels (~1000 Watts).

#### 4.4.1 High Frequency Electromagnetic analysis

The high frequency electromagnetics module of ANSYS 7.1 is used in the first stage of simulation to find out the electric fields within the dielectric load exposed to microwave power within a cavity. The ANSYS program has a preprocessor, a solver, and a postprocessor. The preprocessor provides facilities for describing the high-frequency structure to be simulated, the excitation to be applied, and the boundary conditions or other constraints to be imposed. The solver generates the element descriptions, assembles the element matrices into global finite element matrices, imposes the appropriate boundary conditions, constraints, and excitation sources, and then solves the equations. The postprocessor provides vector plotting and contour plotting of the cartesian components of the electric and magnetic fields (ANSYS 7.1, Help, 2003)

Geometric modeling: Geometric modeling was done using the ANSYS preprocessor. The geometric primitives used for the modeling process were all volumes, i.e. three-dimensional solids were created for each entity such as the cavity, waveguide and the dielectric load. The solid model in the wire frame form is as shown below

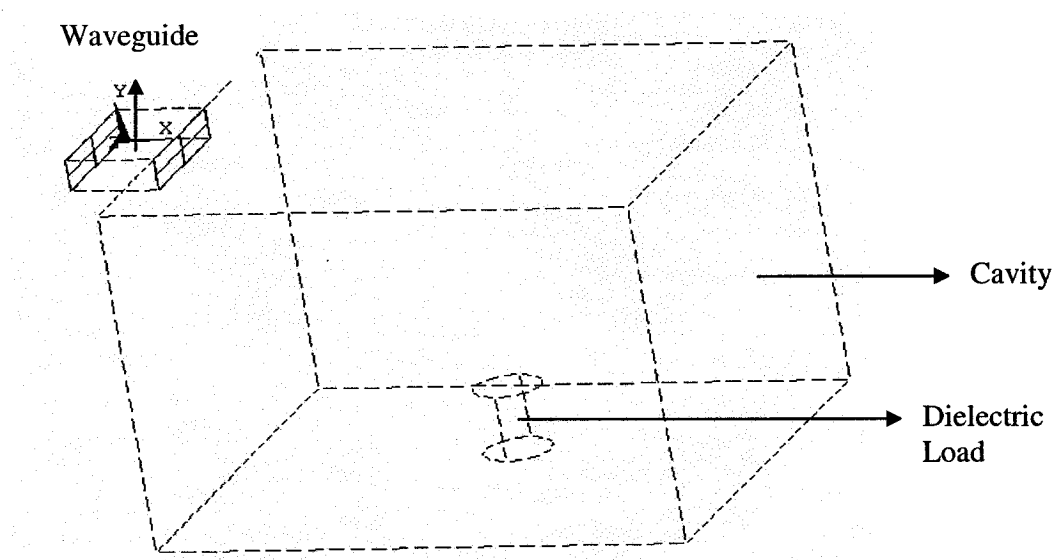


Figure 4.1 Geometric model for the high frequency electromagnetic analysis

**Table 4.2 Dimensions for high frequency electromagnetic analysis**

Entity	Cavity	Waveguide	Dielectric Load
Dimensions (in mm)	267 x 270 x 188	50 x 78 x 18	Diameter = 38.1 Depth = 40

The cavity dimensions and the waveguide dimensions were selected based on the maximum degrees of freedom that could be handled using the university version of ANSYS 7.1 and dimensions of the dielectric load was the same as experimental specimen.

**Mesh Generation:** In this step the above solid model was suitably meshed using the ANSYS mesher options. In particular, for the high frequency electromagnetic analysis the model should have 10 elements per wavelength to obtain accurate results. The elements located at the ports should have as close to a 1:1 aspect ratio as possible in the direction of the wave propagation (ANSY 7.1, Help 2003). The effect of varying the number of elements per wavelength on the maximum electric field intensity is shown in section 4.5.

The element used for generation of the mesh was high frequency tetrahedral 10 noded element (HF 119). HF119 models 3-D electromagnetic fields and waves governed by the full set of Maxwell's equations in linear media. It is based on a full-wave formulation of Maxwell's equations in terms of the time-harmonic electric field (E). This element has one degree of freedom (DOF) i.e. the covariant component of the electric field (Ax). It is defined by up to 10 geometric nodes with Ax DOF on element edges and faces. The physical meaning of the Ax DOF in this element is a projection of the electric field E on edges and faces. Electric field components (Ex, Ey and Ez) and the magnitude of electric field intensity are the solution outputs associated with element (ANSY 7.1, Help 2003).

The material properties for modeling the above entities is given in table 4.3, for the purpose of the analysis the dielectric load selected was as limestone with sulphide mineral (pyrite). This particular rock was selected as the dielectric load because of the

availability of the thermal and electrical properties of the calcite and the pyrite phases of the limestone.

**Table 4.3 Material properties for electromagnetic analysis**

Entity	Relative Permittivity	Relative Permeability	Loss tangent
Cavity	1	1	-
Waveguide	1	1	-
Dielectric load (Calcareous Rock *)	8.4	1	0.0416

\*(Tian, Q.J. *et al.*, 2002)

Boundary conditions and loads: The boundary condition used for the present high frequency electromagnetic analysis was the perfect electric wall boundary condition, i.e. tangential electric field intensity is equal to zero ( $E_t = 0$ ).

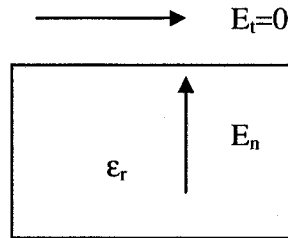


**Figure 4.2 Schematic Representation of the boundary condition**

For the present analysis excitation in the form of a waveguide modal source was used. Here an input port and an output port were defined for the waveguide and the input port was excited with a harmonic frequency of 2450 MHz. Three input power values of 150W, 750W and 1000W were used for the present analysis for excitation source. The microwave excitation powers were selected based on the maximum and minimum powers permitted in the actual experimental setup, which is described in chapter 5.

Finally the finite element model was solved for the harmonic analysis using the sparse direct solver of ANSYS to get the electric field distribution within the dielectric load. However, it has to be noted that this study is mainly concerned with the dielectric losses

at microwave frequencies and hence only electric fields are extracted. If a material exhibits high magnetic loss as well, magnetic fields can also be extracted depending on the permeability of the material.

#### 4.4.2 Transient thermal analysis

A transient thermal analysis was carried out as the next stage of analysis to simulate the temperature profiles for different microwave input power (Salsman *et al.*, 1996).

Because of the fact that calcite has a very low value of dielectric loss factor, microwave heating of the calcite was not included in the model and heating of the pyrite phase was considered (Chen *et al.*, 1983). For the calculation of the microwave power dissipation density of the pyrite phase, the electric fields within the dielectric load obtained from the high frequency electromagnetic analysis and the dielectric loss factor  $\epsilon''$  (figure 4.3) are used.

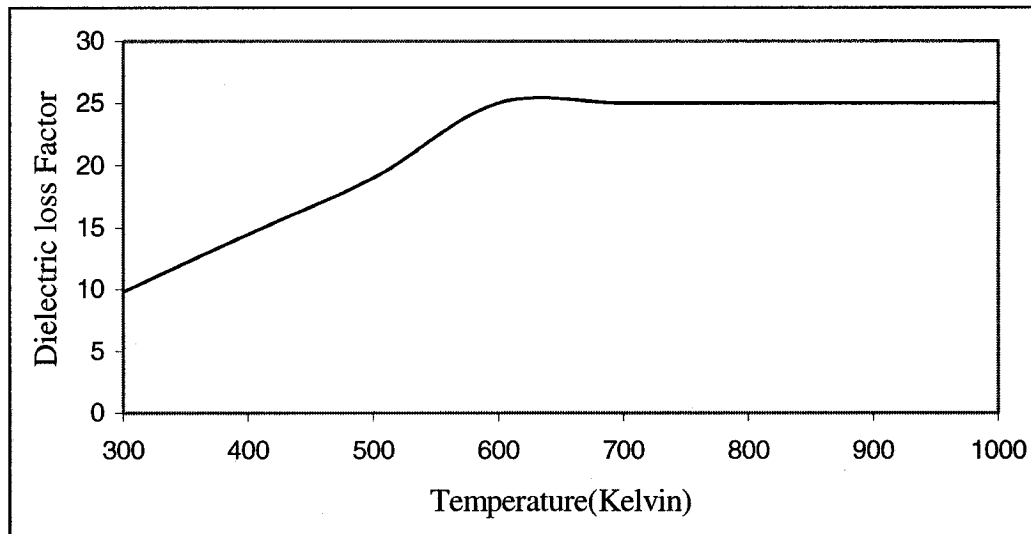
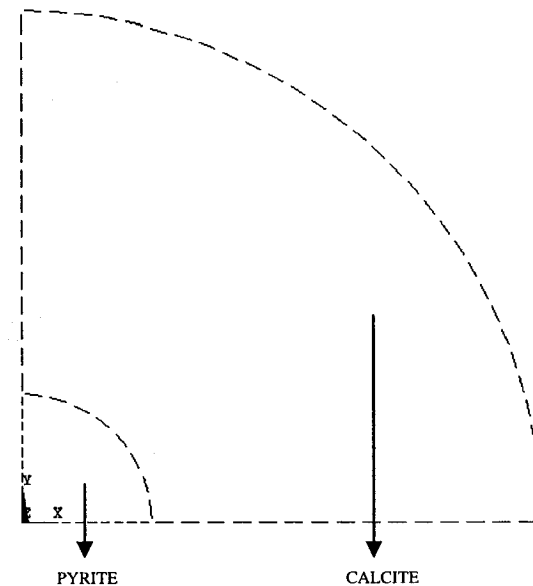


Figure 4.3 Variation of dielectric loss factor with temperature for pyrite (Whittles *et al.*, 2003)

***Geometric modeling:*** The simulation was geometrically and computationally simplified by considering a very small (4mm diameter) hemispherical portion of the cylindrical rock (limestone). A single hemispherical pyrite particle of diameter 1mm was considered, surrounded by a calcite host rock of diameter 4mm. Further, the axial symmetry of the hemisphere allows the modeling in two dimensional domain. Figure 4.4 shows the geometry of the model.



**Figure 4.4 Geometric model for the transient thermal analysis**

***Mesh generation:*** The geometric model was meshed using a 2D thermal element (plane 55) available in the ANSYS element library. In the present analysis this element was used as an axisymmetric ring element with a 2-D thermal conduction capability. The element has four nodes with a single degree of freedom, temperature, at each node. The effect of number of elements on the solution is shown in section 4.5. For the present analysis plane 55 was chosen because it has the axisymmetric capabilities and it can be switched between physics environment of ANSYS for an equivalent structural element (i.e. plane 42). For the present analysis 25 elements per edge was used because of the fact that the model dependency on the mesh is not huge (section 4.5).

The material properties for pyrite and calcite phases as listed below

**Table 4.4 Thermal conductivity as a function of temperature of calcite and pyrite (Whittles *et al.*, 2003)**

Mineral	Thermal Conductivity (W/m K)		
	273K	373K	500K
Calcite	4.02	3.01	2.55
Pyrite	37.90	20.50	17

**Table 4.5 Specific heat capacity as a function of temperature of calcite and pyrite (Whittles *et al.*, 2003)**

Mineral	Specific Heat capacity (J/Kg K)		
	298K	500K	1000K
Calcite	819	1051	1238
Pyrite	517	600	684

**Table 4.6 Density of the mineral phases (Salsman *et al.*, 1996)**

Mineral	Density (kg/m <sup>3</sup> )
Calcite	2680
Pyrite	5018

**Boundary conditions and loads:** The external boundary of the model was assumed to be thermally insulated. Calcite and pyrite were assumed to be perfectly bonded and initially at ambient temperature (Salsman *et al.*, 1996).

The thermal behavior of the model is described by the energy equation (Salsman *et al.*, 1996),

$$\rho C_p (\partial T / \partial t) = 1/r \partial / \partial r (kr \partial T / \partial r) + \partial / \partial z (k \partial T / \partial z) + Pd \quad (4.12)$$

Where,

T = Temperature (Kelvin)

r and z = Spatial co ordinates in (mm)

t = Time (seconds)

$\rho$  = Density (Kg/m<sup>3</sup>)

$C_p$  = Specific heat capacity (J/Kg K)

$K$  = Thermal Conductivity (W/m K)

$P_d$  = Volumetric heat source term due to microwave radiation ( $W/m^3$ ) calculated from eqn (4.10).

Microwave power absorption densities for pyrite at 2450MHz at various temperatures and input microwave powers were calculated. The input microwave power for the present analysis was kept at 150W, 750W and 1000W. The microwave power absorption density as a function of temperature was introduced as a volumetric heat source into the model and the transient temperature field was evaluated for various time intervals.

#### 4.4.3 Estimation of thermal stresses

Thermal stresses due to the differential microwave heating were extracted for various microwave power absorption densities and time intervals. The methodology was fairly simple, the analysis was stepped in to the coupled field mode of ANSYS and the temperature field obtained as a result from the transient thermal analysis was input as the load and the resulting thermal stresses were calculated assuming a linear elastic material model for the pyrite and calcite phases.

The stress-strain relationship to cover the thermal strains and stresses are combined with equations of equilibrium for a isotropic material to predict the thermal response of the model (Timoshenko, S.P., *et al.*, 1970).

$$\varepsilon_{rr} = 1/E\{\sigma_{rr} - \nu(\sigma_{\theta\theta} + \sigma_{zz})\} + \alpha T \quad (4.13)$$

$$\varepsilon_{\theta\theta} = 1/E\{\sigma_{\theta\theta} - \nu(\sigma_{rr} + \sigma_{zz})\} + \alpha T \quad (4.14)$$

$$\varepsilon_{zz} = 1/E\{\sigma_{zz} - \nu(\sigma_{\theta\theta} + \sigma_{rr})\} + \alpha T \quad (4.15)$$

$$\frac{\partial \sigma_{rr}}{\partial r} + \frac{\partial \tau_{rz}}{\partial z} + \frac{(\sigma_{rr} - \sigma_{\theta\theta})}{r} = 0 \quad (4.16)$$

$$\frac{\partial \tau_{rz}}{\partial r} + \frac{\partial \sigma_{zz}}{\partial z} + \frac{\tau_{rz}}{r} = 0 \quad (4.17)$$

Where,  $\varepsilon_{ij}$ ,  $\sigma_{ij}$ ,  $\tau_{ij}$  are strains, normal stresses and shear stresses in index notation with  $i$  and  $j$  representing the indices represented by the 3 different spatial coordinates  $r$ ,  $\theta$  and  $z$ .

Since the analysis was stepped in to a coupled field mode the geometry and mesh properties of the model remained the same as in the transient thermal analysis but with the exception that the elements were changed to two dimensional structural element (plane 42).

The element is defined by four nodes having two degrees of freedom at each node: translations in the nodal  $x$  and  $y$  directions. The material was assumed to behave as a linear isotropic elastic medium with mechanical properties determined by the elastic modulus and Poisson's ratio (table 4.7 and 4.8)

**Table 4.7 Strength Properties of calcite and pyrite (Salsman *et al.*, 1996)**

Mineral	Young's modulus (GPa)	Poisson's ratio
Calcite	797	0.32
Pyrite	292	0.16

**Table 4.8 Thermal Coefficient of expansion as a function of temperature (Whittles *et al.*, 2003)**

Mineral	Thermal Coefficient of Expansion (1/K)			
	373K	473K	673K	873K
Calcite	13.1 x10 <sup>-6</sup>	15.8 x10 <sup>-6</sup>	20.1 x10 <sup>-6</sup>	24 x10 <sup>-6</sup>
Pyrite	27.3 x10 <sup>-6</sup>	29.3 x10 <sup>-6</sup>	33.9 x10 <sup>-6</sup>	-

## 4.5 Results and discussions

In this section firstly the results obtained from the high frequency electromagnetic analysis are presented followed by the microwave power absorption densities, temperature profiles and thermal stresses distribution.

The results of the high frequency electromagnetic simulation is shown below

**Table 4.9 Maximum electric field intensity at different input microwave powers**

Microwave Input power at 2450MHz (In Watts)	Maximum electric field intensity with the Dielectric (Ei in Volts/cm)
150	126.79
750	283.51
1000	327.37

It is seen from the Maxwell's equations that the electric field intensity is a function of number of variables such as the geometry of the load, geometry of the applicator, the dielectric constant of the load and the input microwave power. Changing any one of these variables will change the electric field intensity. In the present simulation it is assumed that the impedance of the load is perfectly matched with that of the waveguide, and hence the values of the electric field intensity are slightly higher than that obtained in an actual microwave cavity. The values obtained for the electric field intensity could not be directly validated with the experimental results because of the limitation on the number of degrees of freedom in the university version of ANSYS, but the values are within the bound because the electric field intensity does not exceed the breakdown voltage for air (which is 30 K V/cm, Meredith *et al.*, 1998). It can be seen that the electric field intensity

Chapter 4  
Simulation of Microwave heating

---

increases with the increase in the input microwave power. However, this increase is not linear because of the fact that the value of electric field intensity is governed by number of factors as stated above. A typical contour for the electric field intensity is shown in figure 4.5 and 4.6.

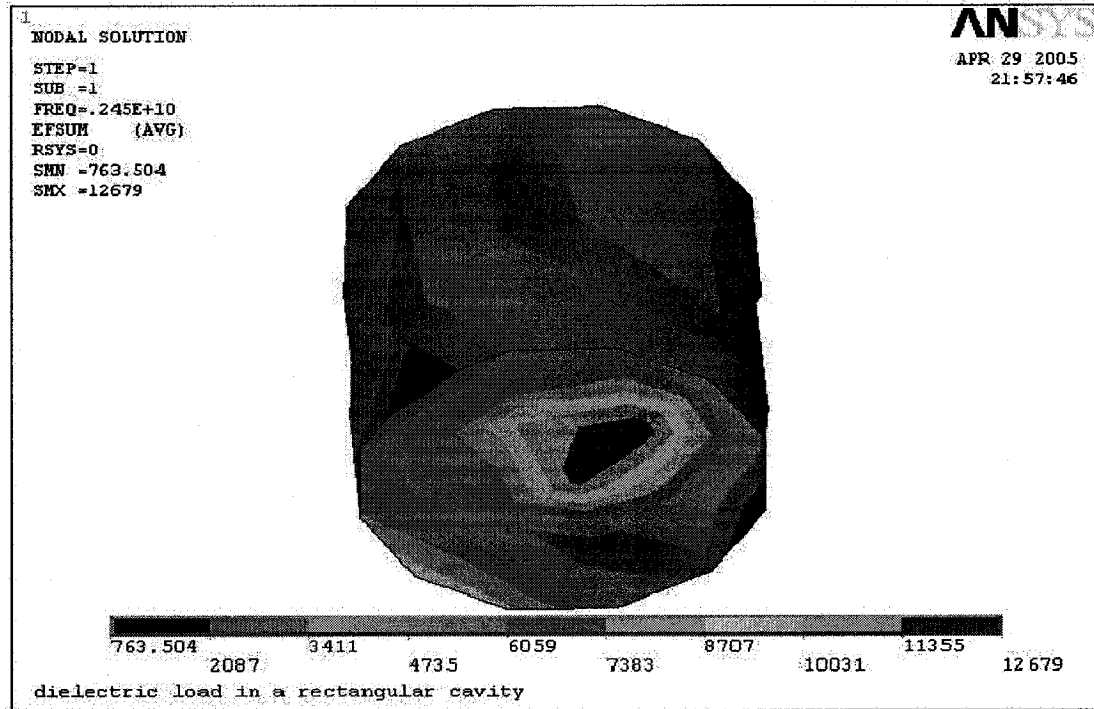


Figure 4.5 Typical contour plots for the electric field distribution within the dielectric load for an input power of 150Watts at a microwave frequency of 2450MHz

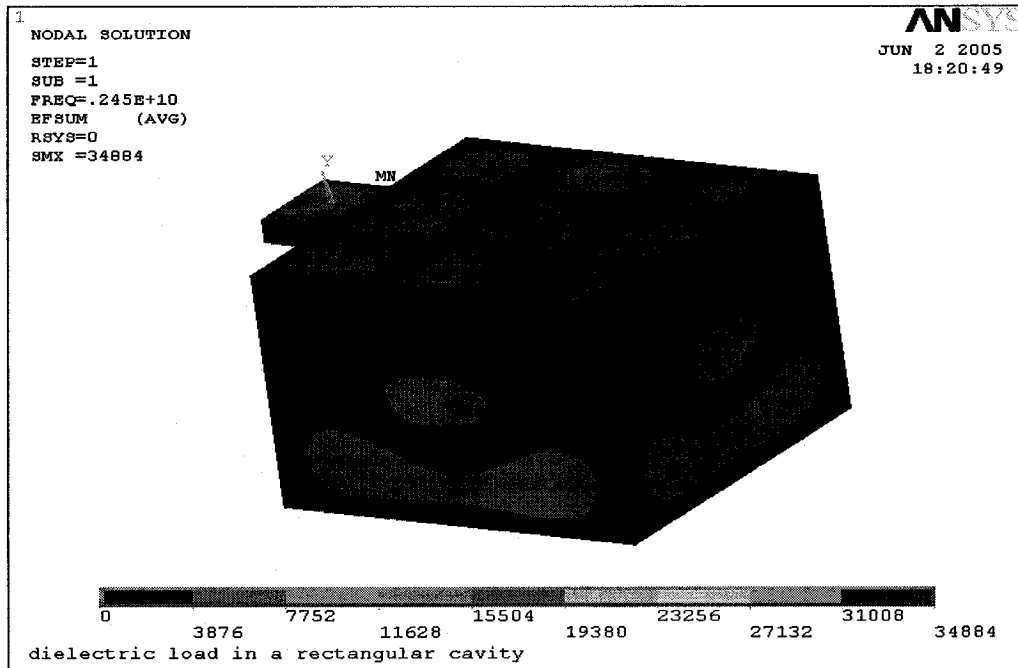


Figure 4.6 Typical contour plot showing the electric field distribution for the whole electromagnetic structure for an input power of 150Watts at a microwave frequency of 2450MHz

The results obtained for the microwave power absorption density of pyrite phase at different microwave input power are presented below.

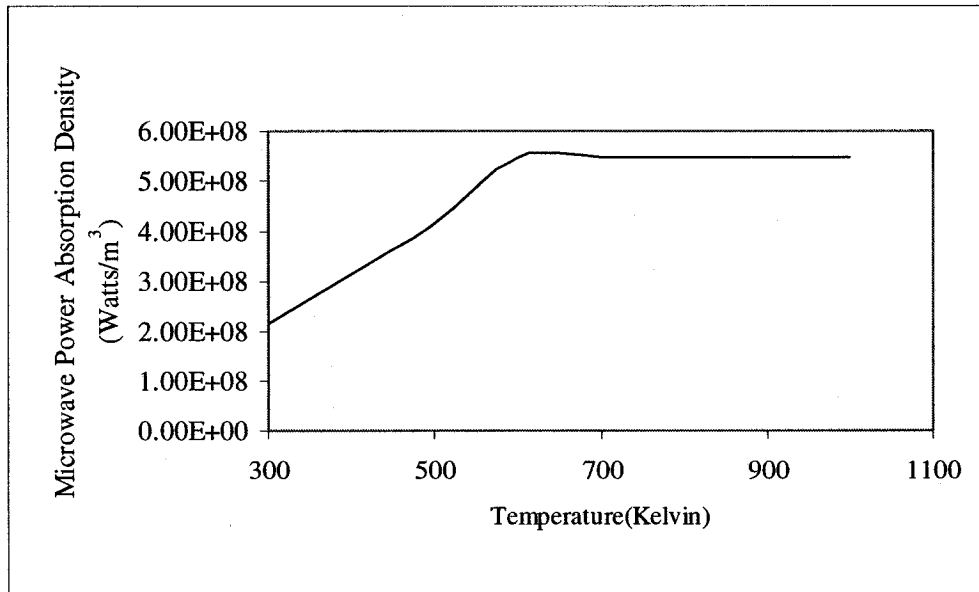
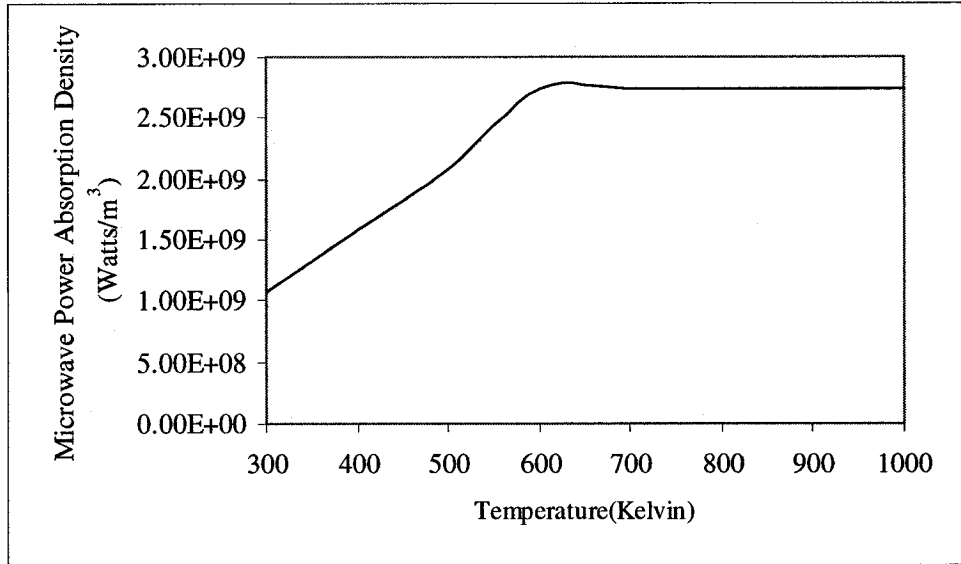
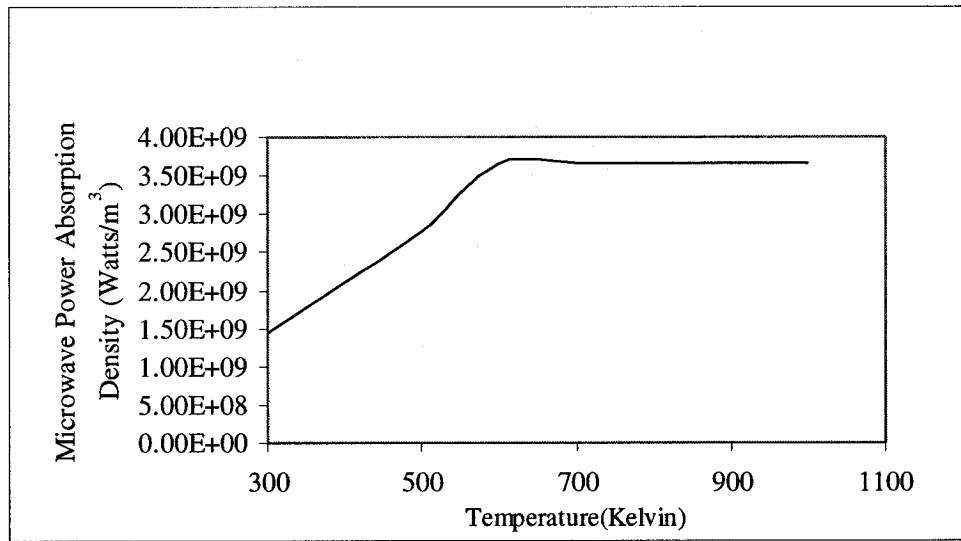


Figure 4.7 Microwave power absorption density of pyrite at 2450Mhz, 150W cavity at various temperatures



**Figure 4.8** Microwave power absorption density of pyrite at 2450MHz, 750W cavity at various temperatures



**Figure 4.9** Microwave power absorption density of pyrite at 2450MHz, 1000W cavity at various temperatures

The value of maximum electric field intensity obtained from the high frequency electromagnetic analysis was used for the computation of microwave power absorption density ( $W/m^3$ ) from eqn (4.10) for different power levels of 150W, 750W and 1000W, as a function of temperature. Figures 4.7, 4.8 and 4.9 show that microwave power

absorption density follows the same trend as the dielectric loss factor and has a linearly increasing trend with temperature up to 600 K and beyond that the power absorption density is a constant. This trend essentially indicates that as the temperature of the load increases the ability of the load to dissipate microwave energy in to heat also increases and this results in a higher rate of temperature increase within the load.

The temperature profiles as a result of microwave heating at three different microwave input powers and exposure times are presented below

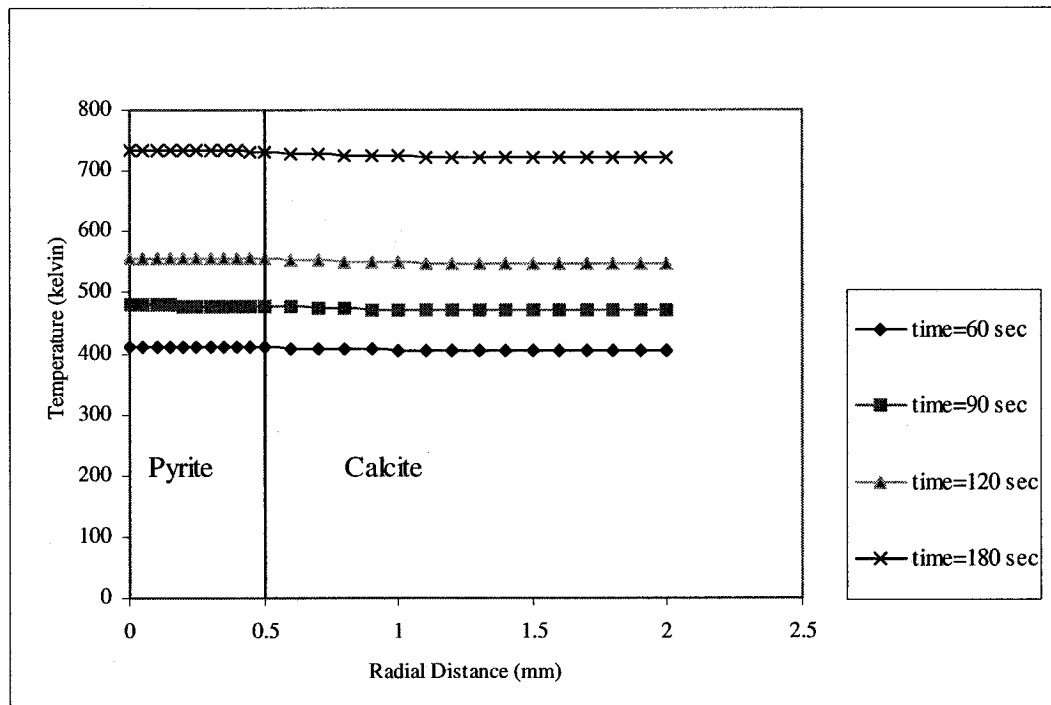


**Figure 4.10 Temperature profiles at different microwave heating times and at input microwave power of 150 W, 2450 MHz**

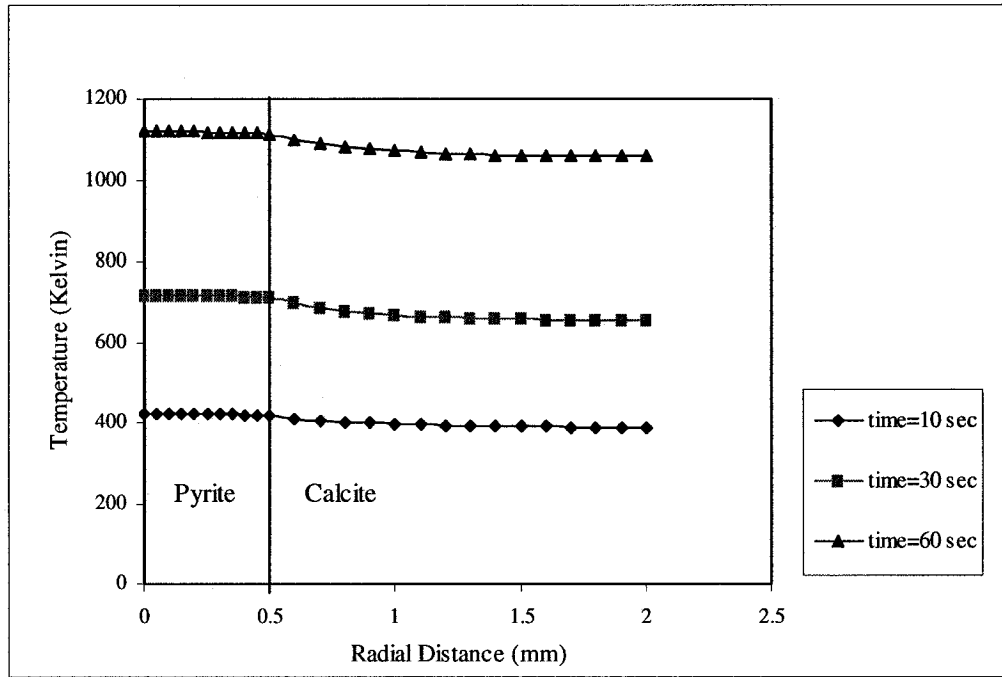


Figure 4.11 Temperature profiles at different microwave heating times and at an input microwave power of 750 W, 2450 MHz.

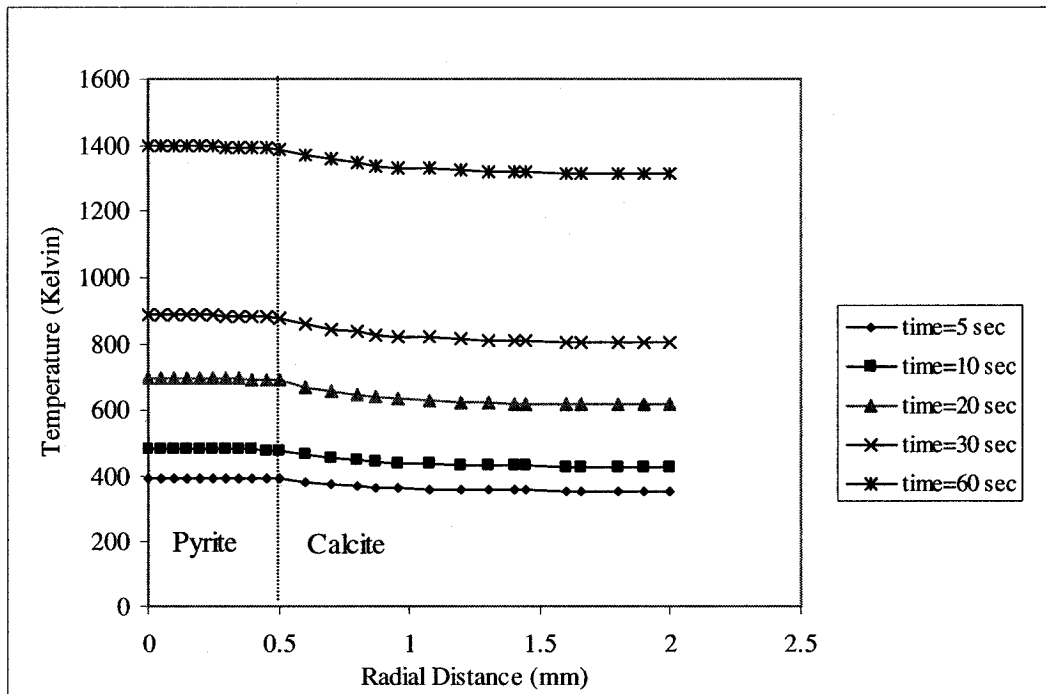


Figure 4.12 Temperature profiles at different microwave heating times and at input microwave power of 1000 W, 2450 MHz.

Simulation results of the transient temperature distributions are shown in figures 4.10, 4.11 and 4.12 for three different input microwave power levels at 2450 MHz. The results of the peak temperature in the simulation indicate, that at longer microwave exposure times higher peak temperatures are obtained.

From fig 4.10 it is seen that pyrite phase takes 180s to reach a temperature of 400K for an input power of 150W, and takes around 5 seconds to reach that temperature when the input power is increased to 1000W as shown in figure 4.12. This shows that the microwave power density has a large influence on the temperature increase with heating time.

From figure 4.12 it is seen that very high temperatures are obtained at a much shorter duration of 30s when compared to that in fig 4.10 and 4.11, this is because of the fact that, as the input power is increased the electric field intensity increases proportionally and this results in higher energy deposition in shorter time intervals.

It is also seen from fig 4.11 and 4.12 that the temperature gradient between the pyrite and calcite phases is higher as the input power is increased and at shorter intervals of time. This is because at lower exposure times and higher input powers the rate of temperature increase is relatively fast and provides less time for the diffusion of heat in to the calcite phase. The temperature profile plot also indicates that the temperature gradient across the calcite and pyrite phases is higher at longer microwave exposure times when the microwave input power is constant. This trend is more apparent when the individual plots are examined as shown in figures 4.13 and 4.14. Here it can be seen that, for an input microwave power of 750 W, the temperature gradient across pyrite and calcite is 34 K for 10 s and 63 K at 60s.

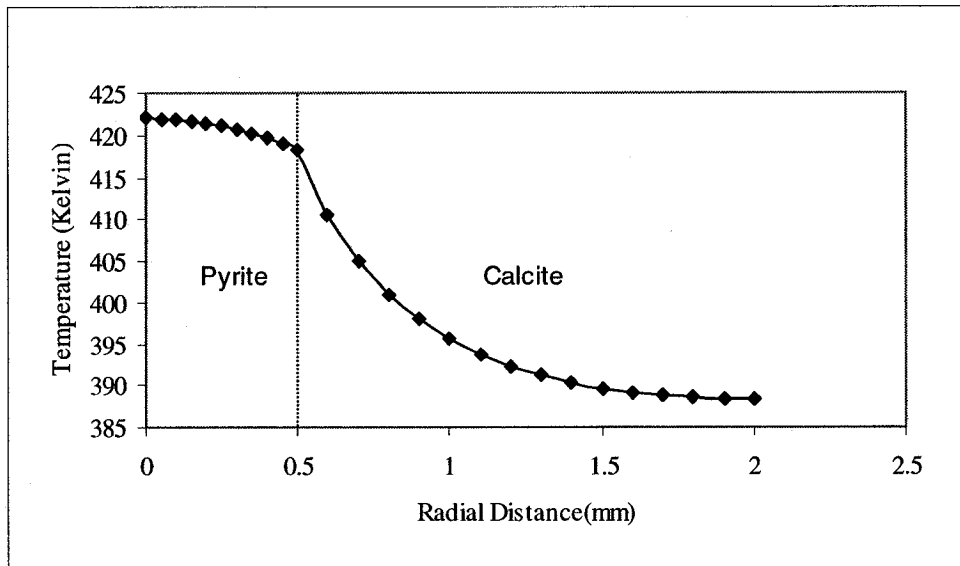


Figure 4.13 Temperature profile at a microwave heating time of 10s and at input microwave power of 750 W, 2450 MHz.

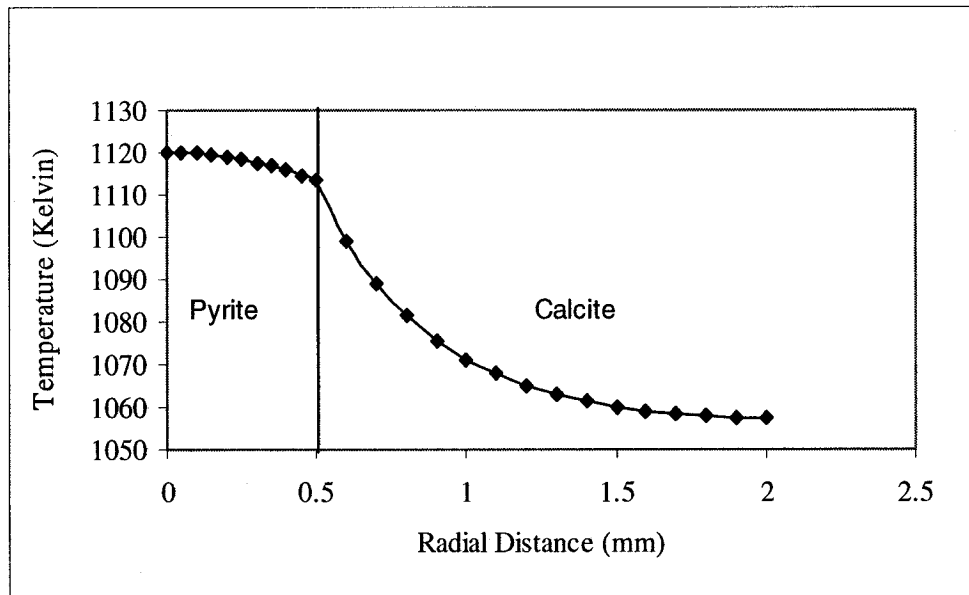


Figure 4.14 Temperature profile at a microwave heating time of 60s and at input microwave power of 750 W, 2450 MHz.

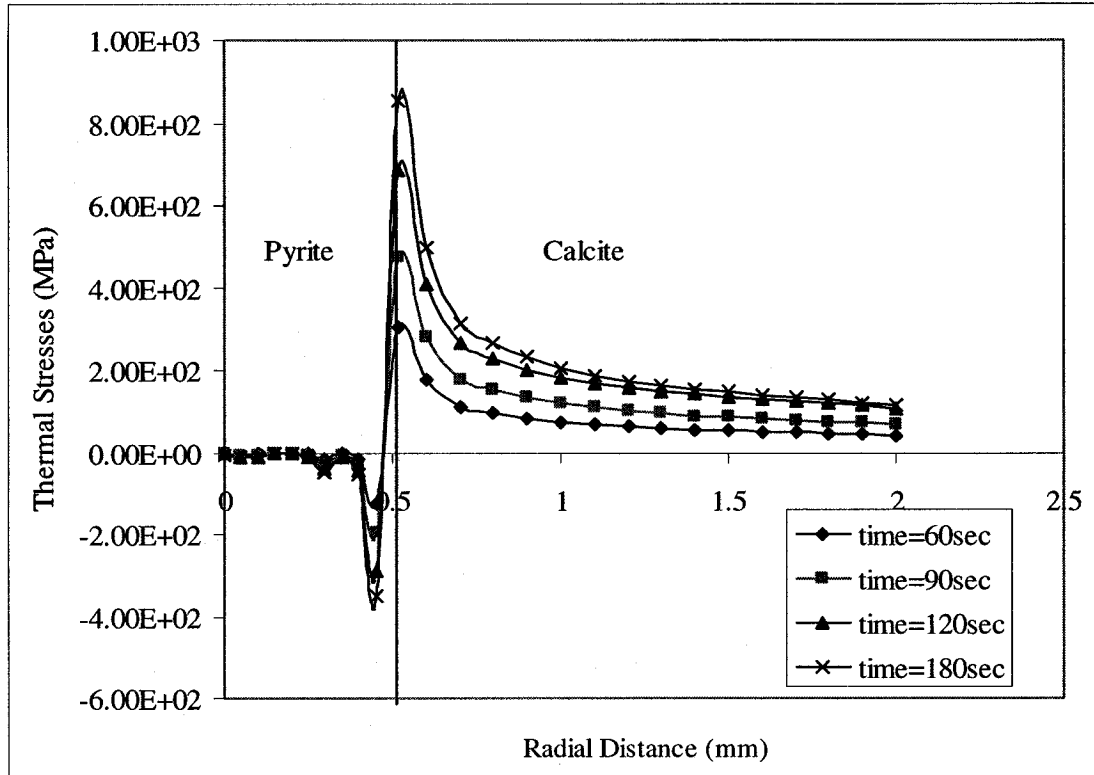


Figure 4.15 Stress profile for a microwave input power of 150W at various exposure times

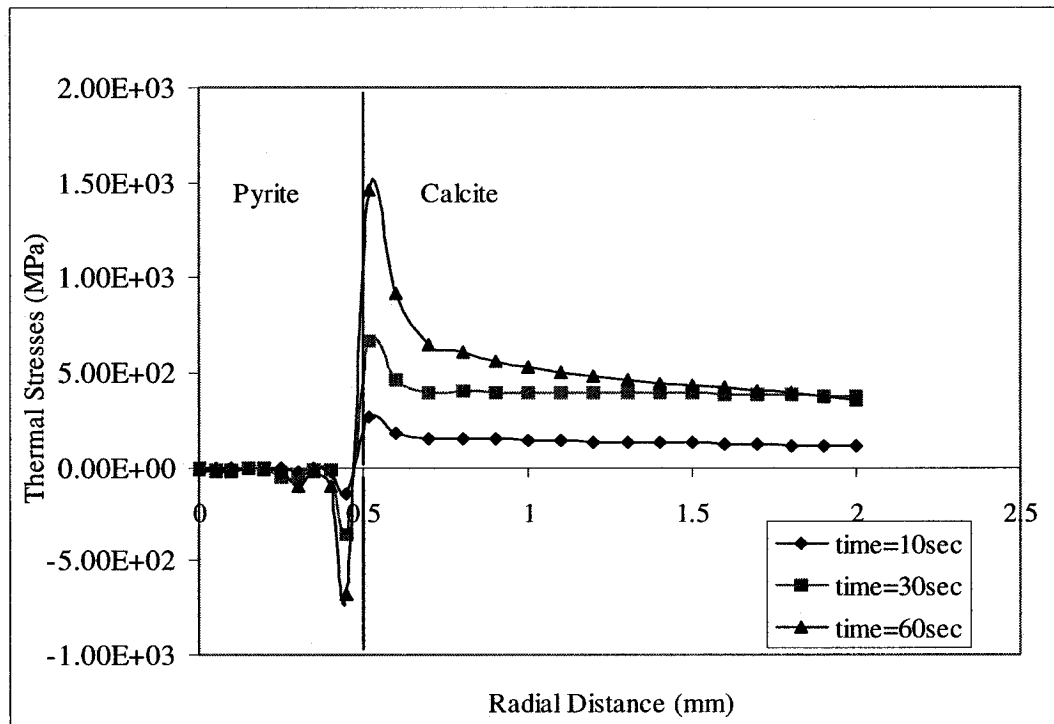


Figure 4.16 Stress profile for a microwave input power of 750W at various exposure times

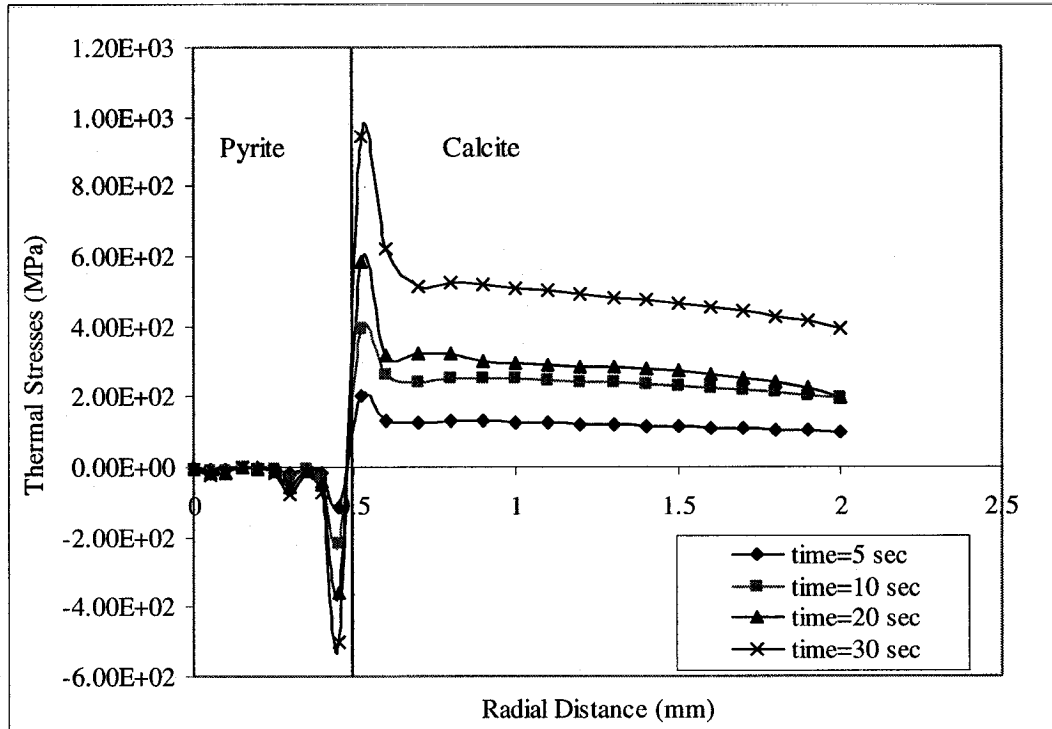


Figure 4.17 Stress profile for a microwave input power of 1000W at various exposure times

Simulation results of the thermal stress (maximum principal stresses) profile are shown in figures 4.15, 4.16 and 4.17 for three different input microwave power levels at a frequency of 2450 MHz. The results from the simulation indicate that within the pyrite phase a state of compressive stress exists and the stress state changes to tensile just near the calcite pyrite interface.

For the same input microwave power it is seen that as the time of exposure is increased the stresses also increase likewise because of higher energy deposition rate. For the same period of microwave exposure the plots show that higher stress gradients are obtained at the calcite pyrite interface at higher input powers. Say for example comparing the individual plots as shown in figures 4.18 and 4.19, it can be seen that for the same microwave time exposure of 10s, a tensile strength of 400 MPa is obtained for 1000W microwave input power as opposed to 250 MPa for a microwave power input of 750W.

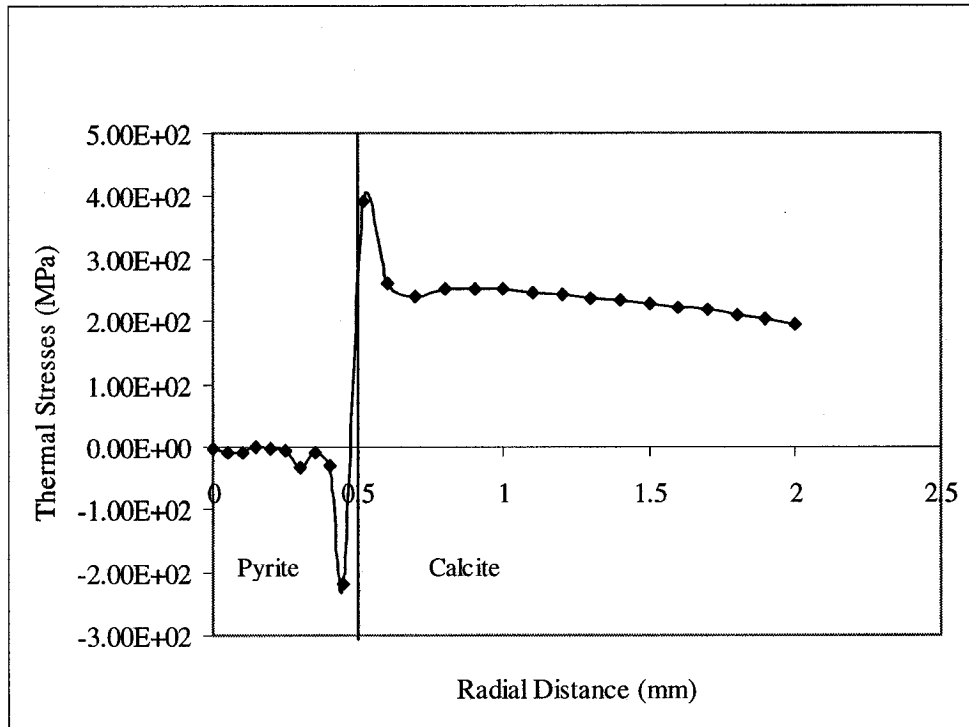


Figure 4.18 Stress profile for a microwave input power of 1000W for microwave exposure time of 10seconds

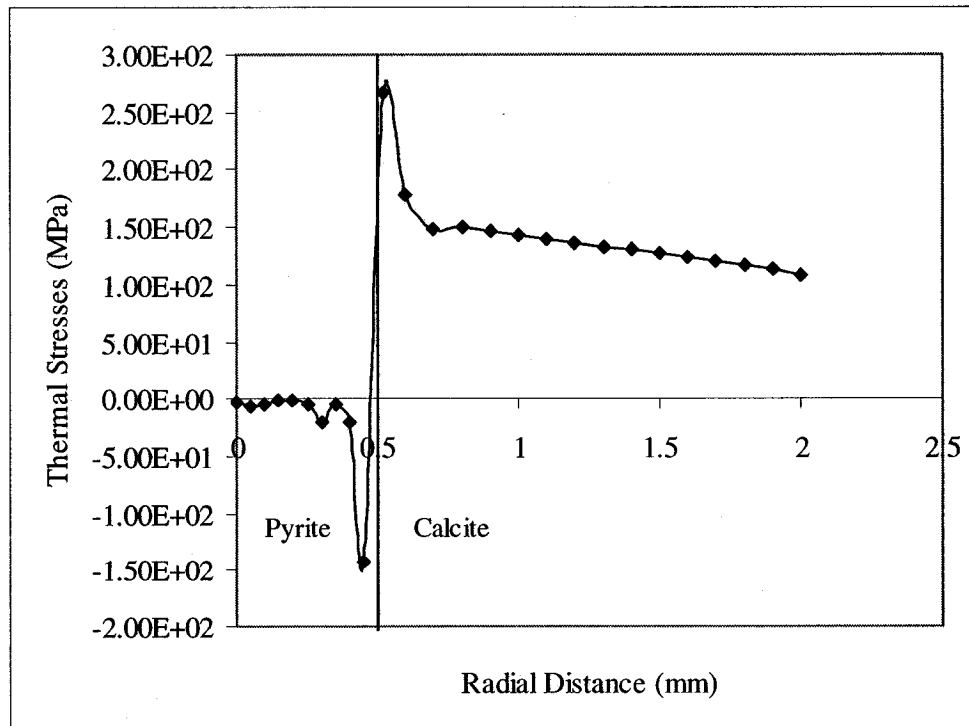


Figure 4.19 Stress profile for a microwave input power of 750W for microwave exposure time of 10 seconds

It is also seen that the magnitude of compressive stresses within the pyrite phase does not exceed the overall unconfined strength of the rock. Typically unconfined compressive strength of limestone is in the range of 125 to 130 MPa (Whittles *et al.*, 2003). However the tensile strength at the interface of calcite and pyrite exceeds the tensile strength of the rock, which for a limestone is substantially lower than the unconfined compressive strength. This trend shows that substantial damage occurs at the interface than at the individual mineral phases.

Even at a low microwave input power of 150W, a peak tensile stress of 200MPa is predicted near the interface indicating that low power microwaves can in fact induce thermal damages in the rock. The thermal damage induced from low power microwaves would be more pronounced whenever there are both microwave responsive and microwave non-responsive mineral phases present in a rock. This creates a thermal mismatch between the different responsive and nonresponsive mineral phases thereby creating stresses of very high magnitude sufficient enough to induce some damage at the grain boundaries. It should also be noted here that a linear elastic material behavior was assumed, because of the non-availability of appropriate properties to employ other material models (Eg: Concrete based material model: which describes the brittle failure case as in rocks). As a consequence of this the values predicted for the stresses are higher.

The trends of the results obtained for the temperature profiles and stress profiles agree well with Salsman *et al.* (1996), Whittles *et al.* (2003) and Jones *et al.* (2005). The loading conditions and the geometry used by these authors are different than that used in the present simulation.

Mesh refinement studies on the high frequency electromagnetic model is shown in figure 4.18 (for a microwave input power of 750 W). The solution for the maximum electric field within the dielectric load starts to converge at 9 elements per wavelength. Hence for the present analysis a mesh density of 10 elements per wavelength was used. However, the mesh could not be refined further because of the constraint on the nodal degrees of freedom in the university version of ANSY 7.1. Nevertheless, the mesh used proved

acceptable as the values of the maximum electric field intensity does not exceed the break down voltage range for air (~30 kV/cm) (Meredith, R. 1998).

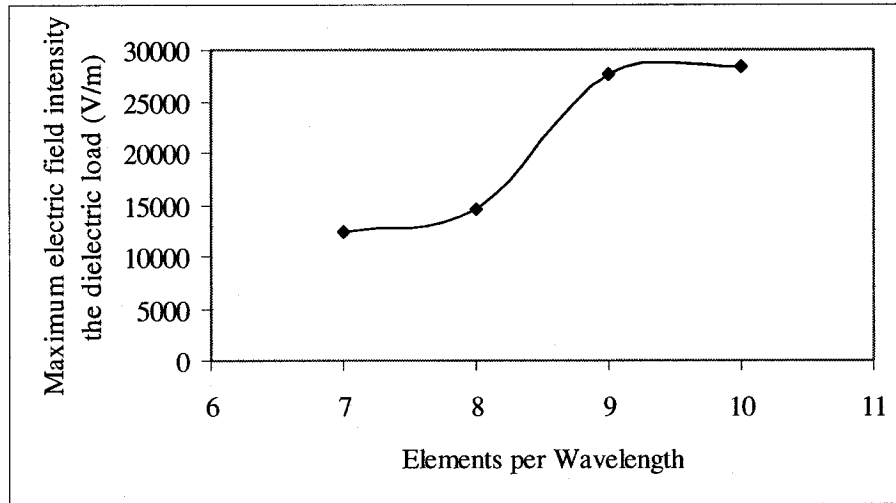


**Figure 4.20** Solution dependency of the high frequency analysis on the mesh size

Mesh refinement studies were done on the axisymmetric model employed for transient thermal analysis and thermal stress analysis. The study was done for one of the loading cases where the input microwave power was 750W and the time of exposure was 30s. It is seen that there is a very slight variation in the maximum temperature of the pyrite phase as the number of elements per edge is increased. This is because the geometry used for the transient thermal is not very complex and also the contact effect between the pyrite and calcite phases is neglected. For the present analysis 25 elements per edge was used.

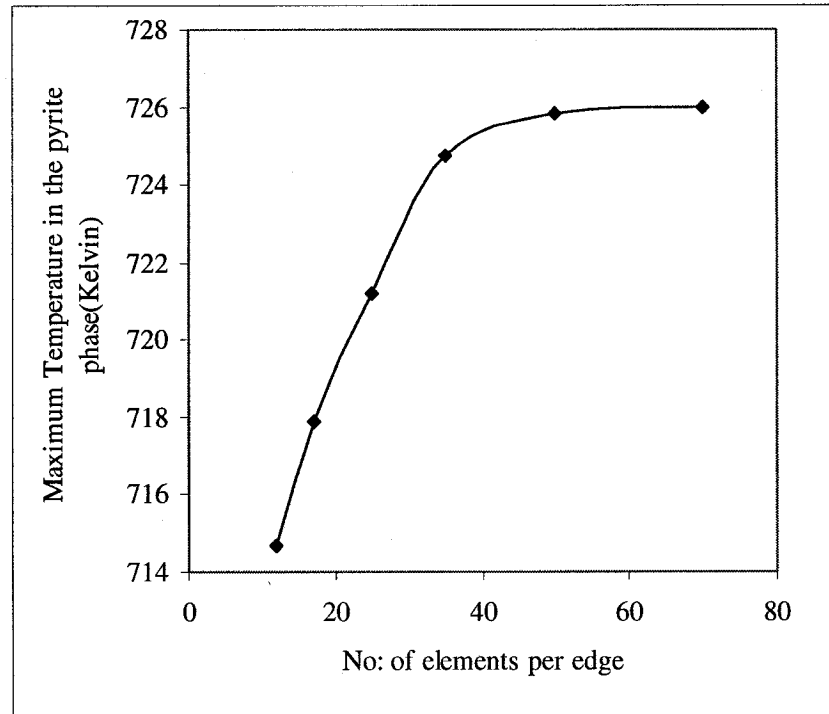


Figure 4.21 Solution dependency of the transient thermal analysis on the mesh size

## 4.6 Conclusion

Electric field intensity was computed within a dielectric load, as well as the temperature profile and stress profile across the calcite pyrite interface was computed for different microwave input powers and times. The results obtained indicate that large temperature gradients and thermal stresses can be obtained across calcite pyrite phases with relatively low microwave input powers. The pyrite phase which is a thermal inclusion constrained within the calcite matrix is subjected to rapid internal heating. The thermal stresses developed at the thermal inclusion boundary is tensile in nature and actually exceeds the tensile strength of the rock by many orders, essentially indicating crack formations, however this phenomenon can be better quantified by the use of more accurate material models. Also the simulation methodology can be applied to other rocks as well provided, the thermal and electrical properties of the rock constituents are known.

# CHAPTER 5

## EXPERIMENTAL STUDIES

---

*As outlined in chapter 2 and chapter 3, very high power microwaves have been used for rock destruction. In most cases the main objective is to actually melt the rock or bring it to its softening temperature using very high power microwaves (>10 KW). Simulation results of chapter 4 give a first order indication of extent of thermal stresses and temperatures that can be obtained in a calcareous dielectric load with microwave responsive and non-responsive phases at microwave power levels within 1000 W. Very limited experimental data is available on the effect of low power microwaves on rocks. Hence in this chapter preliminary studies are undertaken to study the impact of low power microwaves on one of the selected terrestrial rocks (basalt).*

*In the present chapter details about the experimental apparatus, setup materials and experimental procedures are outlined. Finally the chapter concludes with results obtained from these initial exploratory studies.*

## 5.1 Introduction

The works of Lindroth *et al.* (1988,1993) and Okamoto, R. *et al.* (1982) suggest that rocks can be thermally weakened by the application of high power microwaves (in the range of 25KW-75KW). Use of such high power levels might prove prohibitive and uneconomical for outer space applications, which are limited by mission requirements (section 2.2).

In the present chapter the impact of low power microwaves (~100 to ~150W) on terrestrial basalt is studied. Basalt was selected as the test specimen for the study for the following reasons:

- Basalts are the closest terrestrial analogs of Lunar and Martian rocks and hence it was selected for the present study (table 5.1) (Lindroth *et al.*, 1988, Economou, 2001).
- Also because of the fact that basalt is one of the hardest and most common igneous rocks and occurs with abundance on the surface of Earth. Drilling or excavating such rocks is still a challenge on the terrestrial environment.

The present study was highly exploratory in nature because of the fact that there was no previously available data as to how terrestrial basalt might respond to low power microwaves (~150W).

The objective of the experiments were set at determining the temperature rise in the rock at different time intervals for a constant input of microwave power and determine the strength of the microwaved specimens using simple point load testing.

**Table 5.1 Comparison of chemical composition of terrestrial basalt with Lunar and Martian composition (Lindroth *et al.*, 1988, Economou, 2001)**

Components	Basalt	Lunar Composition	Martian Composition
SiO <sub>2</sub>	47.5	41.22	40.9
TiO <sub>2</sub>	1.8	7.49	0.8
Al <sub>2</sub> O <sub>3</sub>	14.6	13.82	10
FeO	7	15.74	20.0
Fe <sub>2</sub> O <sub>3</sub>	7.2	0	-
MnO	0.19	0.20	0.5
MgO	7	7.90	10.3
CaO	6.3	11.98	6.1
Na <sub>2</sub> O	3.8	0.44	3.1
K <sub>2</sub> O	0.8	0.14	0.5
P <sub>2</sub> O <sub>5</sub>	-	0.10	0.9
H <sub>2</sub> O	-	-	-
CO <sub>2</sub>	1.5	-	-
S	0.002	0.13	-

## 5.2 Theory of point load strength test

Uniaxial compression test is a time consuming and expensive test that requires specimen preparation. When extensive testing is required for preliminary information, alternative tests such as the point load test can be used to reduce the time and cost of compressive strength tests.

The point load test is a standard test method suggested by ISRM (1973) to determine the point load strength index. In essence, point load testing involves compressing a piece of rock between two points, as illustrated in figure 5.6. Point-load index is calculated as the ratio of the applied load  $P$  to the square of the distance  $D$  between the loading points (Beinawski, 1975). Rock samples in different shapes such as core, block, and irregular

lumps can be tested by this method. But it is applicable to hard rock with compressive strength above 15 MPa. The testing equipment can be used either in laboratory or in the field. The description of the equipment used for the present study is given in section 5.3. The fact that point load tests have close correlation with uniaxial compressive strength and can be performed at much lower costs than uniaxial compression test and also with no sample preparation makes this test very attractive. However, the results obtained from point load tests have to be used with care, as they are not as reliable as those from the uniaxial compression tests (Broch *et al.*, 1972).

### 5.2.1 Calculation

Uncorrected point load strength index,  $I_s$ , is calculated as:

$$I_s = P/D_e^2 \text{ (MPa)}$$

Where:

$P^*$  = failure load, N

$D_e$  = equivalent core diameter (mm)

#### 5.2.1.1 Size Correction Factor

$I_s$  varies as a function of  $D_e$ , therefore a size correction must be applied to obtain a unique point load strength value for the rock sample. The size corrected point load strength index,  $I_{s(50)}$ , of a rock specimen is defined as the value of  $I_s$  that would have been measured by a diametral test with  $D = 50$  mm.

The size correction was obtained using the formula:

$$I_{s(50)} = F \cdot I_s$$

The "Size Correction Factor F" can be obtained from the chart in Fig 5.1 or from the expression:

$$F = (D_e/50)^{0.45}$$

---

\* Failure P is obtained by multiplying the hydraulic pressure at failure with the effective ram area, if the failure load is calibrated in terms of hydraulic pressure.

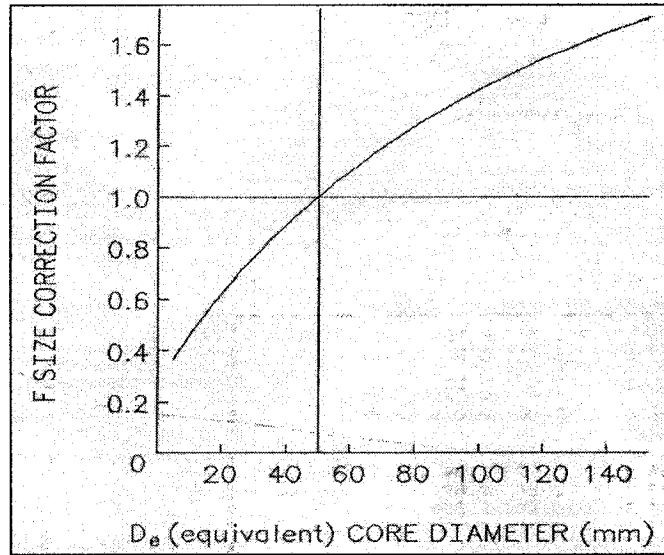


Figure 5.1 Size Correction Factor Chart (ASTM, 1991)

The uniaxial compressive strength can then be estimated by using Fig 5.2 or the following formula:

$$\sigma_c = C I_{s(50)}$$

Where:

$\sigma_c$  = uniaxial compressive strength

C = factor that depends on site- specific correlation between  $\sigma_c$  and  $I_{s(50)}$

$I_{s(50)}$  = corrected point load strength index

The values for C can be obtained from table 5.2

Table 5.2 Generalized value of C (ASTM, 1991)

Core Size (mm)	Value of "C"(Generalized)
20	17.5
30	19
40	21
50	23
54	24
60	24.5

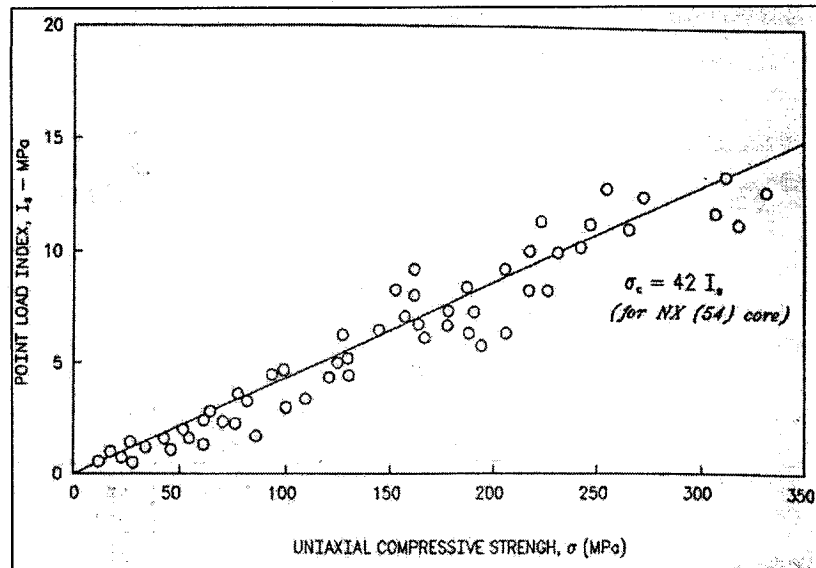


Figure 5.2 Relationship between point load strength index and uniaxial compressive strength (ASTM, 1991)

### 5.3 Experimental Setup

The experimental apparatus used for this study was a standard batch type microwave dryer and a standard point load tester.

#### 5.3.1 Microwaving setup

The microwaving setup consists of a microwave generator (750W and 2450 MHz), 3 port circulator, 3 stub tuners and a cavity (40cmx35cmx25 cm). The microwave generator has the capability of variable power operation with continuous microwave power output. The microwaves generated are transmitted to the main cavity through a series of rectangular waveguides. A 3-port circulator ensures that the microwaves reflected from the cavity were directed to the dummy load, where the reflected microwaves are absorbed. Reflected and incident powers were monitored by the power meters integral with the microwave generator. The reflected microwave power was maintained at a near zero value during each run by manually adjusting a three stub tuner inserted at the top of the waveguide assembly. Standard infrared camera was used for the purposes of temperature

measurements. Photograph of the experimental setup used for the present study is shown in figure 5.3.



**Figure 5.3 Photograph of the microwaving setup**

### **5.3.2 Point load tester**

A standard portable point load-testing machine was used in the present study. The unit consists of loading platens, loading system (ram and loading frame) and a pressure gauge. The point load tester uses a high-pressure hydraulic ram with a small hydraulic pump as the loading system. The loading platen consists of a set of hardened steel cones with a radius of curvature of 5mm and an angle of cone equal to  $60^\circ$ . Load is measured by monitoring the hydraulic pressure in the jack by means of the pressure gauge. Specimens up to 100mm in diameter can be used. A sliding crosshead and steel pins allows quick adjustment of clearance. The maximum capacity of the point load tester is 5 tons. The photograph of the point load testing apparatus used is shown in figure 5.4.

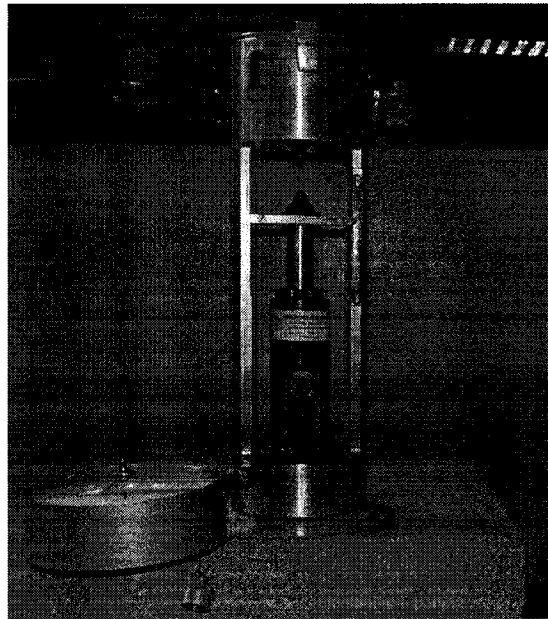


Figure 5.4 Photograph of the point load tester

### 5.3.3 Test Specimens

As mentioned earlier the test specimen chosen for the present work was basalt, obtained from a quarry in New Jersey County, USA. Rock samples in the form of uncut lumps were obtained from the quarry. The uncut samples were suitably cored using a diamond-coring bit into long cylindrical specimens with a diameter of 38.1mm (1.5 inches). These specimens were later cut to obtain a  $L/D > 1$ ,  $L$  being the length of the specimen. A diamond band saw was used for the purpose. A total of 35 specimens were cored from the basalt lumps.

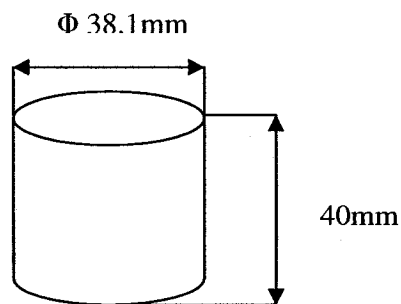


Figure 5.5 Dimensions of the rock specimen

The basalt(used for the present study) texture consists of large crystals of olivine, augite, pyroxene and plagioclase minerals set in fine crystalline or glassy matrix in addition to some iron oxides. Megascopic and microscopic description of the specimen used for the present study is given in table 5.3.

**Table 5.3 Megascopic and microscopic description of the rock (Lewis, J.V., 1907)**

Megascopic description of the rock	Microscopic Description
A greenish-black rock with aphanitic structure and local red bands due to iron oxide stains	Microphenocrysts of augite (some glomeroporphyritic) are set in a matrix of thin laths of labrodarite, granular clinopyroxene and dark; essentially opaques glass which subordinate and interstitial (interstitial texture). Some of the glass been altered to a brown, iron rich chlorite: some of the plagioclase to sericite.skeletal magnetite is a widespread accessory.

## 5.4 Experimental Procedure

### 5.4.1 Microwaving experiments

The rock specimens were divided into 5 sets with each set containing seven specimens. One set of specimens (termed the control specimens) was not exposed to microwave radiation in order to constitute the control specimens. The remaining four sets of specimens were used for the microwave studies. Each set of specimens was exposed to different time intervals of microwave radiation.

The decision on the input power density and the total time of exposure for the sample sets were somewhat arbitrary as no previous data was available. Also the microwaving equipment had a limitation to handle temperatures in excess of 175 °C. So it was decided to select a lower power density of 1W/gram. The time interval for the exposure was varied from 60s, 120s, 180s, and 360s.

The following experimental procedure was followed

- a. The mass of the cylindrical rock specimens was determined using an electronic balance with an accuracy of  $\pm 0.01$ . Their average weight was 140g.
- b. Water in a glass container weighing approximately the same as rock specimens was then placed in the microwave cavity on a one-inch teflon stand and the generator was switched on. This was done to fine tune the reflected microwave power to a zero value. After tuning the reflected microwave power to zero the water in the cavity was removed before the start of the experimental runs.
- c. A rock specimen was then placed in the microwave cavity on the teflon stand and its position inside the cavity was adjusted in such a way to get the least reflected power. The position of least reflected power was then marked off in order to place all the rock specimens at the same position of minimum reflected power.
- d. Rock samples were then placed in the cavity one at a time and then the generator was switched on. The power input was kept at 1W/g. Seven replicates were used for each time interval. The time of exposure for the sample sets is as shown in table 5.4.
- e. Temperature measurements of the rock specimens were taken before and after the microwave exposures using an infrared camera. Temperature was measured at different positions on the specimens and an average temperature was recorded.
- f. Later the samples were placed in a steel crucible and were allowed to cool down to room temperature under ambient conditions.

**Table 5.4 Microwave exposure times used**

Sample set	Time of exposure (in seconds)
Set 1	60
Set2	120
Set3	180
Set4	360

### 5.4.2 Point load strength testing

For the present work diametral testing of the unmicrowaved and microwaved samples were carried out. For the diametral point load testing the load is applied to the specimen as shown in figure 5.6

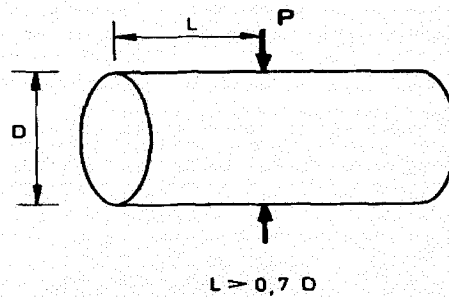


**Figure 5.6 Schematic representation of the loading points in point load testing**

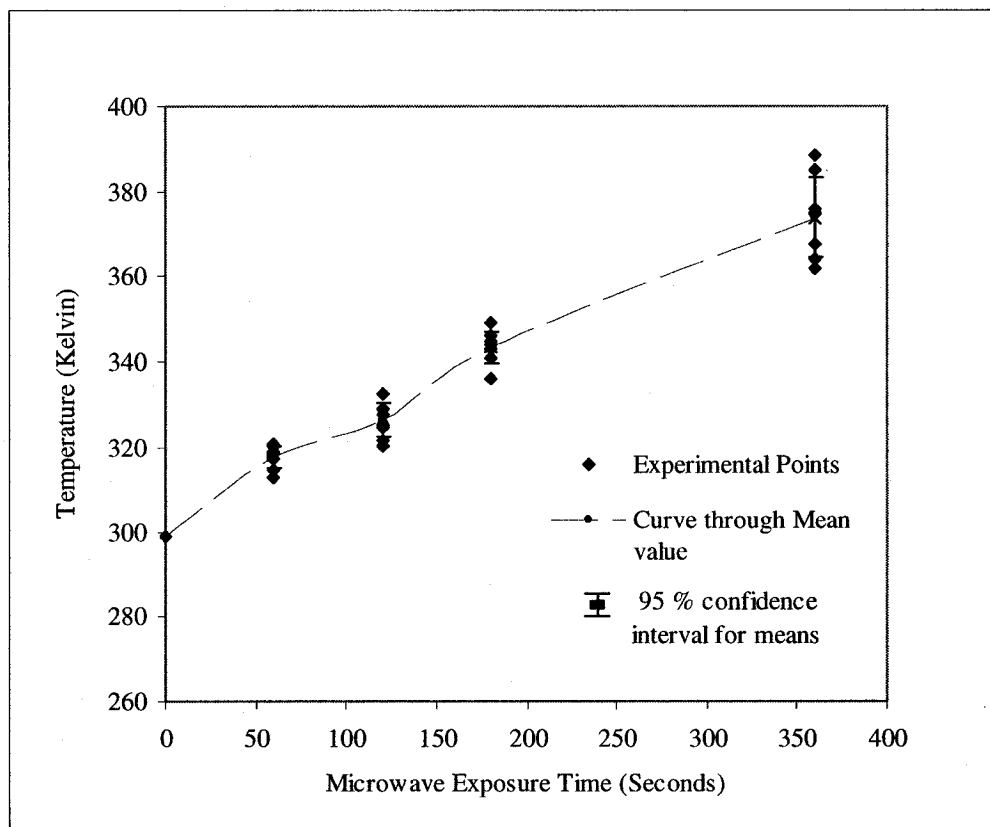
Following testing procedure was followed

1. The rock specimens were inserted in to the test device and the platens were closed to make contact along the core diameter. It was ensured that the distance,  $L$ , between the contact points and the nearest free end was at least 0.5 times the core diameter.
2. The sample was loaded steadily using the hydraulic hand loading system until failure occurred. Hydraulic pressure at failure was recorded
3. The procedure was repeated for all the samples

- The uncorrected point load index, corrected point load index and the compressive strength of the rock specimens were found out following the procedure shown in section 5.2

## 5.5 Results and discussion

The experimental results of rock specimen (basalt) temperature for different microwave exposure times at a constant microwave power density of 1W/g is presented. Also the results of the point load strength tests for the rock specimens are presented.



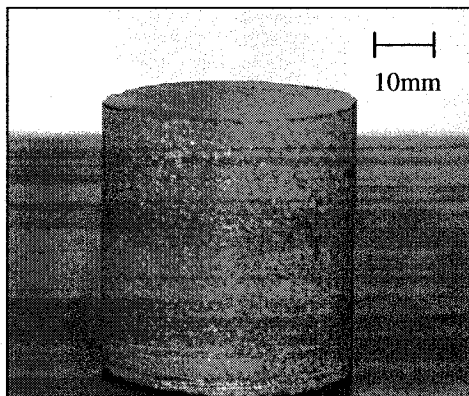
**Figure 5.7** Temperatures of the rock specimens at different microwave exposure times

Figure 5.7 shows the variation of temperature with different microwave exposure times at a constant microwave power density of 1W/gram. It can be seen from the graph that there is a steady increase in the temperature roughly at a rate of 287 K (14 °C) per minute. The highest average temperature obtained was 374K (101°C) at an exposure time of 360s. Temperatures up to 388K (115 °C) were recorded for some samples when exposed for

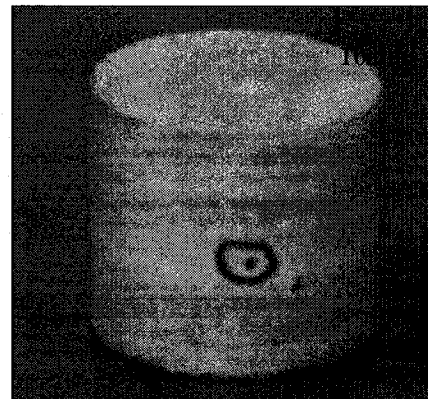
360s. These results show that the basalt rock specimens used are quite receptive to the microwave radiation and they could heat up considerably well for a very small input of microwave power. Also, it has to be noted that temperature values can reach much higher values in the interior of the rock because of local accumulation of microwave energy.

This is partly because of the presence of the microwave responsive metallic or semi-conducting mineral phases such as sulphides and iron oxides. Also pyroxene has a strongly polarizable structure that significantly increases the high temperature dielectric constant of pyroxene containing basalt (Lindroth *et al.*, 1988)

The specimens were allowed to cool after the microwave heating intervals, it was observed that the specimens exposed at 60s and 120s did not show observable cracking (figure 5.8 (a) and (b)). However the specimens exposed at 180s and 360s showed some amount of cracking as shown in figure 5.9 and 5.10.



(a)



(b)

**Figure 5.8 Specimens after 60 seconds (a) and 120 seconds (b) microwave exposure times**

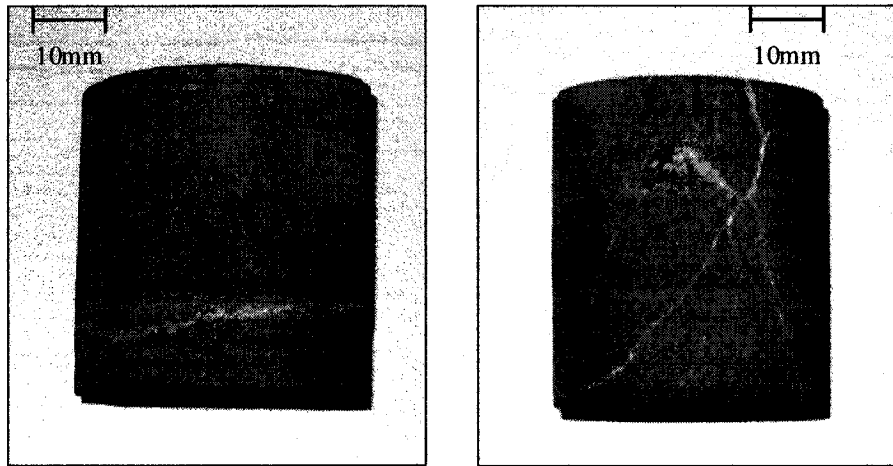


**Figure 5.9** Some specimens that showed cracking after 180seconds microwave exposure times

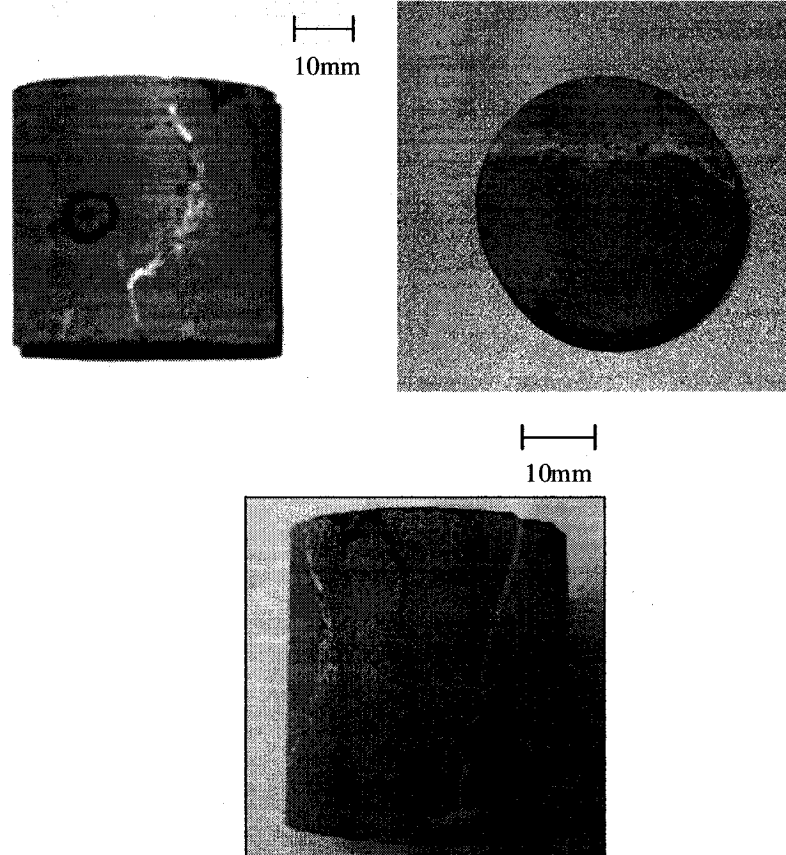


**Figure 5.10** Some specimens that showed cracking after 360seconds of microwave exposure times  
As indicated by the results of the simulations for a calcareous rock (chapter 4) the magnitude of the tensile stresses developed at the grain boundaries of the microwave responsive minerals and non responsive matrix exceeds the strength of the rock, which

essentially indicates that damage which was initiated at the grain boundary can actually propagate into the matrix, there by weakening the matrix. Even in the present experiments, a similar phenomenon is observed. Because the basalt rock specimen used is composed of minerals which are very good microwave absorbers like magnetite and iron rich chlorite embedded in a matrix of labrodarite and glass, which are very poor absorbers of microwaves (Chen *et al.*, 1984, Walkiewicz *et al.*, 1988). This mineral composition of the present rock samples makes it susceptible to differential heating when exposed to microwave radiation, there by facilitating the development and propagation of thermal cracks. These cracks are quite apparent at higher microwave exposure times as shown in the figure 5.9 and 5.10. Conversion of moisture that may be present in the rock sample in to steam, creating regions of localized high pressures might also lead to cracks, however this phenomenon may not be quite dominant because of the fact that basalt is a dense fine grained volcanic rock. Another possibility of crack formation might also be due to the expansion of the entrapped gas pockets within the voids of the rock, because presence of voids is quite common in aphanitic rocks like basalt

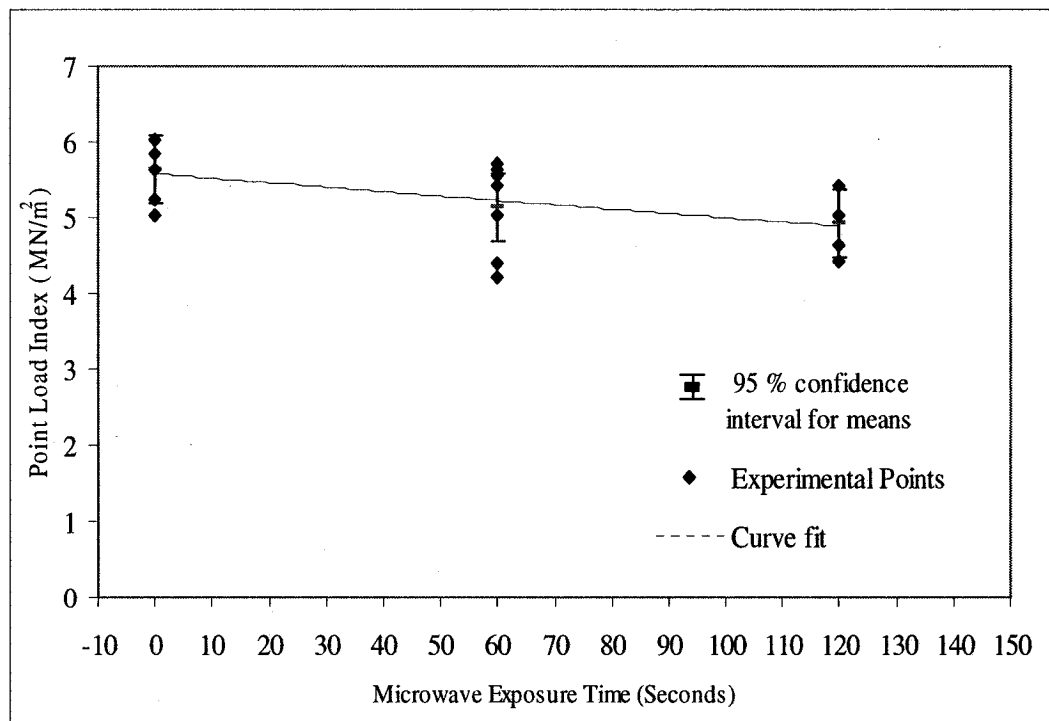


Figure 5.11 Experimental results of the point load tests

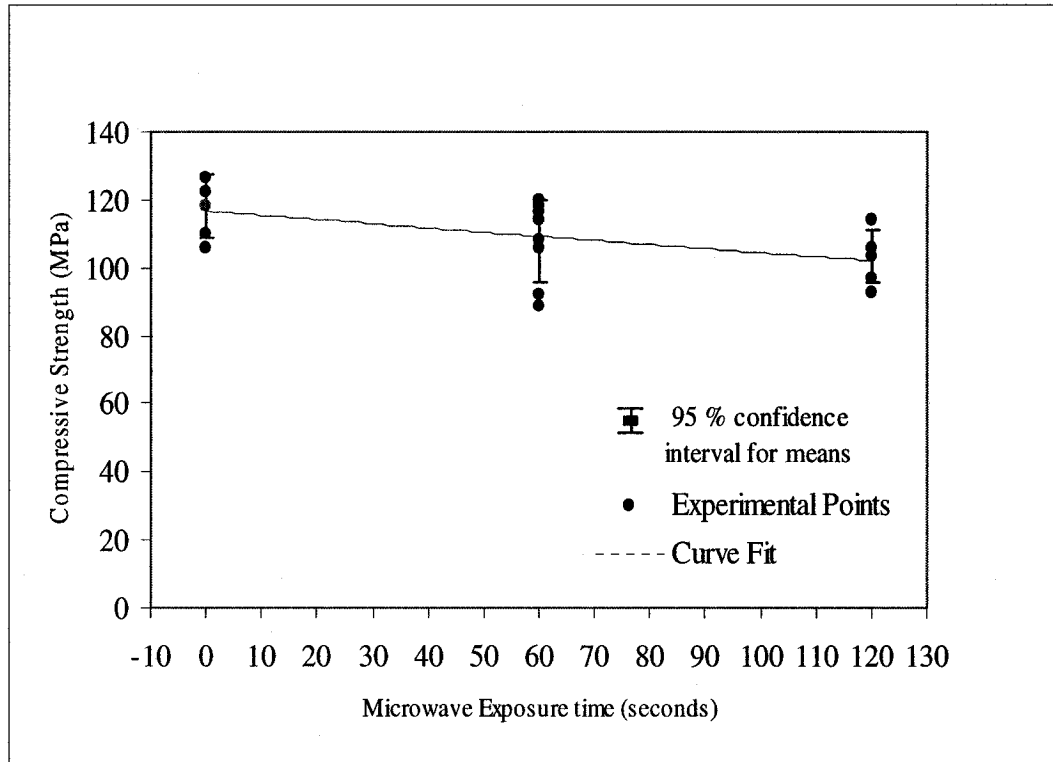


Figure 5.12 Correlated compressive strengths from point load index

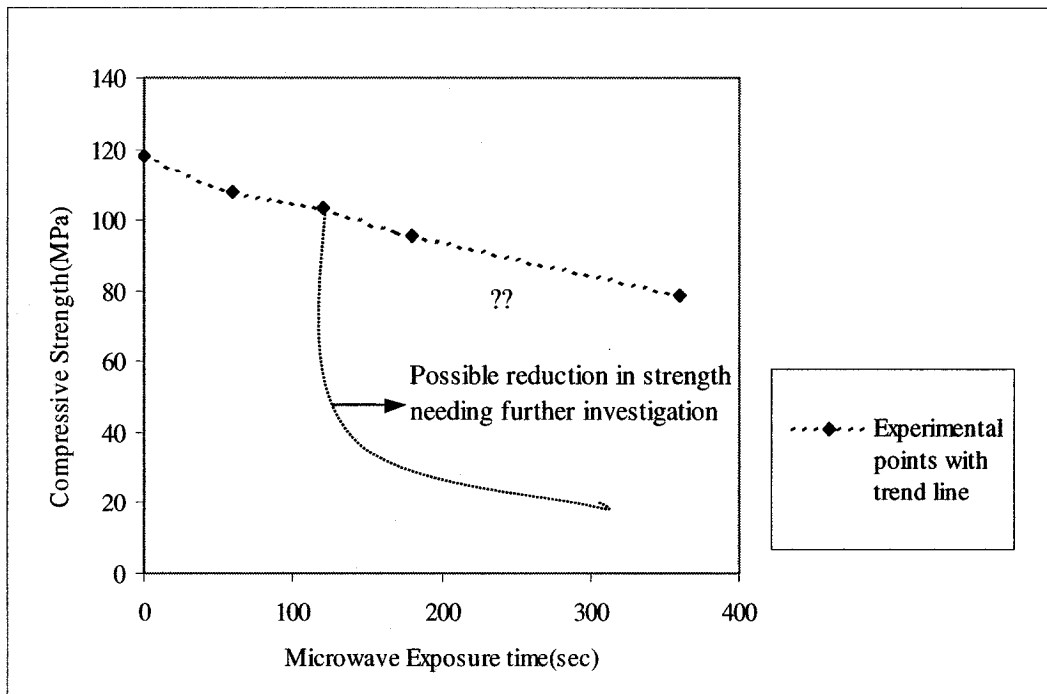


Figure 5.13 Mean Compressive strengths at different Microwave exposure times

**Table 5.5 Average point load index and compressive strengths at different times of microwave exposure**

Microwave exposure time (Seconds)	Sample set	Size corrected Point load index (MN/m <sup>2</sup> )	Compressive strength (MPa)
0	Control Set	5.62	118.25
60	Set 1	5.13	107.87
120	Set2	4.93	103.46
180	Set3*	4.55	95.74
360	Set4*	3.73	78.546

\* Obtained from trend corrected values

The results of the point load tests are shown in figure 5.11, and the correlated compressive strength obtained from the point load index tests are shown in figure 5.12. Typical failure pattern of the specimens by point load testing is shown in figure 5.14. The mean compressive strength for microwave exposure times of 180s and 360s is shown in figure 5.13, these values are obtained from the trend line. Since some of the specimens at 180s and 360s microwave exposure time showed cracking, their strength might as well be very low as indicated in the figure 5.13, however this observation needs further investigation and more sensitive testing techniques.

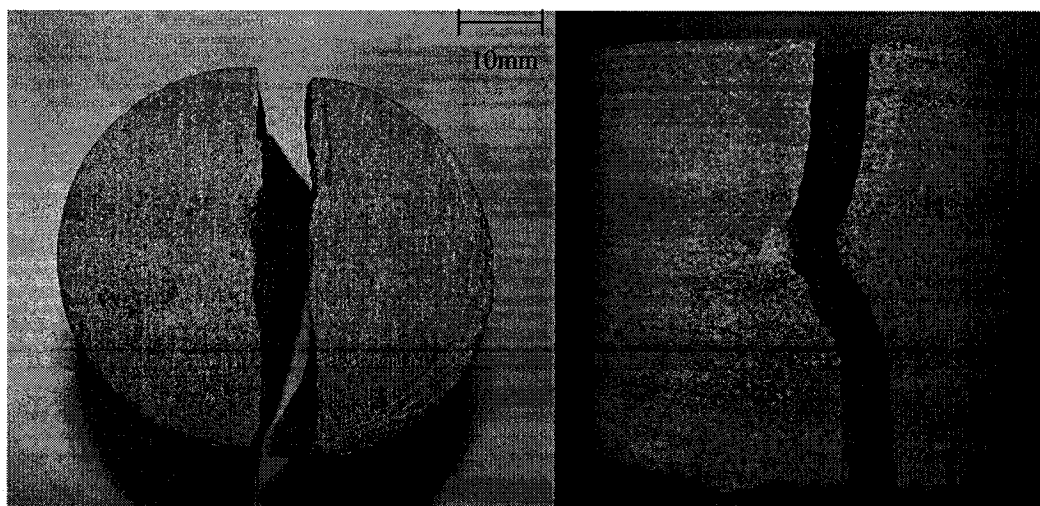


**Figure 5.14 Typical failure patterns of the specimens during the diametral point load testing**

The point load index (figure 5.10) and hence the compressive strength (figure 5.11) show a decreasing trend with an increased exposure to microwaves, giving a preliminary indication that low power microwaves does have the potential of reducing the strength of the basalt rock specimen.

It should be noted here that point load tests could be done for the control set (not exposed to microwaves) and specimens exposed to 60 seconds and 120 seconds of microwave radiation only. The specimens that were exposed to 180 seconds and 360 seconds of microwave radiation could not be tested because of the fact that they had both localized micro cracks and macro cracks (shown in figures 5.8 and 5.9) due to microwave radiation. When they were loaded in the point load tester they showed the tendency of local failure at the point of loading as shown in figure 5.15. As indicated earlier in the discussion the rock matrix is weakened by thermal cracks due to increased microwave exposure. This weakened matrix actually makes the specimen susceptible to indentation by point load platens rendering the test unsuitable for the specimens exposed to higher microwave times. However, this very same phenomenon makes it ideal to facilitate percussion or rotary drag drilling. Drilling involves disintegration of the rock mass by fracturing the rock at the bit rock interface under the action of different cutting forces. Now if the rock matrix already has induced cracks as in the present case, easier penetration is achieved with a much less applied thrust.

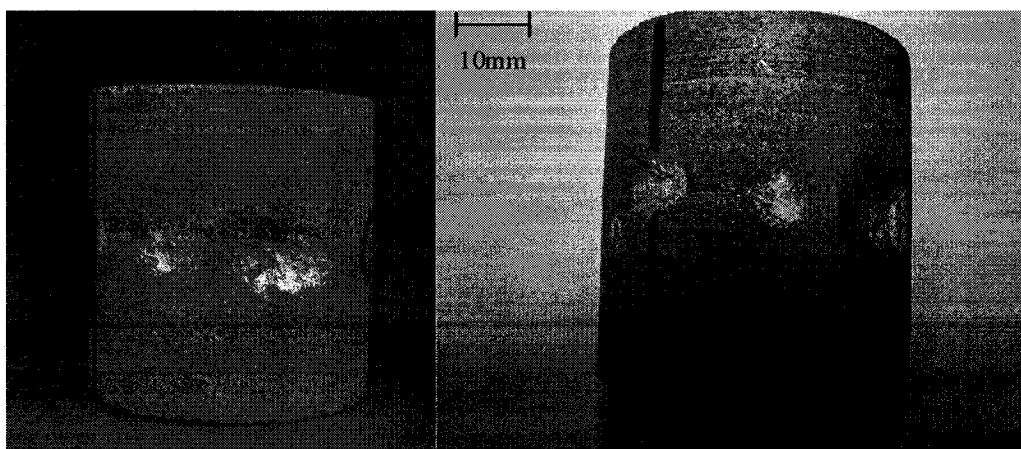


**Figure 5.15 Specimen showing local failures at the point of loading during point load tests after microwaving.**

Because once the rock matrix has cracks it means that a rock which was earlier quite hard, has now become soft, so a drilling or an excavation technique suitable for soft rocks can actually be applied in place of a much more energy demanding mechanical processes.

For example, as a cursory step the effect of microwaves on the rate of drilling during a typical percussive drilling process (for the top hammer having power of drill 14–17.5 kW, blow frequency, 3000–6000 blows/min, bit diameter, 76–89 mm) can be quantified considering the fact that compressive strength of the rock has close correlation with drilling rate of percussive drilling as shown in figure 5.16 (Kahraman, S., *et al.*, 2003)

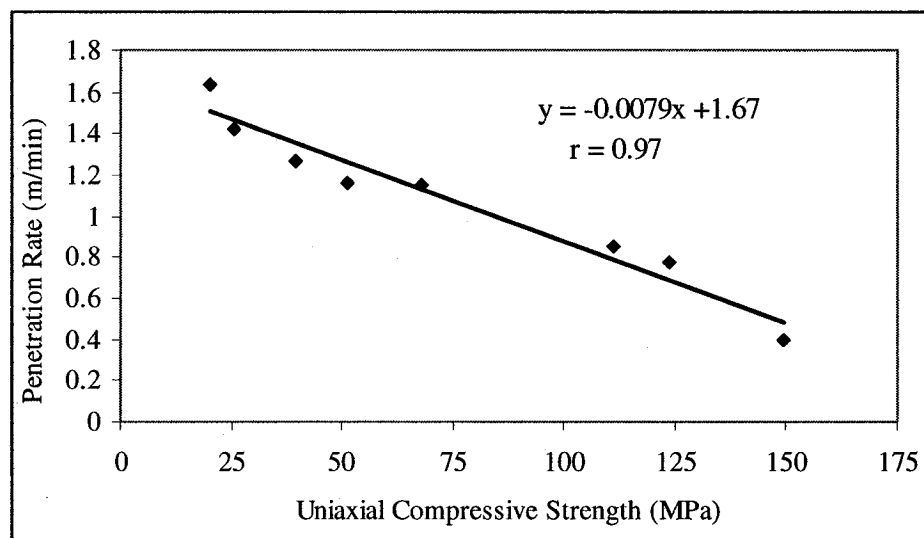


Figure 5.16 Penetration rate vs. uniaxial compressive strength for percussive drilling (Kahraman, S *et al.*, 2003)

A plot between the microwave exposure times for the rock sample and penetration rate for the percussive drilling process indicates that penetration rate increases with increasing microwaving times (figure 5.17). It is seen that there is an increase of 42% (at a microwave exposure time of 360s) in penetration rate as compared to unmicrowaved samples. Since the specimens exposed to higher microwave times had local failures and cracks as well, at the point of loading during the point load tests it might also be the case that we might expect higher penetration rates when compared to that in figure 5.17. However, this result needs further investigation and extensive testing so that a correlation between different microwave parameters (power, time of exposure and frequency) and the drilling parameters can be obtained. This kind of correlation will be helpful in terms

of evaluating the energy balance and economics when microwaves are used in conjunction with drilling processes

In essence it can be concluded that basalt which is considered one of the hardest rocks and very difficult to drill or excavate has actually weakened because of numerous thermal cracks due low power microwave exposure. This result is quite promising because of the fact that such weakened rocks can be drilled or subjected to subsequent breakages using reduced mechanical energies.

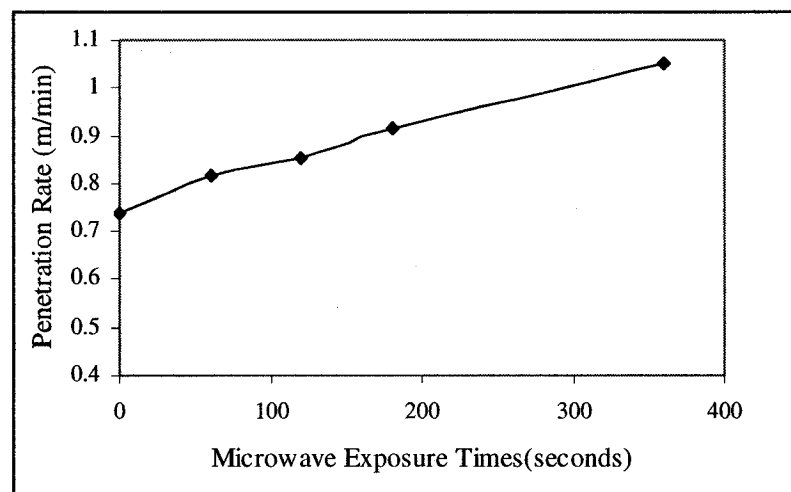


Figure 5.17 Penetration rate vs. Microwave exposure times for percussive drilling

These preliminary results got by the use of low power microwaves with the aim of thermally creating cracks without actually melting them agrees well with Lindroth *et al.* (1988). Lindroth *et al.* (1988) demonstrate that high power microwaves (25KW) could fragment and actually melt low  $\text{TiO}_2$  basalt. However, in the present study the objective was not to melt the rocks but to induce cracking by means of exposure of the rock sample to low power microwaves and subsequently apply mechanical methods of rock breakage.

In the present study a multimode cavity was used as the microwave applicator because of its mechanical simplicity and versatility. Use of single mode applicators or focused microwave beam (Jerby *et al.*, 2002) could induce more damage in to the rocks. Because

with in multimode applicators there are a number of mixed modes, which tend to lower the power handling capabilities of such cavities.

## 5.6 Conclusions

It is concluded that the initial exploratory experiments to assess the effect of low power microwaves on basalt were quite successful. This initial set of results show that the basalt specimen used was responsive to low power microwave radiation and showed a near linear temperature increase with time. The point load strength tests give an indication that the microwaved samples did weaken due differential thermal heating of different mineral phases in basalt. A phenomenon most desirable if one wants to facilitate mechanical breakage of rocks after microwave exposure in the context of drilling.

# **CHAPTER 6**

## **CONCLUSIONS AND RECOMMENDATIONS**

---

## 6.1 Conclusions

A broad review was carried out to provide information in terms of research that has been done in the area of mining in space. The focus was more on Lunar and Martian environments. The present work was categorized in reviewing the research work done in terms of different mine unit operations like drilling, blasting, excavation and comminution and beneficiation applied to space environments. Technologies for different mine unit operations most suitable for space environments was identified. Basic design principles and issues as applicable to Lunar and Martian environments are discussed.

Extraterrestrial drilling applications has received a lot of attention of all the mine unit operations because of its importance in terms of initial subsurface exploration, anchorage and explosive emplacement. There has been work done in developing multitasking-excavating machines for space. Chemical explosives have been developed that can be used in space environments and in fact some were tested on the Lunar surface for seismic experiments. Not much work has been done in developing comminution and beneficiation methodologies for outer space except for those mentioned in chapter 2.

In the second phase of the thesis the scope of the project was narrowed down for identifying a technology that can be applied to space with possible terrestrial applications. From the literature review in chapter 2 it was concluded that optimal combination of mechanical methods and novel energy methods would be the most ideal option for space applications. Microwave assisted rock breakage was identified as one such technology that could be applied to space applications. It is concluded that apart from Lindroth *et al.* (1988) there has been no work done in applying microwaves to assist mechanical breakage of rocks in space environments.

In chapter 3 a brief review of microwave assisted rock breakage applied to terrestrial environment is given. It can be concluded that even in terrestrial environment this process is not so well understood in terms of optimal usage of microwaves for rock destruction.

In chapter 4 it was attempted to numerically simulate the microwave heating effects in a simulated rock using the finite element approach as a first step before actually commencing the experiments. Temperature profile and thermal stress were computed for different microwave input powers and heating times for a calcareous rock.

The results of the simulation indicated that a rock with microwave responsive phase and a microwave non-responsive phase developed thermal stresses of large magnitudes exceeding the actual strength of the rock.

In chapter 5, initial exploratory experimental studies are undertaken. One of the terrestrial rocks (basalt) is selected because of its petrographic similarity to Lunar and Martian rocks and tested for its low power microwave susceptibility.

From the initial results it was concluded that these basalts were quite receptive to microwaves at a low power intensity of 150W. They showed a temperature increase of up to 388 K (115°C) for a 360 seconds exposure time. Some specimens also showed thermal cracking when exposed at 180 seconds and 360 seconds. The point load strength tests indicated that there was a decreasing trend in terms of the point load index as the microwave exposure time was increased. Also, from the preliminary analysis it is seen that improvements in drilling rates can be achieved because of the reduction in the strength of the rock sample.

In essence it can be concluded that the technology investigated in the present work potentially meets the space design criteria listed in section 2.2 namely:

- Lowering the machine mass by actually lowering the mechanical energy requirement.
- Operational and design simplicity by allowing the use of simple drilling system (Eg: use of rotary drag system in place of complex rotary percussive system) that would not have been possible in case of hard rocks.
- Low energy requirement, since low power microwaves are used.

Since the present technology is still in infancy it needs extensive testing and concept realization in terms of actually integrating two different forms of energies (microwaves and mechanical energies) optimally. However, the initial results are quite promising and show that this technology has the potential to meet the space design requirements

## 6.2 Recommendations

Future work could look in to the following aspects, as an extension of the present work.

- Characterize terrestrial basalts more thoroughly when exposed to microwaves of different levels of power in the low power range and frequencies.
- Use of non-destructive testing methods to qualitatively assess the extent of thermal damage caused by microwave radiation.
- Use of more sensitive rock testing methodologies to assess the reduction in strength of the rock after microwave exposure.
- Use of mechanical methods (Eg: drilling or excavation) of rock removal after the rock has been exposed to microwaves to investigate the breakage efficiency, reduction in the mechanical energy and overall energy balance of the combined methods.
- In terms of numerical simulation use of contact based models to accurately model the interface between different mineral phases. Use of finer mesh near the interface to ensure more accurate estimates of the stress gradients. Use of accurate rock failure material models to quantify the extent of damage and the actual reduction in the strength of the rock after exposure to microwaves.
- Developing electromagnetic analysis methodology to estimate the field strength in case of surface exposure of the dielectric. Modeling the electromagnetic structure with the inclusion of impedance differences between different elements of the

structure to give more accurate values of the electric field intensity and finally validating the numerical model with the experimental results

- Finally testing the response of the rock specimens in simulated vacuum and temperature conditions (similar to outer space conditions) when exposed to microwaves.
- Conception and design of microwaving equipment, which can be used in field for exposing rocks to microwave radiation.
- Conception and design of equipment with an optimal integration of both microwave and mechanical energies for rock destruction processes.

## REFERENCES

---

Anon. (1960), "*Moon presents unique problems for drillers*", Oil and Gas Journal, v 58, n 47, Nov 21, p 255 + 257.

ANSYS 7.1 Help, 2003, Intranet HTML Documentation for ANSYS 7.0 Help, ANSYS, Inc., Canonsburg, PA.

Benaroya, H., Bernold, L.E., Chua, K.M., (2002), "*Engineering, design and construction of Lunar bases*", Journal of Aerospace Engineering. Vol. 15, no. 2, Apr, pp. 33-45.

Bernold, L. E. (1991), "*Experimental studies on mechanics of Lunar excavation*", Journal of Aerospace Engineering, v 4, n 1, Jan, p 9-22

Bieniawski, Z. T. (1975), "*Point-load test in geotechnical practice*", Engineering Geology, v 9, n 1, Mar, p 1-11

Blacic, J. D., Rowley, J. C., Cort, G. E. (1986), "*Surface drilling technologies for Mars*", NASA Center for Aerospace Information report, May, p12.

Blacic, J.D., Dreesen, D.S., Mockler, T. (2000), "*Report on conceptual system analysis of drilling systems for 200m depth penetration and sampling of Martian subsurface*", Report, Los Alamos National Laboratory, Oct.

Blair, B. R. (1998), "*Use of space resources - a literature survey*", Proceedings of the International Conference and Exposition on Engineering, Construction, and Operations in Space, Space 98, p 651-665.

## References

---

- Blair, B.R. (1996), "*Fluidized drilling for Lunar mining applications*", Proceedings of the International Conference on Engineering, Construction, and Operations in Space, v 2, p 813-820
- Boles, W.W., Scott, W.D., Connolly, J. F. (1997), "*Excavation forces in reduced gravity environment*", Journal of Aerospace Engineering, v 10, n 2, p 99-103.
- Boles, W .W., Kirby, Baird, S. (2002), "*In situ resource utilization: Excavation to support other operations*", Space and Robotics 2002, p 148-154
- Briggs, G A., Gross, A.R., (2002), "*Technical challenges of drilling on Mars*", AIAA Aerospace Sciences Meeting & Exhibit, 40th, Reno, NV, Jan. 14-17.
- Briggs, G.A., Cannon.H., Domville, S., Glass, B., Mckay, C., George, J., Derkowski, B., (2003), "*Automated, low mass, low power drill for acquiring subsurface samples of ground ice for astrobiology studies on Earth and on Mars*" Third International Conference on Mars Polar Science and Exploration, October 13-17, Alberta, Canada.
- Broch, E., Franklin, J.A. (1972), "*The point-load strength test.*", Int. J. Rock Mech. Min. Sci. Volume 9, pp. 669–697
- Burns, M., Gardner, L.A. (1966), "*Rotary-Percussive system favored for Moon drilling*" Technology week including missiles and rockets, Vol 18, n5, pp 33-36.
- Chen, T.T., Dutrizac, J.E., Haque, K.E., Wyslouzil, W, Kashyap S (1984), "*The relative transparency of minerals to microwave radiation*", Canadian Metallurgical Quarterly 123(3): 349-51
- Church, R.H., Webb, W.E.; Salsman, J.B., (1988), "*Dielectric properties of low loss minerals*", Report of Investigations - United States, Bureau of Mines, n 9194, 27p,

## References

---

- Cohen, B Y., Sherrit, S., Dolgin, B.P., Bridges, N., Bao, X., Chang, Z., Yen, A., Saunders, R.S., Pal, D., Kroh, J., Peterson, T. (2001), "*Ultrasonic/sonic driller/corer (USDC) as a sampler for planetary exploration*", IEEE Aerospace Conference Proceedings, v 1, p 1263-1271.
- Cox, R.M., (2000), "*Fragmentation of Lunar rock with explosives*", Space 2000, p 805-812.
- Das, B., (1991), "*Soil Mechanics Laboratory Manual*", Engineering Press Inc. 1982  
Annual Book of ASTM Standards, 1991
- Delinois, S.L. (1966), "*Challenge of 70's -Mining on the Moon*", Mining Engineering, v 18, n 1, Jan 1966, p 63-66.
- Dick, R.D., Fourny, W.L., Goodings, D.J., (1992), "*Use of explosives on the Moon*", Journal Of Aerospace Engineering, No: 1,Jan pp 59-69
- Economou,T., (2001), "*Chemical analyses of Martian soil and rocks obtained by the Pathfinder Alpha Proton X-ray spectrometer*", Radiation Physics and Chemistry, v 61, n 3-6, p 191-197.
- Fernandez, R., David, C. (2004), "*Mars analog research and technology experiment (MARTE), a simulated Mars drilling project*", European Space Agency, (Special Publication) ESA SP, n 545, March, p 237-238.
- Finzi, A.E., Lavagna, M.; Rocchitelli, G. (2004), "*A drill-soil system modelization for future Mars exploration*", Planetary and Space Science, v 52, n 1-3, January/March, p 83-89
- Gandhi, O.P., (1981), "*Microwave Engineering and Applications*", Pergamon Press, New York, 2nd Ed.

## References

---

- Gertsch, L E.,Gertsch, R.E.(1990) , “*Application of Lunar criteria to three terrestrial mining methods*”, Proceedings of Space 90, April 22-26, volume 1, p 284-293.
- Gertsch, R. E., Gertsch, L.E.; Kent, S.R. (1990), “*Lunar surface mines and mining machinery. Design criteria*”, Proceedings of Space 90 April 22-26, volume 1, p 274-283
- Gertsch, R. E. (1983), “*Method for mining Lunar soil*”, Advances in the Astronautical Sciences, v 53, p 337-346.
- Goodings D.J., Lin, C.P, Dick, R.D., Fournery, W.L., Bernold, L.E. (1992), “*Modeling effects of chemical Explosives for excavation on Moon*”, Journal Of Aerospace Engineering 5,No: 1,Jan, pp 44-58.
- Hall, R.A., Green, P.A. (1992), “*Transfer of terrestrial technology for Lunar mining*”, Proc 3 Int Conf Eng Constr Oper Space III, p 1150-1161
- Hamelin, M., Asikainen, L.,Kitzinger, F.(1993) , “*Blasting with electricity. Paving the way into 21st century mining*”, Innovative Mine Design for the 21st Century, p 805
- Hartman, H.L, Mutmansky, J.M. (2002), “*Introductory Mining Engineering*”, J. Wiley, 570p
- Haque, K.E.(1999), “*Microwave energy for mineral treatment processes - a brief review*” International Journal of Mineral Processing, v 57, n 1, p 1-24
- Hayt, W.H., (1974), “*Engineering Electromagnetics*”, McGraw-Hill Book Company, 3<sup>rd</sup> Ed, 487p.

## References

---

- Hill, III., Shenhar, J., Lombardo, M. (2003), "*Tethered, down-hole-motor drilling system - A benefit to Mars exploration*", *Advances in Space Research*, v 31, n 11, p 2421-2426.
- Horneck, G., Facius, R., Reitz, G., Rettberg, P., Khan, B.C., Gerzer, R.(2001), "*Critical issues in connection with human planetary missions: Protection of and from the environment*" *Acta Astronautica*, v 49, n 3-10, Aug 11, p 279-288
- Jerby.E, V.Dikhtyar, O., Aktushev, U., Groszlick, (2002), "*The microwave Drill*", *Science*, Vol 298 Oct, pp587-589.
- Joachim, C.E. (1988), "*Extraterrestrial excavation and mining with explosives*", *Eng Constr Oper Space Proc Space* 88, p 332-343.
- Jones, D.A., Kingman, S.W., Whittles, D.N., Lowndes, I.S. (2005), "*Understanding microwave assisted breakage*", *Minerals Engineering*, Volume 18, Issue 7, June, Pages 659-669.
- Kahraman, S., Bilgin, N., Feridunoglu, C., (2003), "*Dominant rock properties affecting the penetration rate of percussive drills*", *International Journal of Rock Mechanics and Mining Sciences*, v 40, n 5, July, p 711-723.
- Kingman, S.W., Rowson, N.A. (1998), "*Microwave treatment of minerals - a review*" *Minerals Engineering*, v 11, n 11, Nov, p 1081-1087.
- Kingman, S.W., Vorster, W., Rowson, N.A., (2000), "*The Influence of mineralogy on microwave assisted grinding*", *Minerals Engineering*, v 13, n 3, Mar, , p 313-327.
- Kingman, S.W., Jackson, K., Cumbane, A., Bradshaw, S.M., Rowson, N.A., Greenwood, R., (2004), "*Recent developments in microwave assisted comminution*", *International Journal of Mineral Processing*, v 74, n 1-4, Nov 19, p 71-83.

- Klosky, J.L, Sture, S., Ko, H.Y., Barnes, F. (1996), "*Vibratory excavation and anchoring tools for the Lunar surface*", Proceedings of the International Conference on Engineering, Construction, and Operations in Space, v 2, p 903-911.
- Klosky, J.L, Sture, S., Ko, H.Y., Barnes, F. (1998), "*Helical anchors for combined anchoring and soil testing in Lunar operations*", Proceedings of the International Conference and Exposition on Engineering, Construction, and Operations in Space, Space 98, p 489-494
- Lauriello, P. J.; Fritsch, C. A. (1974), "*Design and economic constraints of thermal rock weakening techniques*" International Journal of Rock Mechanics and Mining Sciences & Geomechanics Abstracts, v 11, n 1, Jan, 1974, p 31-39.
- Lewis, J.V., (1907), "*Petrography of the Newark igneous rocks of New Jersey*", New Jersey Geol Survey Ann Report, Pp 148-467.
- Lewis, J., Mathews, M.S., Guerreiri, M.L. (1993), "*Resources of near-Earth space*", University of Arizona Press, P 51.
- Lindroth, D.P., Podnieks E.R. (1988), "*Electromagnetic energy applications in Lunar mining and construction*", Proc Lunar Planet Sci Conf 18,1988 p365-373.
- Lindroth, D.P. Berglund, W.R.; Morrell, R.J.; Blair, J.R (1993) "*Microwave assisted drilling in hard rock*" , Tunnels and Tunneling, v 25, n 6, Jun, 1993, p 24-27.
- Magnani, P.G., Re, E., Ylikorpi, T., Cherubini, G., Olivieri, A. (2004), "*Deep drill (DeeDri) for Mars application*", Planetary and Space Science, v 52, n 1-3, January/March, p 79-82.
- Mancinelli, R.L. (2000), "*Accessing the Martian deep subsurface to search for life*", Planetary and Space Science, v 48, n 11, Sep, 2000, p 1035-1042.

- Mason, L.W. (1992), "*On the beneficiation and comminution of Lunar regolith*", Proc 3 Int Conf Eng Constr Oper Space III, p 1127-1138.
- Mason, L.W. (1992), "*Beneficiation and comminution circuit for the production of Lunar Liquid Oxygen (LLOX)*", Proc 3 Int Conf Eng Constr Oper Space III, p 1139-1149.
- Maurer, W.C. (1968) "*Novel drilling techniques*", Pergamon Press, Oxford; New York 114p.
- Metaxas, A.C., Meredith, R.J., (1983), "*Industrial Microwave Heating*" Peter Peregrines, London, UK.
- Meredith, R.J. (1998), "*Engineer's Hand book of Industrial Microwave heating*", The institution of electrical Engineers, London, UK.
- Nantel, J. (1996), "*Improvements in mining technology*", Proceedings of the International Conference on Engineering, Construction, and Operations in Space, v 2, p 806-812.
- Nathan, M.P., Barnes, F., Ko, H.Y., Sture, S. (1992), "*Mass and energy tradeoffs of axial penetration devices on Lunar soil stimulant*", Proc 3 Int Conf Eng Constr Oper Space III, p 441-457.
- Nathan, M.P., Barnes, F., Sture, S., Ko, H.Y., Lund, W. (1992), "*Comparison of the efficiencies of a new class of Lunar excavation tools*", American Society of Mechanical Engineers, Aerospace Division (Publication) AD, v 31, Space Exploration Science and Technologies Research, p 141-151
- Nekrasov, L. B., Rikenglaz, L.E., Kolokolova, O. V. (1974), "*Optimization of the input of electromagnetic energy in rock breaking by multistage ETM units*", Soviet Mining

## References

---

- Science (English translation of Fiziko-Tekhnicheskie Problemy Razrabotki Poleznykh Iskopaemykh), v 10, n 4, Jul-Aug, 1974, p 456-460
- Noever, D.A., Smith, D.D., Sibille, L., Brown, S.C., Cronise, R.J., Lehoczky, S.L. (1998), "*High performance materials applications to Moon/Mars missions and bases*", Proceedings of the International Conference and Exposition on Engineering, Construction, and Operations in Space, Space 98, p 275-285.
- Peeters, M., Blair, B. (2000), "*Drilling and logging in space: an oil-well perspective*", Space 2000, p 739-747
- Phillips, M. (1971), "*Drilling holes in the Moon*", Engineering, v 211, n 2, May, p 172-173.
- Podnieks, E.R., Siekmeier, J.A. (1993), "*Terrestrial mining technology applied to Lunar mining*", Space Manufacturing 9-High frontier Accession, Princeton, NJ, pp301-308
- Podnieks, E.R., Siekmeier, J.A. (1992), "*Lunar surface mining equipment study*", Proc 3 Int Conf Eng Constr Oper Space III, p 1104-1115
- Podnieks, E.R., Schmidt, R.L. (1990), "*Lunar mining. Surface or underground?*", Proceedings of Space 90 April 22-26, volume 1, p 315-324
- Poirier, S., Fecteau, J.M., Laflamme, M., Brisebois, D. (2003), "*Thermal rock fragmentation - Applications in narrow-vein extraction*", CIM Bulletin, v 96, n 1071, May, p 66-71
- Protasov, Yu. I. Kuznetsov, V. V., Merzon, A. G.; Chernikov, V. A., Retinskii, V. S. (1984), "*Study of electrothermomechanical destruction of hard rocks with a rotary heading machine*", Soviet Mining Science (English translation of Fiziko-Tekhnicheskie Problemy Razrabotki Poleznykh I, v 20, n 6, Nov-Dec, p 462-467

## References

---

- Roepke, W.W. (1975), “ *Experimental system for drilling simulated Lunar rock in ultrahigh vacuum*”, Report NASA CR 146419, Jan, 12p.
- Rostami, J., Blair, B., Eustes, A. (1998), “*Review of the issues related to extraterrestrial drilling*”, Proceedings of the International Conference and Exposition on Engineering, Construction, and Operations in Space, Space 98, p 437-450.
- Salsman, J.B., Williamson, R.L., Tolley, W.K., Rice, D.A., (1996), “*Short-pulse microwave treatment of disseminated sulfide ores*”, Minerals Engineering, v 9, n 1, Jan, p 43-54.
- Sanga, C.M.E. (2002), “*Microwave Assisted Drying of Composite materials: Modeling and experimental validation*”, PhD thesis, McGill University, Canada.
- Santamarina, J. Carlos (1989), “*Rock excavation with microwaves: a literature review*”, Found Eng Curr Princ Pract, p 459-473
- Schrunk, D., Sharpe, B., Cooper, B., Thangavelu, M. (1999), “*The Moon, resources, future development and colonization*”, New York: Wiley.
- Smith, J.W (1999), “*Analysis of Microwave heating of Dielectric materials*”, PhD thesis, University of Minnesota, USA.
- Taylor, G.J., Martel, L. M.V. (2003), “*Lunar prospecting*”, Advances in Space Research, v 31, n 11, p 2403-2412.
- Tian, Q.J., Gong, P.; Xu, B.; Wang, X.; Guo, H.; Tong, Q. (2002), “*Reflectance, dielectric constant and chemical content of selected sedimentary rocks*”, International Journal of Remote Sensing, v 23, n 23, Dec 10, p 5123-5128

## References

---

Timoshenko, S.J., Goodier, J.N., (1971), "*Theory of elasticity*", McGraw-Hill book company, 3<sup>rd</sup> Edition.

Walkiewicz, J. W., Kazonich, G., McGill, S. L., (1988), "*Microwave heating characteristics of selected minerals and compounds*", *Minerals & Metallurgical Processing*, v 5, n 1, Feb, p 39-42.

Watson, P.M. (1988), "*Explosives research for Lunar applications: A review*", *Eng Constr Oper Space Proc Space* 88, p 322-331.

Whittles, D.N., Kingman, S.W.; Reddish, D.J.(2003), "*Application of numerical modeling for prediction of the influence of power density on microwave-assisted breakage*" *International Journal of Mineral Processing*, v 68, n 1-4, January, p 71-91.